Downstream Purification and Analysis of the Recombinant Human Myelin Basic Protein Produced in the Milk of Transgenic Cows

A thesis presented in partial fulfillment of the requirements for the degree of

Doctor of Philosophy

in

Chemistry

Massey University (Palmerston North)
New Zealand

Medhat Ahmed Abdel-Hamid Al-Ghobashy

2009

Abstract

Downstream purification and analysis of a model biopharmaceutical protein (recombinant human myelin basic protein) is described. The recombinant protein was expressed in the milk of transgenic cows and was found exclusively associated with the casein micellar phase. Binding of milk calcium to the active sites of a cation exchanger resin was used beneficially in this study in order to gently disrupt the casein micelles and liberate the recombinant protein. This approach was found superior to the conventional micelle disruption procedures with respect to product recovery, resin fouling due to milk components and column hydrodynamic properties. Further purification was carried out using Ni^{2+} affinity chromatography and resulted in purity more than 90% and a total recovery of 78%. A capillary electrophoresis total protein assay employing large volume sample stacking and a microsphere-based, sandwich-type immunoassay were developed and validated. Both methods were successfully integrated with the downstream purification protocol in order to evaluate various quality attributes of the recombinant protein. A one-step capillary isoelectric focusing protocol was developed in order to monitor the recombinant protein in milk samples. The results showed extra protein bands in the transgenic milk that had isoelectric points significantly lower than the theoretically calculated one which indicated that the protein had been modified during expression. The association between the recombinant protein and bovine milk caseins was explored at the molecular level using the surface plasmon resonance technique. Results showed a calcium-mediated interaction between the recombinant protein and the phosphorylated caseins. This selective interaction was not noted between the human myelin basic protein and milk caseins which indicated mammary gland-related posttranslational modifications, most likely phosphorylation. The co-expression of the recombinant protein and caseins in the mammary gland, along with the ability of the recombinant protein to form calcium bridges with caseins explained its association with the casein micellar phase in the transgenic milk. Despite this and owing to the low expression levels of the recombinant protein in milk, light scattering investigations using diffusing wave spectroscopy showed no significant differences between the transgenic and the non-transgenic milk samples with respect to the average micelle size and the micelle surface charges.

Acknowledgements

I would like to thank my supervisors A/Professor Dave Harding and Dr Bill Williams for their support and help throughout every step of this thesis. Via their wide collaborative network, I enjoyed working with experts from quite diverse backgrounds here at Massy University and at other New Zealand research institutes.

In addition, I would like to thank Dr Goetz Laible and his research team, in particular Brigid Brophy (Ruakura Research Centre, Agresearch Ltd) for providing the transgenic milk samples and their useful co-operation. I would like to express my deep gratitude to Dr Gill Norris (Institute of Molecular Biosciences, Massey University), Dr Kate Palmano (Fonterra Research Centre) and Dr Thomas Backstrom and his research group, in particular Evelyn Spittle (Malaghan Institute for Medical Research). I am also grateful to Dr Don Otter (Fonterra Research Centre) and Professor Ashton Partridge and his research team, in particular Dr Krishanthi Jayasundera (NRC, MacDiarmid Institute) for useful discussions, teaching me techniques and granting me access to their research labs.

Special thanks to Tracy Edwards (Institute of Molecular Biosciences, Massey University) and Tim Hale (Agresearch Ltd) for their efforts in arrangements for sample transfer between Massey University and Agresearch Ltd. I would like to thank also my colleagues in the lab, in particular Dr Linley Shofield, Dick Poll, Aurelie Cucheval and Chris Burrows.

Finally my family requires a special acknowledgement. Heba, without your love and patience this thesis would be a lot harder. My lovely daughters, Rawan and Jana, this thesis meant sacrificing many hours together.

Table of Contents

List of Figures

List of Tables

List of Abbreviations

Abbreviation	Definition
Δtm	Difference in migration time
A	Integrated peak area
ANOVA	Analysis of variance
BA	Benzyl alcohol
BGE	Background electrolyte
BME	β-Mercaptoethanol
BSA	Bovine serum albumin
CA	Carrier ampholytes
CAP	Calcium phosphate nanoparticles
CB	Comassie Blue protein stain
cDNA	Complementary deoxyribonucleic acid
CE	Capillary electrophoresis
CIEF	Capillary isoelectric focusing
CIP	Clean-in-place
CK	Cholecystokinin flanking peptide
CM	Carboxymethyl
CMC	Critical micelle concentration
CN	Casein
CNF	Casein fraction
CNM	Casein micelles
CS	Carbonic anhydrase II
cv	Column volume
CZE	Capillary zone electrophoresis
DAD	Diode array detector
DP	Deep Purple protein stain
DWS	Diffusing wave spectroscopy
EDC	1-Ethyl-3-[3-dimethylaminopropyl]carbodiimide hydrochloride

EDTA	Ethylenediaminetetraacetic acid disodium salt dihydrate
ELISA	Enzyme linked immunosorbent assay
EOF	Electroosmotic flow
EtA	Ethanolamine
Fc	Flow cell
FS	Fused silica
GDL	Glucono-δ-lactone
GST	Glutathione-S-transferase
h	Peak height
HEPES	4-(2-Hydroxyethy)-1-piperazine ethanesulfonic acid
His tag	An amino acid motif in proteins which consists of polyhistidine residues, often at the C- or N-terminus.
hMBP	Human myelin basic protein
HRP	Horse radish peroxidase
HSDC	High sensitivity detection cell
I.D.	Internal diameter
ICH	International conference on harmonization of technical requirements for registration of pharmaceuticals for human use
IEF	Isoelectric focusing
IMAC	Immobilized metal affinity chromatography
LA	Lactalbumin
LF	Lactoferrin
LG	β-Lactoglobulin
LLOQ	Lower limit of quantitation
LOD	Limit of detection
LP	Lactoperoxidase
LVSS	Large volume sample stacking
mAb	Monoclonal antibody
MBP	Myelin basic protein
MFGM	Milk fat globule membrane
MFI	Median fluorescence intensity

mRNA	Messenger ribonucleic acid
MS	Multiple sclerosis
MSD	Mean square displacement
MW	Molecular weight
MWCO	Molecular weight cut off
NC	Nitrocellulose
NHS	N-Hydroxysuccinimide
O.D.	Outer diameter
OG	Orange G
PA	Migration time-corrected integrated peak area
PBS	Phosphate buffered saline
PEO	Polyethylene oxide
PQ	ProQ Diamond protein stain
PTM	Posttranslational modifications
QC	Quality control
R^2	Correlation coefficient
rhMBP	Recombinant human myelin basic protein
RN	Ribonuclease A
RT	Room temperature
RU	Resonance unit
SA-PE	Streptavidin-coupled *R*-phycoerythrin
SDS	Sodium dodecylsulfate
SDS-PAGE	Sodium dodecylsulfate-polyacrylamide gel electrophoresis
SF	Serum fraction
S-NHS	N-Hydroxysulfosuccinimide
SPBB	Sulfopropyl Sepharose big beads
SPR	Surface plasmon resonance
Tg	Transgenic
TGmilk	Milk obtained from transgenic cows by natural lactation
$TGmilk_h$	Milk obtained from transgenic heifers by hormonal induction
tm	Migration time

$W_{1/2}$	Peak width at half height
WF	Whey fraction
WTmilk	Milk obtained from wild type, control cows

Chapter 1

1 Introduction

1.1 Biopharmaceuticals: history and current situation

Biopharmaceuticals is a term used to describe drugs that are produced using biotechnology and does not include those produced by direct extraction from non-engineered biological sources. They are proteins including antibodies or nucleic acids used for therapeutic or in vivo diagnostic purposes. Since the 1970s, the total number of patents granted for biopharmaceuticals has risen significantly; from 30 applications in 1978 to 34,527 in 2001. This dramatic rise could be attributed to the completion of the human genome project, with genes and sequences arising out of the project providing new routes for drug discovery. The great collaboration between different disciplines including molecular biology, molecular genetics, bio-engineering, protein / carbohydrate / nucleic acid chemistries and pharmaceutical sciences has contributed to the ever increasing trend toward biopharmaceuticals (Arakawa & Philo, 2002; Luke, Doina, & Simon, 2002; G. Walsh, 2003).

Since the commercial production of the first recombinant therapeutic drug, human insulin, in 1982, (Humulin; Genentech, USA), the number of biotechnology products available in the market continued to grow from 84 (2000) to 148 (2003). As of 2006, 418 biotechnology medicines have been in development for more than 100 diseases. During 2007, fifteen biopharmaceuticals were approved in the US and / or the EU, with only five of them being “biosimilar” to already existing lead products. These biosimilar drugs demonstrated the comparability of the active ingredients obtained using different manufacturing technologies and indicated the increase in the competition in the biopharmaceutical industry. Currently, the time gap between the approval of a lead biopharmaceutical entity and that of a generic product is less than two years, compared to 8 – 10 years in the early days. As a result, few new biopharmaceuticals are likely to enjoy high market shares and thus the development of more efficient production strategies is required (Jagschies, 2008; Little, Paquette, & Roos, 2006; Tauzin, 2006; G. Walsh, 2008).

1.2 Second generation biopharmaceuticals

Throughout the 1980s, the recombinant technology was used to produce proteins with identical amino acid sequences to their human counterparts. Techniques such as site-directed mutagenesis along with the increased understanding of protein structure-function relationships allowed the production of proteins of altered, "engineered" amino acid sequences. Several beneficial therapeutic and technical outcomes have been achieved using this approach such as the reduction / elimination of product immunogenicity (humanization), the alteration of the pharmacokinetics profiles in order to generate long acting drugs and the production of novel multi-acting "fusion" proteins. The same technology was employed to graft peptide sequences (tags) to recombinant proteins in order to facilitate product recovery and testing such as the polyhistidine tag (His tag) and the glutathione-S-transferase tag (GST tag) (Gary Walsh, 2000, 2003, 2006).

1.3 Sources of biopharmaceuticals

Escherichia coli and mammalian cell lines are still the main sources of biopharmaceuticals. However, it is generally believed that prokaryotes are unable to carry out the complex posttranslational modifications (PTM) which are required for the activity and the stability of the product. Mammalian cell culture is a technically demanding, slow and expensive technique. On the other hand, yeast, insect and plant cell cultures provide good economic alternatives. They require shorter fermentation cycles and have lower risk of transmitting mammalian pathogens. These systems can carry out glycosylation yet in a pattern different from that produced by the human machinery, which may have functional and safety implications (Clark, 1998; Gary Walsh, 2006).

1.3.1 Pharming

"Pharming" is a new brand of farming that involves the production of human pharmaceuticals in genetically modified plants and farm animals. Despite the early enthusiasm for plant expression systems, several technical barriers remain to be overcome. Differences in glycosylation patterns between mammalian and plant systems represent a

formidable hurdle as some plant-derived sugar motifs are highly immunogenic in man (Gary Walsh, 2006). On the other hand, a wide variety of farm animals, such as cows, goats, pigs, sheep and chickens are being used to generate proteins of therapeutic interests. They became the preferred production facility since they have many advantages such as flexibility in production capacity and product delivery in a convenient form such as milk, egg, blood, urine and seminal fluid (Clark, 1998; Gavin, 2001; Nikolov & Woodard, 2004). The mammary gland is generally the preferred bioreactor due to its ability to carry out complex PTM in a pattern similar to that of the human machinery. The large volumes of milk, the high levels of protein expression and the ease of milk collection without detriment to the animal contributed to the popularity of the use of the mammary gland as a bioreactor. Regulatory elements derived from genes encoding abundantly expressed milk proteins were used to target the expression of foreign proteins in the mammary gland of transgenic (Tg) animals and in some cases very high levels of expression have been achieved (J. Denman et al., 1991; Laible & Wells, 2007; Melo Eduardo, Canavessi Aurea, Franco Mauricio, & Rumpf, 2007; Pollock et al., 1999; Salamone et al., 2006; van Berkel et al., 2002; Velander et al., 1992; Wright et al., 1991).

1.4 Quality control of biopharmaceuticals

Human proteins expressed in heterologous systems are of an unpredictable nature and assessment of their activity and stability is of primary importance. Some variability is not only anticipated but is also acceptable as long as it is well understood by the manufacturer. Comparison of the recombinant product with its human counterpart or to a lead product is essential in order to evaluate the product biosimilarity. The guidance documents published by the International Conference on Harmonization of Technical Requirements for Registration of Pharmaceuticals for Human Use (ICH) provide specific information on product testing and acceptance criteria of the biotechnology-derived products. ICH brings together the regulatory authorities of Europe, Japan and USA as well as experts from the pharmaceutical industry. Its primary objective is to provide recommendations and guidelines for various product registration requirements in order to obviate the need for duplicate testing of new biopharmaceuticals. Various aspects of

bioanalytical method validation have also been discussed in the literature and in the guidelines issued by the registration authorities around the world (Doblhoff-Dier & Bliem, 1999; Findlay et al., 2000; Hildebrand, 2005; Krause, 2006; C. Zhang & Van Cott, 2007).

1.4.1 Quality control of transgenic protein pharmaceuticals

For those biopharmaceuticals produced in the milk of Tg animals, early milk collection by hormonal induction of the heifers ($TGmilk_h$) allows the prediction of whether the transgene would be expressed in milk during the natural lactation (TGmilk). It helps also set up a preliminary purification strategy as well as a biochemical characterization protocol of the product. Once acceptable expression levels of the recombinant protein in the TGmilk have been achieved, close monitoring of the expression levels and patterns is required in order to establish the acceptance limits for different sources of variability. A strategy for product recovery at scale has to be designed employing as few steps as possible with the least number of denaturants in order to maintain activity and good yields. A well designed battery of analytical methods has to be integrated with the purification strategy since no single method is sufficient for evaluation of all the quality attributes of such large molecules. Product testing has to be also carried out for each animal at different stages of lactation and over different lactation cycles to ensure production consistency (Doblhoff-Dier & Bliem, 1999; Hildebrand, 2005; Kelner & Bhalgat, 2007; Krause, 2006; Mueller, Gempeler, Scheiwe, & Zeugin, 1996; Nikolov & Woodard, 2004; Volkin, Sanyal, Bruke, & Middaugh, 2002; C. Zhang & Van Cott, 2007).

ATryn, a recombinant human anti-thrombin, is the first biopharmaceutical of a transgenic source to gain a marketing approval (GTC Biotherapeutics, USA). ATryn was produced in the milk of transgenic goats and represented a good example of the effort and the time required to produce and characterize a transgenic biopharmaceutical product (Echelard, Meade, & Ziomek, 2005). The first, healthy transgenic goat was born in 1992 and the marketing approval for ATryn was granted in 2006[*].

[*] (http://www.gtc-bio.com/products/atryn.html).

In the following sections, the production of the recombinant human myelin basic protein (rhMBP) in the milk of genetically modified cows and early attempts carried out for the purification of this recombinant protein is reviewed. At first, the role of myelin basic protein in health and disease and why it has been considered as a potential biopharmaceutical is discussed.

1.5 Myelin basic protein

1.5.1 Physiological role

The myelin sheath is one of the defining characteristics of all gnathostomates (verebrates with jaws). It is comprised of a multi-lamellar, compact structure formed of lipids (70%) and proteins (30%). Myelin basic protein (MBP) represents 30% and 5 - 15% of the myelin protein in the central and peripheral nervous systems respectively. It is localized in the space between the opposing membrane layers and is responsible for the compactness of the myelin sheath layers, thereby insulating nerve fibers for efficient transmission of impulses (Vanrobaeys, Van Coster, Dhondt, Devreese, & Van Beeumen, 2005). Figure 1 shows a diagrammatic representation of a myelinated neuron while Figure 2 shows a magnified cross section of such a neuron showing the insulating, multi-lamellar myelin layers.

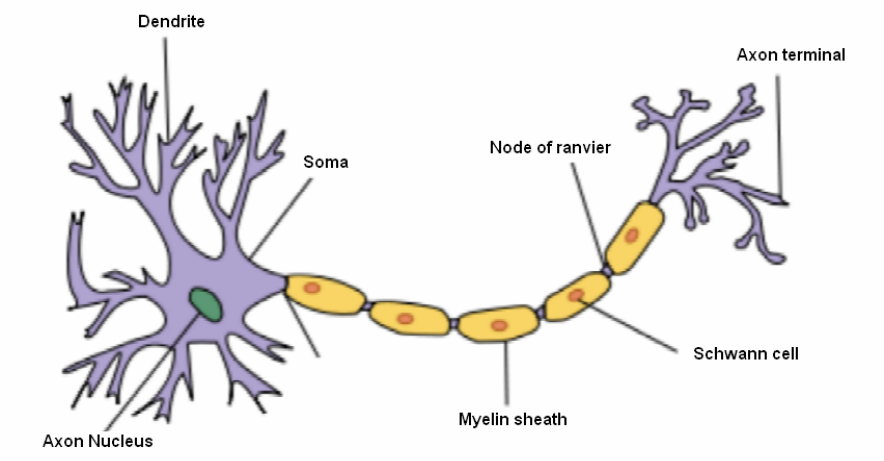

Figure 1: Diagrammatic representation of a myelinated neuron.

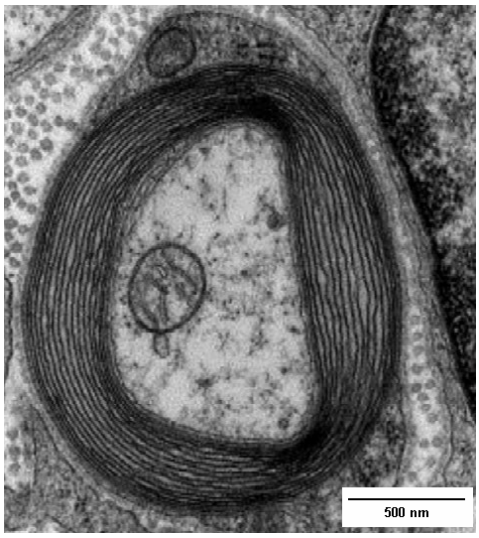

Figure 2: Transmission electron micrograph of a cross section of a myelinated neuron showing the multi-lamellar structure of the myelin sheath.

1.5.2 Pathology of multiple sclerosis

Multiple sclerosis (MS) is an autoimmune human disease of multi-factorial origin, characterized by an active degradation of the myelin sheath. The human myelin basic protein (hMBP) has been considered as the autoantigen in demyelination diseases in general and in MS in particular. The presence of the hMBP in the cerebrospinal fluid at levels higher than normal (> 4 ng/ml) is a marker of active inflammation and myelin breakdown. Without this insulation, information from nerves would be transmitted inefficiently, which results in weakness, sensory loss or other neurologic dysfunction (Tzakos et al., 2004; Vanrobaeys et al., 2005).

1.5.3 Biomolecular characteristics of myelin basic protein

MBP is a typical example of an "intrinsically unstructured" or a "natively unfolded" protein in solution but it has a meaningful structure in the myelin sheath or in the presence of other biological molecules. The conformationally adaptive structure of the hMBP along with its highly basic character allows an efficient interaction between the hMBP and the negatively charged phospholipids in the myelin sheath which wraps concentrically around nerve fibers as discussed above (Beniac et al., 1997; Eylar, 1970; Harauz et al., 2004; Maatta, Coffey, Hermonen, Salmi, & Hinkkanen, 1997; Tzakos et al., 2004).

The hMBP is a product of the differential splicing of a single mRNA transcript resulting in four molecular weight (MW) isoforms: 21.5, 20.2, 18.5 and 17.2 kDa with the 18.5 kDa protein representing the major isoform. Further microheterogeneity exists due to a myriad number of PTM (N-terminal acylation, phosphorylation, methylation, deimination, deamidation, ADP-ribosylation) that result in a variety of charge isoforms. Of these types of PTM, three have significant roles in the physiology of MBP and the pathology of MS. Deimination (irreversible) of arginine to citrulline limits the ability of MBP to maintain a compact myelin sheath and is pivotal to the pathology of MS. Phosphorylation (reversible) alters the conformation of MBP, the ability to interact with the phospholipid bilayer and renders it less susceptible to proteolysis. Although methylation (irreversible) of arginyl residues of MBP is correlated with compact and healthy myelin, it was found to increase in MS patients as well (Chantry & Glynn, 1986; Cruz & Moscarello, 1983; Harauz et al., 2004).

The complete amino acid sequence of the 18.5 kDa hMBP isoform has been investigated and the following results were obtained: it contains 170 residues with a high abundance of basic residues (12 Lys and 19 Arg) distributed randomly and giving the protein a very basic character (pI 12.5). The relatively low abundance of acidic residues (9 Asp and 2 Glu) also contributed to the overall basic character of the protein. The hMBP primary structure exhibits many characteristics of an intrinsically unstructured protein, particularly in the enrichment of proline (19 Pro), an amino acid associated with open conformations, and in the low abundance of the hydrophobic residues. Myelin basic protein

shows a high degree of sequence conservation in various species which indicated the importance of maintaining its structural properties and the sites of PTM (Cheifetz, Moscarello, & Deber, 1984; Deibler, Martenson, & Kies, 1972; Harauz et al., 2004).

It has been reported that hMBP can bind in vitro and in vivo to a wide variety of proteins (calmodulin, actin, tropomyocin, tubulin, clathrin, α2-macroglobulin, heat shock protein and several myelin and non-myelin proteins), amphipathic molecules (lipids and surfactants) and various divalent cations. Many of these interactions have either a physiological or pathological significance while for the other interactions the significance is still unknown which indicates a complex structure-function relationship of hMBP (Boggs, Rangaraj, Gao, & Heng, 2006; Eylar, 1970; Harauz et al., 2004).

1.5.4 A possible treatment for multiple sclerosis

Multiple sclerosis is as yet a disease without a fully effective treatment and largely of unknown pathogenesis. With the existence of multiple independent epitopes in hMBP, therapies that eliminate pathologic T-cell responses to multiple epitopes have a distinct advantage over peptide-specific therapies such as anti T-cell receptor. Recent research suggested that administration of neuroantigens to patients can tolerize the autoimmune response. The human myelin basic protein was investigated for its antigenic epitopes and was studied as a model for an immunomodulatory vaccine against MS. Linear and cyclic analogues of several hMBP epitopes have been synthesized and a molecular model which may be useful in the design of an immunomodulatory vaccine has been developed (Beniac et al., 1997; Eylar, 1970; Harauz et al., 2004; Maatta et al., 1997; Tzakos et al., 2004).

1.5.5 Sources and methods of isolation of MBP

Studies of MS autoantigens and the MBP biophysical characteristics require the availability of large amounts of pure protein. Several protocols have been in use for the isolation of the MBP from CNS tissue of different species since 1970s. These procedures were generally based on homogenization and lipid removal of the CNS tissue using organic solvents followed by adsorption of the MBP on cation exchanger resins at acidic pH

(Bizzozero, Odykirk, McGarry, & Lees, 1989; Deibler et al., 1972; Eylar, 1970). The use of such purified MBP encountered many problems such as the presence of contaminants, typically proteolysis products of MBP. These proteolysis products were found to tolerize the MBP-reactive T-cell clones leading to a decreased reactivity to the intact MBP molecules (Oettinger et al., 1993).

Recombinant technology was utilized to produce the 18.5 kDa hMBP (Oettinger et al., 1993; Russo & Brand, 1999) and the 21.5 kDa (Nye et al., 1995) isoforms in *E. coli*. A purification procedure similar to that described above was employed in one case (Oettinger et al., 1993) while protocols employing cation exchange chromatography and immobilized metal affinity chromatography (IMAC) were employed for purification of the rhMBP in the latter cases (Nye et al., 1995; Russo & Brand, 1999). Recombinant bacteria provided a reliable, cheaper source of the hMBP. Lack of the human PTM patterns was the main drawback since the immunogenicity of hMBP was found to increase with the abundance deiminated Arg residues (Harauz et al., 2004). Thus, the production of rhMBP in the milk of transgenic animals was considered.

In the following section, a brief discussion of the characteristics of this unique production matrix (milk) will be discussed along with the previously reported problems associated with the production of recombinant proteins in the milk of transgenic animals.

1.6 Milk proteins

Milk is a complex colloidal dispersion of fat globules and various proteins in an aqueous solution of lactose, minerals and other components. Normal milk contains approximately 87.4% water and 12.6% milk solids. It provides the complete nutritional requirements including protein, fat and carbohydrates for mammalian neonates. Milk shows large inter-species differences which are required to match the specific nutritional requirements of the neonates, growth rate and the energy requirements of each species (Table 1) (Playne, Bennett, & Smithers, 2003). Milk also serves a number of physiological functions via its protein and peptide content such as immunoglobulins, enzymes, enzyme inhibitors, growth factors and anti-bacterial agents. Many factors affect milk composition even within the same species such as the breed, diet, milking frequency and the animal's state of health. Milk proteins can be broadly classified as caseins and whey proteins. About 70 years ago, the term "casein" was adopted as the English word describing the protein precipitated from milk at (pH 4.6). The liquid remaining after precipitation of caseins from skimmed or whole milk was called the whey fraction (Fox, 2003; Playne et al., 2003).

Table 1: Approximate composition of milk (g/L) in various species.

Component		Cow	Human	Buffalo	Goat	Sheep
Total solids		125	129	171	130	163
Proteins		34	10	38	29	55
	Casein proteins	28	4	--	23	--
	Whey proteins	6	5.5	--	6	--
Fat		31	38	75	45	53
Lactose		48	71	49	41	46
Oligosccharides		0.03 - 0.06	3 - 8	--	--	--
Riboflavin (mg/L)		1.57	0.43	1.02	1.14	4.36
Minerals	Ash	7	2	8	8	9
	Calcium	1.14	0.34	1.85	1.30	1.93
	Phosphorus	0.93	0.14	1.25	1.06	0.99

Caseins (CN) are classified into five categories; α-$_{s1}$, α-$_{s2}$, ß-, κ- and γ-CN (ß-casein-derived peptides / proteolysis products) with relative abundance of 38: 10: 36: 13: 3 respectively. The whey (W) fraction is composed of four main acidic proteins that can be captured using anion exchange resin: ß-lactoglobulin (LG), α-lactalbumin (LA), bovine serum albumin (BSA) and immunoglobulins. Lactoferrin (LF) and lactoperoxidase (LP) are two basic whey proteins that are not captured during this process because of their high isoelectric points. The relative concentrations, molecular weights and isoelectric points of major bovine milk proteins are summarized in Table 2. (Fox, 2003; Tremblay, Laporte, Leonil, Dupont, & Paquin, 2003).

Table 2: Approximate composition and molecular weights of bovine milk proteins.

		Concentration (g/Kg)	% of Total Protein	MW (kDa)	pI
Caseins	α_{s1}-CN	10.0	30.4	23.6	4.9 / 5.3
	α_{s2}-CN	2.6	7.9	25.2	4.9 / 5.3
	ß- CN	9.3	28.3	24.0	5.2
	κ- CN	3.3	10.0	19.0	5.8
	γ- CN	0.8	2.43	11.5 - 20.5	
	Total	26.0	79.0		
Whey proteins	LA	1.2	3.6	14	4.4
	LG	3.2	9.7	18.3	5.4
	BSA	0.4	1.2	67	5.1
	Immunoglobulins	0.8	2.4	Up to 1000	5 - 8
	Miscellaneous	0.8	2.4		
	LF	0.1	0.3	77	7.9
	LP	0.03	0.1	78	9.6
	Total	6.5	19.8		
MFGM*		0.4	1.2		
Total		≈ 32.9	100		

* **Milk fat globule membrane**

1.6.1 The complexity of the milk system

Milk contains a few primary proteins as discussed above. However, the milk proteome is still extremely complex due to post translational modifications, numerous genetic variants, low abundance proteins and presence of a naturally occurring proteolysis. An additional level of complexity arises from the fact that milk is a bio-colloid system composed of three phases; dispersed lipid phase, aqueous serum phase and casein micellar phase which contains 70 - 80% of milk proteins. Thus, milk with its unique nature is challenging for chromatographic processing (Fox & Brodkorb, 2008; Manso, Leonil, Jan, & Gagnaire, 2005; O'Donnell, Holland, Deeth, & Alewood, 2004).

Several approaches have been reported in order to reduce the complexity of milk prior to chromatographic processing. However, serious product losses have always been the main concern. Fat globules normally cause problems by blocking packed columns. It has been reported that chromatographic processing of raw milk is possible at elevated temperatures (35 - 37 ^{o}C) (Fee & Chand, 2006). Under such conditions, the stability of recombinant proteins and the risks of bacterial growth have to be considered. The deposition of the casein micelles over the whole length of chromatographic beds results in a gradual increase in back pressure and mass transfer limitations (Pampel, Boushaba, Udell, Turner, & Titchener-Hooker, 2007; Wilkins & Velander, 1992; C. Zhang & Van Cott, 2007).

1.6.2 Downstream purification of transgenic proteins

A recombinant protein expressed in the milk of Tg animals could be associated to some extent with any of the three phases of the milk system. However, it has been reported that most recombinant proteins produced in milk partition into the aqueous phase and thus downstream purification usually begins with lipid and casein removal (Nikolov & Woodard, 2004; Wilkins & Velander, 1992; C. Zhang & Van Cott, 2007).

Owing to its commercial value, the milk system has been studied extensively by the dairy industry and could be considered the best characterized food protein system. A combination of physical and chemical fractionation techniques have been in use for many years (Fox & Brodkorb, 2008; O'Donnell et al., 2004). However, most of the traditional methods are not suitable for processing of milk containing recombinant proteins that are typically pH and temperature sensitive. For example, isoelectric point precipitation of caseins resulted in loss of 50% of activity and only 25% overall yield in the case of tissue-type plasminogen activator separation from transgenic goat milk (J. Denman et al., 1991). It has been reported also that an overall yield of 2.0 - 2.5% for factor IX was obtained upon using acid removal of caseins from transgenic ewe's milk (Niemann et al., 1999).

Several procedures have been employed successfully in order to clarify milk samples prior to chromatographic processing and high product yields were obtained. It has been reported that more than 90% removal of caseins was achieved by deconstruction of the calcium core of the casein micelle using EDTA, followed by precipitation of caseins using insoluble calcium phosphate nanoparticles (CAP). This approach was claimed to be successful in the liberation of recombinant proteins that could be entrapped within the casein micelles (T. Morcol & Bell, 2001; Tuelin Morcol, He, & Bell, 2001). Other approaches using additives such as arginine (J. S. Denman & Cole, 1995) or increasing the milk ionic strength by adding salt (Nuyens & VanVeen, 1999) have been reported in order to disrupt the interaction between casein micelles and valuable proteins in milk.

1.7 Recombinant human myelin basic protein

The rhMBP used in this study was produced in the milk of transgenic cows as a model for production of biopharmaceutical proteins in farm animals (AgResearch Ltd, Ruakura Research Centre, Hamilton, New Zealand). A line of Tg cows which produce the 17.2 kDa isoform of the human protein as N-terminal His tagged fusion protein in their milk has previously been generated employing nuclear transfer technology as summarized in Appendix I (Brophy et al., 2005).

In this study, milk from these cows was used to develop a downstream purification protocol as well as an analytical testing strategy for the rhMBP.

The main objectives of this study were:

- Development of a simple and reliable procedure that can overcome milk-associated processing problems.

- Generation of a validated battery of analytical testing protocols applicable to recombinant proteins which lack traceable enzymatic activity such as the rhMBP.

- Investigation of the possible effects of expression of the model recombinant protein on the physicochemical characteristics of the milk system.

- Exploration of the effects of the mammary gland expression system on the properties of the recombinant protein.

Finally, this downstream purification protocol will be employed to establish a continuous supply of pure rhMBP to the multiple sclerosis research group at Malaghan Institute of Medical Research (Wellington, New Zealand).

Chapter 2

2 Experimental

2.1 Chemicals and samples

The entire milk collection from consecutive afternoon and morning milking was collected and pooled to form a representative one day milk sample from transgenic cows, either by hormonal induction of the heifers ($TGmilk_h$) or by natural lactation (TGmilk) after the first planned start of calving, and wild type control cows (WTmilk) with, except for the transgene insertions, the same genotype. The milk samples were defatted and freeze-dried for storage. All milk samples used in this study were prepared from milk powder by dissolving suitable amounts in MilliQ water to 10% concentration. Standard brain-derived hMBP (1.0 mg/ml) was purchased from Research Diagnostics (USA) for comparative purposes (cat no. RDI-TRK8M79). The casein standards: α_s-CN, β-CN and κ-CN - cat no. C6780, C6905 and C0406 respectively were purchased from Sigma (USA).

A rat anti-hMBP monoclonal antibody (mAb) (cat no. ab7349) which recognizes amino acids sequence 82 - 87 of hMBP, horse radish peroxidase (HRP)-labeled anti-rat mAb (cat no. A5795) and HRP-labeled anti-His tag mAb (cat no. 15165) were obtained from Abcam (UK), Sigma (USA) and Pierce (USA) respectively and were used for western blotting and dot blotting applications. For the Bio-Plex and Biacore applications, a mouse anti-hMBP mAb (affinity purified – 100.0 μg/ml - cat no. sc-71547) which recognizes the amino acid sequence 130 - 136 of hMBP was purchased from Santa-Cruz Biotechnology (USA). A biotinylated rat anti-mouse (affinity purified – 500.0 μg/ml - cat no. 553388) and a biotinylated anti-His tag mAb (affinity purified – 200.0 μg/ml - cat no. 34440) were purchased from BD Biosciences (USA) and QIAGEN (Germany) respectively.

For the Bio-Plex experiments; N-hydroxysulfosuccinimide (S-NHS), 1-ethyl-3-[3-dimethylaminopropyl]carbodiimide hydrochloride (EDC) and all the buffers used (named as wash buffer, activation buffer, blocking buffer, storage buffer and staining buffer) were part of the Bio-Plex amine coupling kit (Bio-Rad, USA). For the surface plasmon resonance (SPR) experiments, an amine coupling kit containing EDC, N-hydroxysuccinimide (NHS), ethanolamine (EtA) and 4-(2-hydroxyethy)-1-piperazine

ethanesulfonic acid (HEPES)-based buffer; 10 mM HEPES at pH 7.4, 150 mM NaCl, 3 mM EDTA and 0.005% polyoxyethylenesorbitan under a trade name of HEPES-EP were purchased from GE Healthcare (USA).

Two capillary electrophoresis (CE)-grade markers, benzyl alcohol (BA) and orange G (OG) were purchased from MicroSolv, USA and Beckman Coulter, USA respectively. For capillary isoelectric focusing (CIEF) experiments, carrier ampholytes (CA), CIEF Gel and protein standards (ribonuclease A (RN, pI 9.5), carbonic anhydrase II (CS, pI 5.9), β-lactoglobulin A (LG, pI 5.1) and cholecystokinin flanking peptide (CK, pI 3.6)) were obtained as part of the Beckman CIEF kit (Beckman Coulter, USA). Polyethylene oxide (PEO) of different molecular weights (100, 300 and 600 kDa) were obtained from Sigma. The Deep Purple (DP) total protein stain and the ProQ (PQ) Diamond phosphoprotein stain were purchased from GE Healthcare (USA) and Invitrogen (UK) respectively. Nitrocellulose (NC) membranes were obtained from Bio-Rad (USA). Vivaspin centrifugal filters, 500 Da molecular weight cut off (MWCO), were purchased from Vivascience (Germany). All other chemicals were of analytical grade and were obtained from Sigma (USA).

2.2 Instruments

2.2.1 Chromatography

All chromatographic separations were carried out at 4 - 8 ^{o}C using an AKTA Explorer 100 Air controlled by Unicorn 5.11 software (GE Healthcare, Sweden). Hardware and software modifications were carried out in the lab in order to bypass the line of detectors during the sample loading step as shown in Figure 3. These modifications helped avoid fouling of the flow cells of the detectors and obviated the need for extensive clean-in-place (CIP) protocols between runs. Modifications in the software were carried out (in-house) in order to incorporate the bypass function as well as the sequential loading approach in the automated strategies of the Unicorn platform. An offline conductivity monitor was connected to the bypass line in order to monitor the conductivity of the flow-through. The scale of this conductivity monitor was calibrated to the loading buffer conductivity as 0.0% response and the milk conductivity as 100% response.

An electronic module (LabPro Datalogger, Vernier, USA) was used to interface the signal obtained to the PC controlling the AKTA system. The cation exchanger resin Sulfopropyl Sepharose BB (SPBB), empty columns of different column volumes (cv); PD-10, Tricorn 10/100 and XK 16/20 and IMAC prepacked columns; HisGraviTrap – cv 1 ml (Ni^{2+} Sepharose 6 FF) and HisTrap HP – cv 5 ml (Ni^{2+} Sepharose HP) were purchased from GE Healthcare, Sweden.

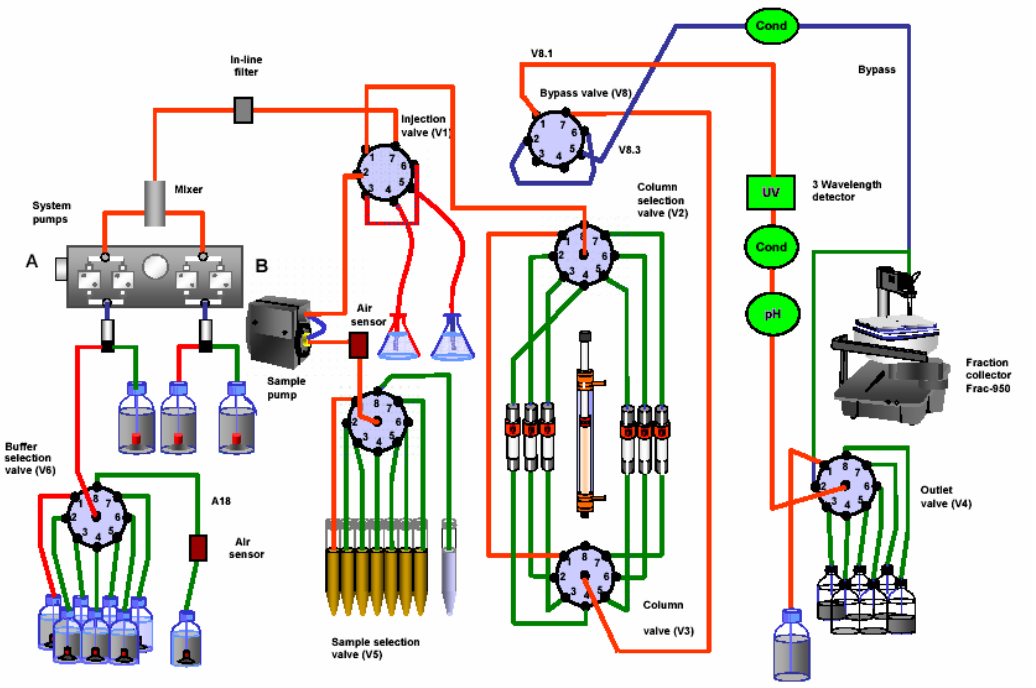

Figure 3: Diagrammatic representation of the modified flow path in the AKTA system: red lines represent the liquid flow path when all valves are at their default positions, green lines represent optional liquid flow paths and blue lines represent the bypass installed to divert the liquid flow away from the system detectors.

2.2.2 Capillary electrophoresis

All CE experiments were carried out at 25 ^{o}C using an Agilent HP^{3D} CE (Agilent Technologies, Germany) controlled by Chemstation software. A diagrammatic representation of the basic components of the instrument is shown in Figure 4. Detection was carried out at 214 and 280 nm using a diode array detector (DAD) which was set to scan a wavelength range of 200 – 600 nm. A special alignment interface, high sensitivity detection cell (HSDC), which increases the detection path length from 75 µm to 1200 µm was purchased from the same manufacturer. Sample plug volume calculations were carried out using the CE Expert software (Beckman Coulter, USA). Coated fused silica (FS) capillaries; eCAP neutral capillaries and ZeroFlow capillaries were purchased from Beckman Coulter, USA and MicroSolv, USA respectively. All bare FS capillaries used, except for those used with the HSDC, were purchased in bulk from Agilent Technologies, Germany and MicroSolv, USA. A capillary cutter (Agilent Technologies, Germany) and a window maker (MicroSolv, USA) were used to prepare all the capillaries employed.

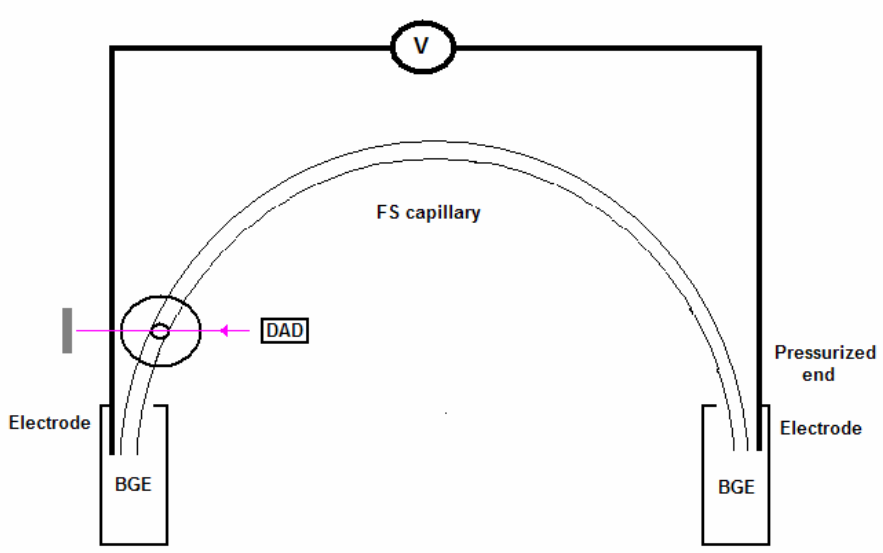

Figure 4: Diagrammatic representation of the basic components of a capillary electrophoresis system with a standard detection window (path length = capillary internal diameter). FS: fused silica, BGE: background electrolyte and DAD: diode array detector.

2.2.3 Bio-Plex suspension array system

The Bio-Plex suspension array system is comprised of a 96-well fluorescent microplate reader, precision fluidics and a dual laser detector with real-time digital signal processing (Figure 5). Sandwich-type assays were performed on the surface of 5.5 µm polystyrene beads which have been color-coded using two fluorescent dyes forming an array of one hundred distinct spectral addresses (Lumenix, USA). The first laser is used to identify the spectral bead address while the second laser determines the quantity of the reporter molecules associated with each antibody matched pair. Since the Bio-Plex system is able to distinguish up to one hundred different types of color-coded beads, up to one hundred different analytes can be assayed in the same sample (Nolan & Mandy, 2006). The system is controlled by Bio-Plex Manager software.

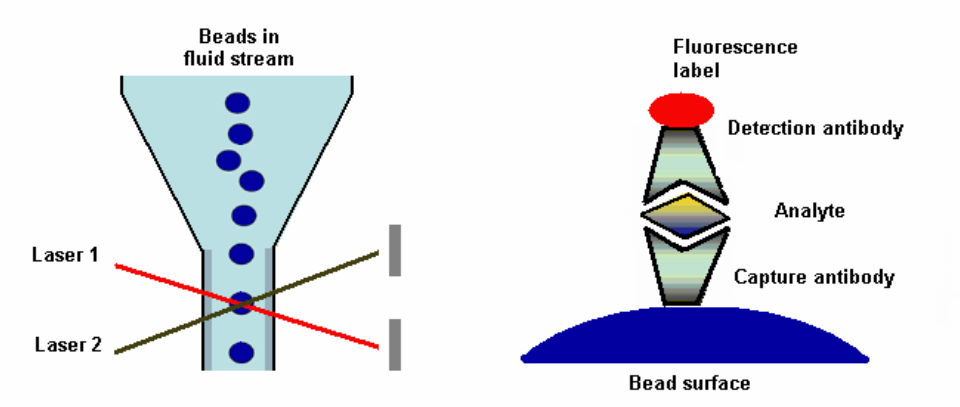

Figure 5: Diagrammatic representation of the precision fluidics and the two-laser beam detector (left) of the Bio-Plex system and a magnified bead surface (right) showing the fluorescent antibody sandwich assembly.

2.2.4 Surface plasmon resonance

Biomolecular interaction experiments using the SPR technology were carried out using a Biacore X100 system (Figure 6). Biacore control software and Biacore evaluation module were used to control the instrument and analyze the data respectively.

All investigations were carried out on the surface of carboxymethyl (CM) dextran, CM5 sensor chips at 25 ^{o}C. The detection principle of the SPR technique involves focusing the polarized light onto a gold sensor surface and the reflected light is monitored. Energy transfer occurs at a critical angle which varies according to the refractive index at the near vicinity of the sensor surface. Thus, as analytes bind to the sensor surface, a change in the mass and hence the refractive index at the surface occurs. By measuring such small changes in real time, the instrument monitors the change in mass as a ligand binds or dissociates from the surface. Data are presented as a sensogram which shows the change in the SPR response (measured in resonance units, RU) with time (Myszka & Rich, 2000; R. L. Rich & Myszka, 2001).

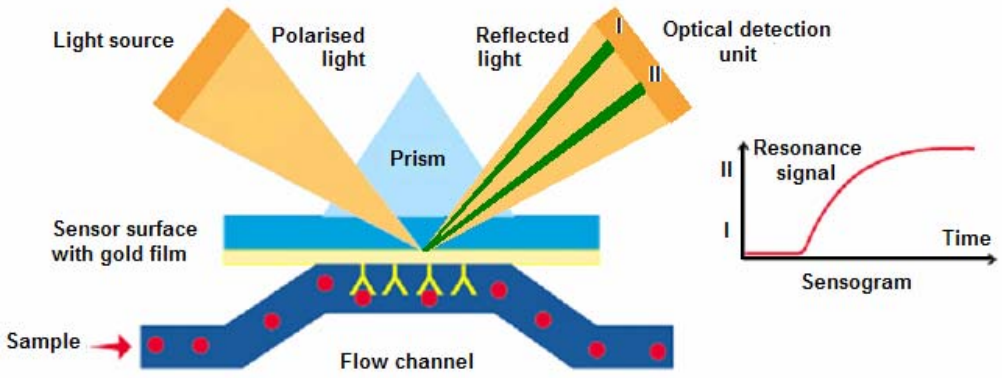

Figure 6: Diagrammatic representation of the detection principle of the surface plasmon resonance technique. I: represents the reflectance angle of light when only a buffer is flowing (baseline) and II: represents the reflectance angle as analytes bind to the sensor surface (binding response). Sensogram: represents the change in response (resonance signal) as analytes bind to / dissociate from the sensor surface in real time.

2.2.5 Diffusing wave spectroscopy

The diffusing wave spectroscopy (DWS) experiments were carried out using a 35 mW He Ne Melles-Griot laser operating at 633 nm. Samples were analyzed in plastic cuvettes of 10 mm width, 50 mm height and 4 mm path length. The transmitted multiply scattered light was collected using a single optical fibre (P1-3223-PC-5, Thorlabs, Germany) and was detected with a photomultiplier tube module (HC120-08, Hamamatsu, Japan) as shown in Figure 7. The auto-correlation functions of the scattered light were obtained using a Malvern 7132 correlator. A more detailed description of the experimental set-up and data analysis has been previously described elsewhere (Hemar & Pinder, 2006; Hemar et al., 2003).

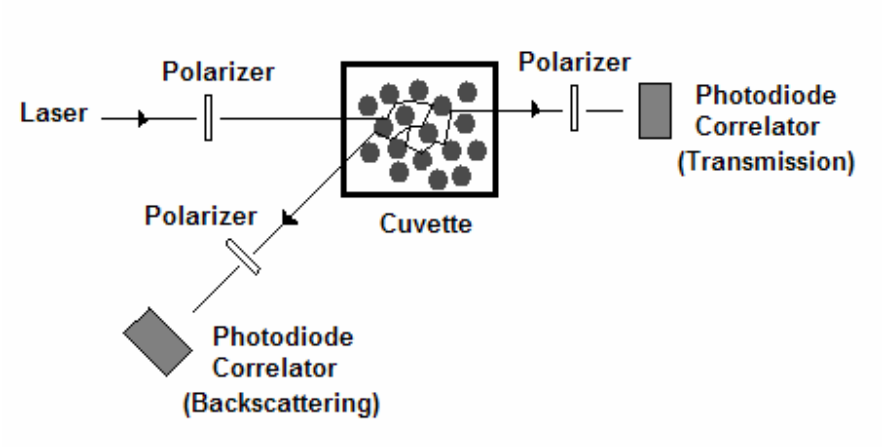

Figure 7: Diagrammatic representation of the basic components of a DWS instrument showing both modes of detection of the emitted laser beam: transmission and backscattering.

2.2.6 Data analysis

Data analysis was carried out using the software integrated with each instrument (as described above) in addition to Minitab and SPSS statistical softwares for experimental design and generation of the calibration curves respectively.

2.3 Methods

2.3.1 Milk fractionation

Two fractionation approaches were trialed in order to locate the recombinant protein in various milk fractions. Isoelectric point precipitation of caseins followed by centrifugation (8000 xg for 10 min) was carried out using (1.0 M) acetic acid to pH 4.6. The supernatant remaining after centrifugation was considered as the whey fraction (WF). The casein fraction (CNF) was prepared by dissolving the pellet in 8.0 M urea. The second fractionation approach was based on the direct pelleting of casein micelles by centrifugation of a milk sample at 8000 xg for 2 h at room temperature (RT). The supernatant was considered as the serum fraction (SF). The pellet obtained was washed twice with MilliQ water then re-suspended in MilliQ water and was considered to contain intact casein micelles (CNM). These protocols were applied to $TGmilk_h$ and WTmilk samples and the obtained fractions were analyzed using reducing sodium dodecylsulfate-polyacrylamide gel electrophoresis (SDS-PAGE) followed by western blotting analysis.

2.3.2 Development of the purification protocol

2.3.2.1 Media screening

A disposable column (PD-10) was packed with 5 ml SPBB resin and used to investigate the usefulness of the direct chromatographic recovery of the rhMBP from milk. A loading buffer of 50 mM HEPES (pH 7.0) was used for column equilibration and washing. Milk samples ($TGmilk_h$ - 10 ml) were loaded onto the column by gravity and elution was carried out using 10 cv of the same buffer in the presence of 1.0 M NaCl. The collected fractions and the supernatant obtained after boiling a sample of the SPBB resin with SDS-PAGE sample buffer were analyzed using SDS-PAGE followed by western blotting analysis. Fractions containing the rhMBP were used to investigate the applicability of the IMAC technique using HisGravi columns (cv 1 ml). A loading buffer of 50 mM HEPES buffer (pH 7.0) containing 0.5 M NaCl and (5 - 50) mM imidazole was used for column equilibration and washing steps. Elution was carried out using the same buffer but

in the presence of 500 mM imidazole. The flow-through fractions and the eluted fractions were analyzed using SDS-PAGE followed by western blotting analysis.

2.3.2.2 Column format

The described modifications to the chromatography system were carried out in order to bypass the line of detectors during the sample loading step and column wash as described above. A Tricorn 10/100 column was packed with 8 ml of SPBB resin and used for optimization of the purification protocol. A loading buffer of 50 mM HEPES (pH 7.0) was used for column equilibration and washing while elution was carried out using a buffer of similar composition but in the presence of 1.0 M NaCl. The TGmilk samples (30 ml) were loaded onto the column using the sample pump at a flow rate of 1.0 ml/min followed by a column washing step (50 mM HEPES pH 7.0 - 6 cv). The flow was diverted through the bypass line to the fraction collector, the flow-through and 3 cv of the washing buffer were collected before returning the flow to the detectors line again. The conductivity of the flow-through was recorded during the sample loading step using an offline conductometer connected to the bypass line. Elution of the retained proteins from the column was then carried out using 50 mM HEPES (pH 7.0) in the presence of 1.0 M NaCl either as a gradient or as a step elution over 10 cv from 0.0 to 1.0 M NaCl. The flow-through fractions and salt-eluted fractions were analyzed using SDS-PAGE followed by western blotting or dot blotting techniques, as required in each experiment.

The fractions containing the rhMBP were pooled together and were further purified using a HisTrap HP column (cv 5 ml). A loading buffer of 50 mM HEPES (pH 7.0) - 0.5 M NaCl - 50 mM imidazole and an elution buffer of the same composition and pH but using 0.5 M imidazole were used. A suitable amount of imidazole was dissolved in the pooled fraction containing the rhMBP up to 50 mM concentration in order to bring the sample composition to the loading buffer composition. Samples were loaded onto the column at 2.5 ml/min followed by 3 cv washing step using the loading buffer. A gradient elution was carried out at 5.0 ml/min over 2 cv followed by 5 cv of the elution buffer. The column effluent was collected in fractions of 2 cv each and fractions containing rhMBP isoforms were pooled together.

2.3.2.3 Factors affecting the dynamic capacity of the cation exchange step

The method described above was used as a template to study various factors affecting the dynamic capacity of the column such as the effects of: i) sample loading flow rate, ii) sample dilution, iii) endogenous milk components and iv) loading the sample in aliquots with a column washing step after each aliquot.

2.3.3 Downstream purification of rhMBP from TGmilk

The optimized method for the direct capture of the rhMBP from TGmilk using the Tricorn 10/100 (cv 8 ml) was scaled-up by a factor of 2.5. A new column (XK 16/20) was packed to 10 cm height (cv 20 ml) and was used for isolation of the rhMBP from TGmilk. A loading buffer of 50 mM HEPES (pH 7.0) was used for column equilibration and washing. Milk samples were loaded at 2.0 ml/min in aliquots of 0.64 cv each followed by 2 cv of loading buffer at 5.0 ml/min. Elution was carried out using the same buffer in the presence of 1.0 M NaCl at 10.0 ml/min in two steps (0.5 M and 1.0 M NaCl – 5 cv each). Column effluent was collected in fractions (2.5 cv each). The fractions containing the rhMBP were pooled together and were further purified using a HisTrap HP column (cv 5 ml) as described above. The collected fractions were analyzed using SDS-PAGE/western blotting. Fractions containing the rhMBP were pooled together and the amount of the rhMBP was estimated using the dot blotting assay.

2.3.4 Stability study

A preliminary qualitative stability study was carried out in order to evaluate the stability of the rhMBP throughout the time and conditions employed for product recovery. The short term stability of the rhMBP in milk, SPBB fractions, IMAC fractions and desalted concentrated fractions (rhMBP stock) was studied over 24 h in order to evaluate the matrix effect on the stability of the rhMBP. TGmilk samples were prepared and processed according to the developed purification protocol. A sample of the pooled IMAC fractions was desalted using 50 mM HEPES (pH 7.0) and concentrated (10x) using Vivaspin centrifugal filters (500 Da MWCO).

The final preparation was considered as “rhMBP stock”. Aliquots of each of the four sample types were incubated at RT, 4 - 8 ^{o}C (purification conditions) and at the specified time (0, 1, 2, 4, 8, 12 and 24 h) aliquots were taken and immediately frozen at - 80 ^{o}C. Samples obtained at t_0 were considered as controls. On the other hand samples incubated for 24 h at room temperature were considered as forced degradation in order to obtain a qualitative estimate for the degradation (if any) for each set of matrix and conditions. Samples were analyzed using SDS-PAGE followed by western detection as previously described.

2.3.5 Preparation of the rhMBP reference standard

An in-house reference standard of the rhMBP was prepared from TGmilk samples. The optimized downstream purification and testing protocols of the rhMBP were applied as described to prepare the reference standard. Sample concentration and buffer exchange to 1.0 mg/ml in 50 mM HEPES (pH 7.0) were carried out at 4 - 8 ^{o}C using Vivaspin centrifugal filters (500 Da MWCO). The identity, purity and integrity of the rhMBP in the final preparation were confirmed using SDS-PAGE followed by western blot detection with anti-hMBP and anti-His tag antibodies. The total amount of rhMBP was determined by dot blot assay using anti-hMBP antibody. The total protein content in the final preparation was determined using a capillary zone electrophoresis (CZE) method as described below. The purity of the final preparation was estimated by comparing the concentration of the rhMBP determined by dot blot to the total protein concentration determined by the CZE method. Short term stability of the rhMBP in the final preparation was studied using western blot analysis as described. The stability over three freeze (- 20 ^{o}C) / thaw (unassisted at RT) cycles over 36 h was evaluated as well. The same procedure was repeated using the WTmilk for preparation of a negative control sample (WTcontrol) equivalent to the in-house rhMBP reference standard. The prepared standard and control samples were stored in aliquots at - 80 ^{o}C and were used for the development and validation of the immunoassays.

2.3.6 Determination of total protein content using CZE

A CZE protocol employing a large volume sample stacking (LVSS) was developed and optimized in order to determine the total protein content in chromatography fractions.

2.3.6.1 Analysis conditions

A background electrolyte (BGE) of 50 mM HEPES (pH 7.0) was used for all electrophoretic runs and sample preparation. All experiments were carried out using bare FS capillaries of 325 µm outer diameter (O.D.), 75 µm internal diameter (I.D), total length of 72 cm and effective length to the detection window of 63.5 cm along with the HSDC. Capillaries were pre-flushed with 0.1 M NaOH, 0.1 M H_3PO_4 for two min each, MilliQ water for five min then 0.1% PEO (100 kDa) in 50 mM HEPES buffer (pH 7.0). Injection was carried out at 50 mbar for 40 s (7.6% of capillary volume and ≈ 9.0% of capillary length to the detection window). Separation was carried out at 25 ^{o}C under negative polarity conditions (-30 kV ≈ -417 V/cm) and detection was carried out at 214 nm with the detection window at the anodic end of the capillary as shown in Figure 8.

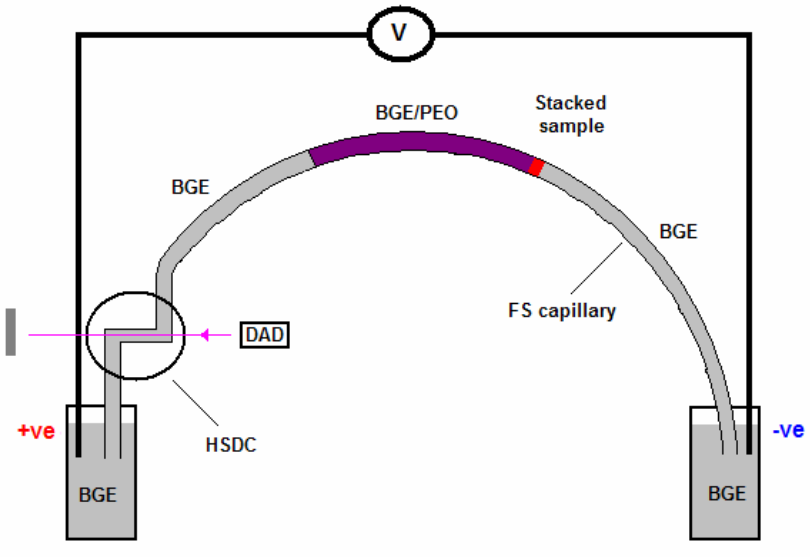

Figure 8: Diagrammatic representation of the experimental setup used in the CZE method showing the large volume stacking principle under negative polarity conditions. FS: fused silica, BGE: background electrolyte, PEO: polyethylene oxide, HSDC: high sensitivity detection cell and DAD: diode array detector.

2.3.6.2 Capillary pre-conditioning

The role of NaOH, H_3PO_4 and water in the regeneration of the FS capillary wall was thoroughly studied while developing the CIEF protocol (see below). In this experiment, the functionality of the dynamic coating polymer was investigated via analysis of a negatively charged marker (4% v/v OG diluted in 50 mM HEPES buffer, pH 7.0 v/v) after preconditioning the capillary with 0.1% PEO in 50 mM HEPES (pH 7.0) as described above. The electrophoregram obtained was compared to that recorded when the capillary was preconditioned with the buffer only. The reproducibility and stability of the dynamic coat was evaluated by analysis of the marker sample over three consecutive runs. The recorded migration times and the current traces over the run time were compared. A similar procedure was followed for the analysis of a denatured BSA sample (1.0 mg/ml) which was prepared by incubation of the protein sample at 95 ^{o}C for five min with 35 mM SDS and 5% v/v β-mercaptoethanol (BME) and analyzed as described above.

2.3.6.3 Effect of SDS concentration

A BSA stock solution (10.0 mg/ml) was prepared in 50 mM HEPES buffer (pH 7.0). Suitable volumes of this stock solution were used to prepare a set of denatured BSA samples (1.0 mg/ml) as described above in the presence of different SDS concentrations (5 - 35 mM). A non-denatured BSA sample was prepared and analyzed under the same conditions for comparative purposes.

2.3.6.4 Stacking conditions

A denatured BSA sample (1.0 mg/ml) was prepared and analyzed as described employing an injection time 10 - 320 s which corresponded to 1.8 - 47.0 % (v/v) of the capillary volume respectively. The electrophoregrams were compared in order to evaluate the efficiency of sample stacking with the injection time / volume.

2.3.6.5 Calibration and validation

A series of BSA standard solutions over a wide concentration range was prepared in the same buffer and analyzed as described above using an injection time of 40 s. Migration time-corrected integrated peak area (PA) for the peaks recorded at 214 nm was plotted vs BSA concentration. Various validation parameters were statistically derived from the calibration curve. The predictability of the calibration curve was evaluated via analysis of a set of BSA standard solutions and the predicted concentrations were compared to the actual ones. The results were compared also to those obtained using the classical Bradford method according to the published protocols (Zor & Selinger, 1996).

2.3.6.6 Effect of salt and application to chromatographic fractions

The effect of the presence of NaCl in chromatography fractions on the stacking efficiency was investigated. A series of BSA standard solutions covering a wide concentration range was prepared in the presence of (0 – 200 mM NaCl). All samples were analyzed using 40 s injection time and the electrophoregrams were compared. For the determination of the total protein content in the chromatographic fractions, samples were either desalted using Vivaspin centrifugal filters (500 Da MWCO) or diluted with 50 mM HEPES buffer (pH 7.0) to salt concentration less than 50 mM before analysis. The protein concentration was then determined from the calibration curve.

2.3.7 Bio-Plex immunoassay

In this assay, a sandwich-type immunoassay on the surface of the fluorescent beads was established, as shown in Figure 9. The mouse anti-hMBP mAb “capture antibody” was covalently immobilized to the surface of one type of the fluorescent beads. The antibody-coupled beads were then incubated with samples containing the antigen “rhMBP”. For the detection of the captured antigen on the surface of the beads, a biotin-conjugated anti-His tag mAb “detection antibody” was employed. The well characterized interaction between the biotin label and the fluorescent marker streptavidin coupled *R*-phycoerythrin (SA-PE) was used to detect the antibody sandwich (Vignali, 2000).

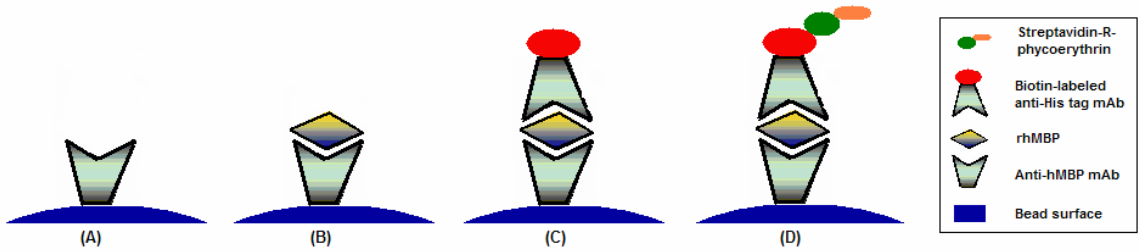

Figure 9: Diagrammatic representation of the steps of the Bio-Plex immunoassay. A: anti-hMBP antibody - coupled beads, B: beads after incubation with samples containing the rhMBP, C: formation of the biotin-labeled antibody sandwich and D: antibody sandwich with the fluorescence label ready for detection by the Bio-Plex system.

2.3.7.1 Coupling of anti-hMBP antibody to the fluorescent beads

Coupling of the anti-hMBP antibody to the surface of the fluorescent polystyrene beads was carried out according to the following in-house optimized protocols based on the manufacturer's guidelines. A buffer exchange step for the antibody preparation was carried out using a phosphate buffered saline - pH 7.4 (PBS) in order to get rid of any amine additives. The final concentration of the antibody was determined by measuring its optical density at 280 nm. Suitable amounts of beads (20 µl ≈ 2.5 x 10^5 beads each) were transferred to three coupling reaction tubes. The beads were obtained by centrifugation and the bead pellet was re-suspended in 80 µl of the activation buffer. Aliquots of 2 µl of 50.0 mg/ml of freshly prepared solution of EDC closely followed by equivalent volumes of freshly prepared S-NHS solution of the same concentration were added to each tube in order to activate the surface of the beads. The bead suspension was incubated for 20 min at RT, away from light under constant rotation (25 rpm).

Activated beads were then washed with 2 x 150 µl PBS (pH 7.4) and then re-suspended in 100 µl PBS. In order to determine the optimal coupling conditions, the coupling reaction was carried out using three different amounts of the anti-rhMBP antibody (1.2, 1.8 and 2.4 µg). Suitable volumes of the antibody preparation equivalent to these amounts were added and the total volume was adjusted to 120 µl with PBS. Beads were then incubated for 2 h under the same conditions. Coupled beads were washed using 500 µl

PBS then incubated with 250 µl of the blocking buffer for 30 min. Beads were then washed with 500 µl of the storage buffer then re-suspended in 50 µl of the same buffer. The concentration of coupled beads in each preparation was determined using a hemocytometer and the efficiency of the surface coverage in each case was evaluated.

2.3.7.2 Validation of the coupling protocol

Aliquots from each bead preparation (≈ 10,000 beads each) were transferred into two sets of microfuge tubes which were labeled as "test" and "control". The biotinylated anti-mouse antibody and the SA-PE solutions were prepared by diluting suitable amounts of each of them with the staining buffer to 2.0 µg/ml. Aliquots of 50 µl of the diluted antibody were transferred to the "test" tubes and equivalent volumes of the staining buffer were transferred to the "control" tubes. All tubes were incubated for 30 min at RT as described above then the supernatant was discarded. Aliquots of 50 µl of the diluted SA-PE were transferred to each of the "test" tubes and equivalent volumes of the staining buffer were transferred to the "control" tubes. All microfuge tubes were incubated for 10 min under the same conditions. The supernatant was then discarded and each of the pellets was re-suspended in 125 µl of the storage buffer then was transferred to a single well of a 96-well microtiter plate. The median fluorescence intensities (MFI) obtained from the "control" and "test" samples for each anti-hMBP antibody amount were then compared to identify the optimal coupling conditions. Coupling of the anti-hMBP antibodies to a larger number of beads was carried out using the optimized protocol. The concentration of the bead stock was determined as described above. Coupled beads were then stored away from light at 4 ^{o}C where they are stable for at least six months.

2.3.7.3 Optimization of the detection step

In order to determine the optimum concentration of the detection antibody, three samples of the rhMBP reference standard over a wide range of concentration were prepared in 50 mM HEPES (pH 7.0). A similar procedure was followed to prepare an equivalent serial dilution of the WTcontrol sample. Aliquots with a volume equivalent to ≈ 10,000 coupled beads were transferred to each well of a 96-well filter plate pre-wetted with the

assay buffer then washed with the same buffer. Aliquots of 50 µl of the prepared test samples and control samples were transferred to the filter plate (in duplicate) and were incubated with the coupled beads for 30 min. Samples were then incubated with different amounts of the biotin-labeled anti-His tag antibody (25 µl of 1:250, 1:500 and 1:1000) for another 30 min. Detection was carried out using the Bio-Plex system after an incubation step with 50 µl SA-PE (1:1000) for 10 min and the optimal dilution factor of the anti-His tag antibody was determined according to the MFI. All incubation steps were carried out at RT, away from light and on the surface of a plate shaker (300 rpm). A washing step was carried out after each incubation step using 3 x 100 µl of the assay buffer. Excess reagents and washing buffers were removed from the filter plate by vacuum filtration. The optimized conditions were used for all subsequent analysis of standard and test samples.

2.3.7.4 Calibration, validation and application of the Bio-Plex method

A serial dilution of the rhMBP standard covering a wide range of concentration was prepared using 50 mM HEPES buffer (pH 7.0) in a 96-well microtiter plate. Blank and WTcontrol samples were included in the same plate. Suitable amounts of the coupled beads were transferred to the desired number of wells of a 96-well filter plate. Aliquots of 50 µl of the prepared samples were transferred from each well of the microtiter plate and added to the corresponding well in the filter plate. Samples were incubated with the coupled beads for 30 min followed by an incubation step with the biotin-labeled anti-His tag antibody (1:1000) for 30 min. The antibody sandwich was detected after another incubation step with the SA-PE system for 10 min. Standard, blank and WTcontrol samples were analyzed in triplicates and the fluorescent signal generated was detected using the Bio-Plex system. A calibration curve was obtained by plotting the MFI vs the rhMBP concentration. The same procedure was used to prepare and analyze all validation samples as well as samples containing unknown concentrations of the rhMBP. The MFI was used to predict the concentration of the rhMBP from the optimized calibration curve. The control and blank samples were included in every plate in order to detect any processing error.

2.3.8 Capillary isoelectric focusing

In this section, a CIEF protocol in dynamically coated capillaries was developed and various conditions affecting the separation efficiency and reproducibility were studied. In CIEF technique, the proteins to be analyzed are mixed with the CA solution, which is by itself a mixture of small molecular weight, zwitterionic compounds having a wide range of pI values that spans the required pH range. Injection is carried out by filling the capillary with this mixture and then an electric field is applied with an acidic buffer at the anode and a cathodic buffer at the cathode. Under these conditions, charged CA and protein molecules migrate through the medium until they reach a region where they become uncharged (at their pI) in a process known as "focusing". Since the CA have small molecular weight, they get focused before the protein molecules forming a pH gradient that stretches over the whole capillary length with the most acidic and most basic ampholytes at the anodic and cathodic ends of the capillary respectively. Mobilization of the focused protein bands past the detector window is then carried out by applying a hydraulic pressure or by addition of salt to one of the BGE solutions (Kilar, 2003; Righetti, 2004; Rodriguez-Diaz, Zhu, & Wehr, 1997).

2.3.8.1 Reference two-step CIEF method

A set of CIEF protein stock solutions: RN (24.0 µg/µl), CS (4.0 µg/µl), LG (4.0 µg/µl) and CK (4.0 µg/µl), a stock of 2% CA / CIEF gel, an anolyte solution (91 mM H_3PO_4 in CIEF gel) and a catholyte solution (20 mM NaOH in water) were prepared as described in the CIEF kit supplier's manual. Aliquots (2 µl) of each protein stock solution were transferred to a CE sample vial containing 100 µl of the 2% CA / CIEF gel and the total volume was adjusted to 110 µl with MilliQ water. The standard mixture was vortexed for 30 s then centrifuged at 8000 xg for 2 min to remove any air bubbles. Analysis was carried out using the coated capillaries obtained from the same supplier: eCAP neutral capillaries, 325 µm O.D., 50 µm I.D, 33 and 24.5 cm total length and effective length respectively. Capillaries were pre-conditioned before each run by flushing with 10 mM H_3PO_4 followed by MilliQ water for 1 min each. Injection was carried out by filling the capillary with the sample using a hydraulic pressure of 950 mbar for two min. Focusing of

protein bands at their pI values was carried out by applying a voltage of 15 kV (455 v/cm) for 6 min. Mobilization of the focused protein bands was accomplished using a hydraulic pressure of 35 mbar, after the focusing step is complete, while the voltage was maintained at 21 kV (636 v/cm) and detection was carried out at 280 nm. Capillaries were post-conditioned after each run by flushing with MilliQ water for 5 min. Figure 10 illustrates the basic experimental setup of the CIEF protocol employed.

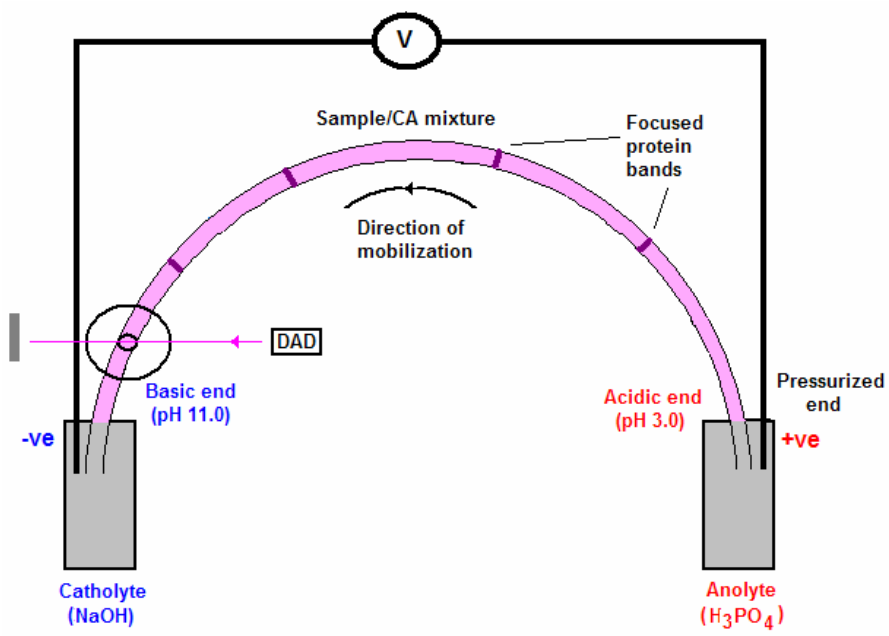

Figure 10: A diagrammatic representation showing the experimental setup employed in the CIEF protocol showing the pH gradient formed along the capillary and the direction of mobilization of the focused protein bands under positive polarity conditions.

2.3.8.2 One-step CIEF in dynamically coated capillaries

All capillaries used in this experiment were bare FS capillaries of exactly the same dimensions as the coated ones described above. New capillaries were flushed with 1.0 M NaOH for 20 min followed by MilliQ water for 10 min before the first run and every morning. Before each run, capillaries were pre-conditioned using 1.0 M NaOH, 0.1 M NaOH and MilliQ water for 5 min each while after each run capillaries were flushed with

MilliQ water for 10 min. A standard protein mixture, anolyte and catholyte solutions were prepared as described above, analysis was carried out using a fixed voltage of 15 kV (455 V/cm) and a hydraulic pressure of 35 mbar applied after 6 min and maintained throughout the run time. Capillaries were post-conditioned after each run by flushing the capillaries with MilliQ water for 5 min. This method was employed to investigate various experimental conditions and to explore the functionality of the BGE additives (CA and PEO polymer)

2.3.8.3 Capillary conditioning

In order to obtain reproducible separations in dynamically coated capillaries, various protocols for conditioning of the surface of the FS capillaries were investigated. The effect of the initial conditioning of the new capillaries (before the first run) and every morning using 1.0 M NaOH followed by MilliQ water (10 min each) compared to 0.1 M NaOH followed by MilliQ for the same time. For surface regeneration before each run, various combinations of base (NaOH), acid (H_3PO_4) and MilliQ water were trialed employing base (0.1 M - 2 min), acid (0.1 M - 2 min) and water for 1 - 10 min. Experiments were carried out in triplicate, the electrophoregrams were compared to those obtained using the one-step CIEF protocol with respect to the ability to resolve the four protein standards, the stability of the current trace and the reproducibility of migration times of the four proteins.

2.3.8.4 Concentration of the anolyte and catholyte solutions

Five combinations of anolyte (H_3PO_4) / catholyte (NaOH) concentrations were studied over a concentration range of 50 - 200 mM H_3PO_4 and 10 - 40 mM NaOH for the anolyte and catholyte respectively in the following order: i) anolyte: 100 mM - catholyte: 10 mM, ii) anolyte: 100 mM - catholyte: 20 mM, iii) anolyte: 50 mM - catholyte: 10 mM, iv) anolyte: 50 mM - catholyte: 20 mM and v) anolyte: 200 mM - catholyte: 40 mM and the electrophoregrams were compared.

2.3.8.5 Functionality of CA

In these experiments, the role of the CA in separations was investigated. Two sets of control samples were prepared and analyzed under the same experimental conditions. The first set was prepared using 2 µl of each of RN, CS and CK in: i) 2% CA in CIEF gel, ii) 2% CA in MilliQ water and iii) 2% MilliQ water in CIEF gel. The second set was prepared without proteins, but using 1 - 3% CA in either MilliQ water or CIEF gel and the electrophoregrams and the current traces were studied.

2.3.8.6 Functionality of PEO polymer

Three stock solutions (0.1, 0.5 and 1%) of each of the 100, 300 and 600 kDa PEO polymers were prepared by dispersing suitable amounts of each polymer in MilliQ water and stirring overnight at room temperature. A set of nine sample matrices (2% CA / polymer solution) was prepared and 100 µl of each sample matrix was transferred into a sample vial. Aliquots of RN and CK (2 µl each) were added to each sample matrix and the total volume was adjusted to 110 µl using MilliQ water. All samples were vortexed for 30 s then centrifuged at 8000 xg for 2 min to remove any air bubbles. This set of standard samples was analyzed employing different voltage values (10 - 20 kV) and hydraulic pressure (0 - 35 mbar).

2.3.8.7 Factorial design analysis

In order to investigate the combined effects of PEO molecular weight (100, 300 and 600 kDa), concentration (0.1, 0.5 and 1.0%) and either voltage (10, 15 and 20 kV) at 35 mbar or pressure (10, 20 and 35 mbar) at 15 kV on method performance, two full factorial design experiments ($3^3 = 27$ runs each) were carried out as shown in Figure 11. Migration times (tm) of two protein standards (RN and CK) and the difference in migration time (Δtm) were used as the response variable in the statistical analysis.

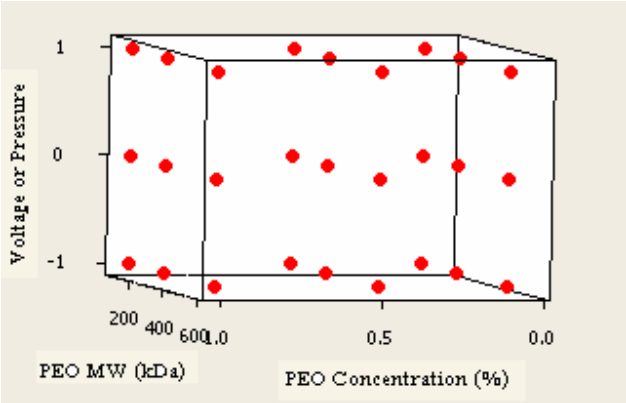

Figure 11: 3D scatter plot of the 3^3 full factorial design experiments showing the experimental conditions investigated (-1, 0 and 1 represent the three levels of either the pressure or the voltage).

2.3.8.8 Determination of the protein isoelectric point

Two sets of validation samples of identical composition (10 samples each) were prepared using the four standard proteins as previously described. Samples of each set were analyzed using the optimized one-step CIEF protocol using two different sets of reagents. The mean migration time of each protein standard in both sets was compared in order to ensure the homogeneity of the experimental error. Results from the two validation sets were then pooled and the mean migration time of each standard protein was calculated. The mean migration times were plotted vs the nominal pI values of the corresponding standard protein and the linear, polynomial and exponential regression models were generated and compared. In order to validate the suggested regression model, results from each set of the validation samples were used to generate a calibration curve and predict the pI values of the standard proteins in the other set.

2.3.8.9 Reproducibility of the migration time and qualitative analysis

FS capillaries from two manufacturers, different sets of BGE and samples were analysed within the same day and over two days to investigate the repeatability and reproducibility of the proposed method respectively.

2.3.8.10 Application to chromatographic samples

The one-step CIEF protocol was used to screen milk samples and chromatographic fractions for the rhMBP. Milk samples (TGmilk and WTmilk) and milk fractions prepared via centrifugation were analyzed after a 10-fold dilution with MilliQ water. Desalted samples of the chromatographic fractions (SPBB and IMAC fractions) obtained as described previously were analyzed in parallel and the results were compared.

2.3.9 Surface plasmon resonance

2.3.9.1 Surface preparation of the immunosensor chip

The anti-hMBP mAb was covalently immobilized to the surface of a CM5 sensor chip. A standard amine coupling protocol was utilized according to the surface preparation wizard in the Biacore control software (Johnsson, Loefaas, & Lindquist, 1991). Briefly, coupling was carried out at 25 ^{o}C using HEPES-EP as the running buffer. The CM-dextran matrix in flow cell-2 (Fc-2) was activated by injection of 100 µl of a freshly prepared mixture of NHS:EDC (1:1 - 10 µl/min). An aliquot of 100 µl anti-hMBP antibody (10.0 µg/ml) in 10 mM acetate buffer – pH 4.5 was injected at 5 µl/min, followed by 70 µl of EtA at 10 µl/min in order to deactivate the residual active sites in the matrix. The surface was then immediately conditioned by injecting three aliquots (15 µl each) of 10 mM glycine HCl buffer, pH 2.5 (30 µl /min) in order to remove non covalently-bound antibodies (typically 10,000 RU were obtained using this protocol). A similar procedure was followed but without the antibody in order to deactivate the CM-dextran matrix in the control flow cell (Fc-1). Signals obtained from Fc-1 were subtracted from those obtained from Fc-2 in order to correct for non-specific binding to the matrix.

2.3.9.2 Optimization of analysis conditions

A standard series of rhMBP was prepared in HEPES-EP buffer in order to evaluate the performance of the sensor chip over a wide concentration range. These preliminary binding assays were carried out using HEPES-EP as the running buffer at flow rate of 10 µl/min. Aliquots of 10 µl of each standard solution were injected at the same flow rate

(binding phase) followed by the running buffer for 200 s (dissociation phase). In order to optimize a surface regeneration strategy for the conditions that were to be employed, a standard solution of the rhMBP standard (10.0 µg/ml) was prepared in 10 mM HEPES buffer – pH 7.4 (HEPES-1) and the same buffer was used as the running buffer (10 µl/min). Three 10 mM glycine-HCl buffers (pH 3.0, 2.5 and 2.0) were prepared and trialled (in triplicate) at the same flow rate for 30 s. The reproducibility of the binding responses as well as the base line values for each buffer was evaluated. In another experiment, a blank sample (HEPES-1), WTcontrol, rhMBP (2.0 µg/ml), hMBP (1.0 µg/ml) samples were analyzed (in triplicate) in order to test the regeneration protocol with the hMBP samples and to investigate matrix interference (if any).

2.3.9.3 Binding experiments

The experimental design employed in this study was based on the covalent immobilization of a "capture molecule" (anti-hMBP mAb) to the surface of the sensor chip. Standard samples containing the "ligand" (rhMBP or hMBP) were then injected. The interaction between the captured "ligand" and different "analytes" (α_s-CN, β-CN and κ-CN) was then investigated in different buffers (Figure 12).

2.3.9.4 Concentration measurements

Two sets of standard solutions of the rhMBP and of the hMBP standards over a wide concentration range were prepared and analyzed using HEPES-1 buffer as described above. Aliquots of 10 µl of each sample were injected at 10 µl/min, allowing a binding time of 60 s and a dissociation time of 120 s. Regeneration of the immunosensor surface was then carried out using 10 mM glycine-HCl (pH 2.0) for 30 s. The obtained responses were plotted vs protein concentration for both ligand molecules (hMBP / rhMBP).

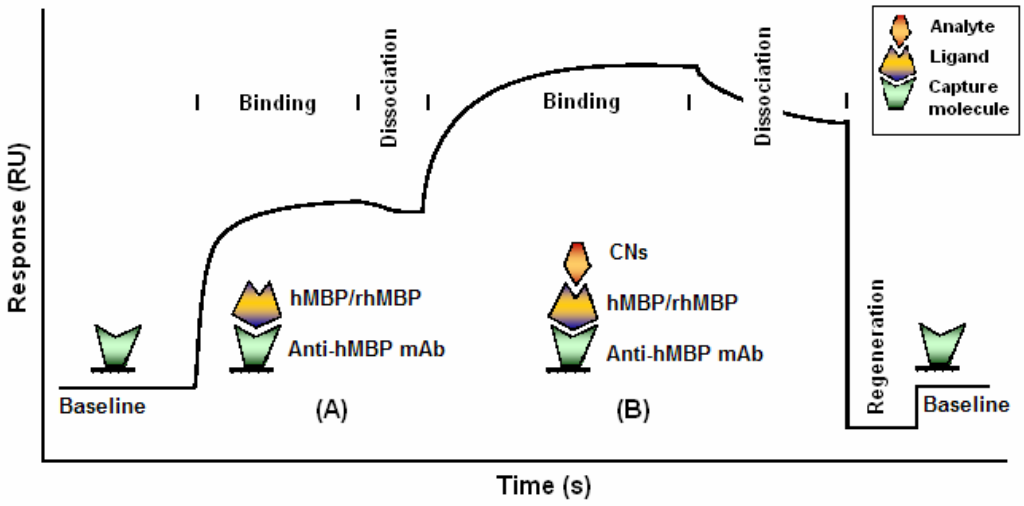

Figure 12: A diagrammatic sensogram showing the experimental set-up employed in the SPR experiments. Baseline: SPR response upon flowing the running buffer on the antibody-coupled sensor surface, (A): SPR response during the binding / dissociation phases upon injection of a ligand molecule (hMBP / rhMBP), (B): SPR response during binding / dissociation phases between the captured ligand and casein molecules.

2.3.9.5 Interaction analysis

Two experiments were carried out to probe the interaction patterns between the analytes (α_s-CN, β-CN and κ-CN) and the ligands (rhMBP or hMBP). In the first experiment, the interaction between all caseins and either the rhMBP or the hMBP was investigated using a set of buffers of different composition (Table 3). Standard solutions of the rhMBP (3.0 ug/ml) and of the hMBP (1.7 ug/ml) were prepared in the HEPES-1 buffer. Stock solutions of α_s-CN, β-CN and κ-CN (1.0 mg/ml each) were prepared in the same buffer and suitable volumes were diluted into the required buffer: HEPES-1, HEPES-2 (150 mM NaCl), HEPES-3 (10 mM $CaCl_2$) and HEPES-4 (150 mM NaCl and 10 mM $CaCl_2$) as described in Table 3 to final concentration of 50.0 ug/ml. Aliquots of 10 µl of either the rhMBP or the hMBP standards were injected followed by 20 µl of casein solutions at the same flow rate. A dissociation time of 300 s was allowed before surface regeneration was carried out as described above.

Table 3: The salt concentration in the buffers employed for studying the interaction between hMBP / rhMBP and caseins using the SPR technique. All buffers were prepared using 10 mM HEPES (pH 7.4).

	NaCl (75 – 300 mM) *	$CaCl_2$ (5 – 20 mM) *
HEPES-1	-	-
HEPES-2	+	-
HEPES-3	-	+
HEPES-4	+	+

* **The exact concentrations are as described in each experiment below.**

In the second experiment, the interaction between rhMBP and α_s-CN was investigated in further detail using the same experimental set-up except for the analyte buffer composition. A set of α_s-CN solutions was prepared in HEPES-1, HEPES-2 in the presence of 75, 150 and 300 mM NaCl, HEPES-3 in the presence of 5, 10 and 20 mM $CaCl_2$ and HEPES-4 containing 10 mM $CaCl_2$ and 75, 150 and 300 mM NaCl. All samples were analysed under the same experimental conditions and the obtained binding responses were studied in order to investigate the effect of buffer additives on the interaction between the rhMBP and α_s-CN.

2.3.10 Diffusing wave spectroscopy

Milk samples were prepared and analyzed at 25 ^{o}C. Tests were carried out for 3 min to ensure low noise intensity autocorrelation functions ($g_l(t)$) which were obtained experimentally by:

$$g_1(t) \equiv \frac{1}{\beta}\left(\frac{\langle I(t)I(0)\rangle}{\langle I\rangle^2} - 1 \right)^{1/2} \qquad (1)$$

where β is a constant characteristic of the optics, and $I(0)$ and $I(t)$ are the intensities of the detected light at time zero and t respectively. In cases where substantial multiple scattering

occurred between entering the sample and arriving at the detector, the light path can be considered as a random walk and the calculation of the autocorrelation function can be performed from the solution to a well-known diffusion problem:

$$g_1(t) = \frac{\frac{L/l^* + 4/3}{z_0/l^* + 2/3}\left\{\sinh\left[\frac{z_0}{l^*}\sqrt{k_0^2\langle\Delta r^2(\tau)\rangle}\right] + \frac{2}{3}\sqrt{k_0^2\langle\Delta r^2(\tau)\rangle}\cosh\left[\frac{z_0}{l^*}\sqrt{k_0^2\langle\Delta r^2(\tau)\rangle}\right]\right\}}{\left(1 + \frac{8t}{3\tau}\right)\sinh\left[\frac{L}{l^*}\sqrt{k_0^2\langle\Delta r^2(\tau)\rangle}\right] + \frac{4}{3}\sqrt{k_0^2\langle\Delta r^2(\tau)\rangle}\cosh\left[\frac{L}{l^*}\sqrt{k_0^2\langle\Delta r^2(\tau)\rangle}\right]} \quad (2)$$

where L (thickness of the sample) >> l^* (photon transport mean free path length; the length scale over which the direction of light is randomized), z_0 the penetration depth (considered equal to l^* in these experiments), $k_o = 2\pi n/\lambda$, the wave vector of the light and $\langle r^2(\tau)\rangle$ is the mean square displacement (MSD) of the particle.

The value of l^* is obtained by performing transmission measurements using latex beads in a water sample (a model colloid suspension with known l^*) as previously described in more detail (M. Alexander, Rojas-Ochoa, Leser, & Schurtenberger, 2002). The inversion of equation 2 can now be carried out with a zero-crossing routine; that is, for each time an experimental g1 is measured, the corresponding value of the MSD required for the theoretical expression to match that value can be found. The crux of the technique is that even though light traversing the sample is multiply scattered, the MSD of the scatterers (the CN micelles) with time can still be obtained. For the initial milk systems, assuming the viscosity of the medium, the measured MSD allows the direct extraction of the micelle sizes (Marcela Alexander & Dalgleish, 2004). Milk samples were analyzed in triplicate as described and the average micelle size of each milk type (TGmilk and WTmilk) was extracted and compared.

In order to compare the acid-gelation behaviour of the TGmilk to that of the WTmilk, samples were prepared in the presence of 0.02% sodium azide as a preservative. Acidification of the milks was achieved by addition of 2.3% glucono-δ-lactone (GDL). The correlation function was recorded for three min every five min, while monitoring the gradual drop in pH, over 4 h. With l^* known, the MSD versus time lag can be obtained by

inverting equation 2 with a zero-crossing routine as described above. However, in this case the slope of the double logarithmic MSD versus lag time plot at high frequency (10^3 - 10^6 Hz) was studied during the acidification process (MSD slope vs pH) as a tool to follow the kinetics of the gel formation as previously described in detail (Donato, Alexander, & Dalgleish, 2007).

2.3.11 Gel electrophoresis and immunoblotting

The 15% SDS-PAGE with Comassie Blue (CB) detection was carried out according to the method of Laemmli (Laemmli, 1970). The protocols for gel staining employing DP and PQ were carried out as described by the manufacturers. Immunodetection was carried out on the surface of NC membranes (0.2 µm) using either rat anti-hMBP mAb followed by a secondary HRP-coupled anti-rat mAb or HRP-coupled anti-His tag mAb. Chemiluminescence detection of the HRP-coupled antibodies was carried out according to published protocols (Leong & Fox, 1990). Optimization of electro-blotting and development protocols was carried out in-house (Brophy et al., 2005). Anti-hMBP mAb was used in all immunodetection experiments unless otherwise specified. A semi-quantitative immunoassay was developed using dot blotting analysis in order to estimate the concentration of rhMBP in chromatography fractions. A serial dilution of each test sample was compared to an equivalent serial dilution of the hMBP standard. Comparisons were carried out by blotting 1 µl of each solution on the surface of a NC membrane. Detection was carried out in a similar way to the membranes obtained by electro-blotting. The signal intensity which was obtained from the rhMBP samples was compared to that obtained from the standard hMBP in order to determine the rhMBP concentration relative to that of hMBP concentration and to the lowest detectable concentration in the hMBP standard series. A Bio-Rad gel imaging system (USA) and a Fujifilm intelligent dark box (Japan) were used for documentation of stained gels and NC membranes respectively.

Chapter 3

3 Downstream Purification of Recombinant Human Myelin Basic Protein

3.1 Background

A line of transgenic cows which produces the rhMBP in their milk has previously been generated and milk obtained by the hormonal induction in the heifers was investigated. Initial western blotting analysis of the $TGmilk_h$ samples using an anti-hMBP mAb confirmed the expression of the rhMBP and revealed that it was exclusively associated with the skimmed milk (Brophy et al., 2005). Therefore, all subsequent investigations were carried out using skimmed milk samples. The rhMBP was detected as one major isoform and several minor isoforms using either anti-hMBP or anti-His tag antibodies. The apparent molecular weight of the rhMBP major isoform was estimated from SDS-PAGE / western blotting analysis to be ≈ 21 kDa. This value was in agreement to the calculated value (21.04 kDa) which was predicted from the rhMBP amino acid sequence (Appendix I) as previously described (Bjellqvist et al., 1993). The dot blotting assay employing an anti-hMBP mAb showed an expression level of 2 - 3 mg/ml in $TGmilk_h$ (Brophy et al., 2005).

At first, various approaches were trialed in order to reduce the complexity of the $TGmilk_h$ samples prior to the purification of the rhMBP. Isoelectric point precipitation of caseins, disruption of the casein micelles via inclusion of additives such as urea and arginine and selective precipitation of caseins using CAP were investigated. The use of isoelectric point precipitation of caseins or denaturants resulted in a poorly soluble product in the final preparation. The use of CAP was found to be more successful than these more aggressive micelle disruption procedures with respect to the solubility of the rhMBP in the final preparation. However, the rhMBP was detected along with the precipitated caseins which explained the low yields obtained (Appendix I) (Brophy et al., 2005). In this study, skim milk from these animals was used to develop a simple, reliable and automated downstream purification strategy for the isolation of the rhMBP from milk. In order to design a strategy that overcomes the problems encountered previously, a systematic study of the starting material was conducted.

3.2 Understanding the starting material

In this experiment, the localization of the rhMBP in the transgenic milk system was investigated in more detail. Two milk fractionation procedures were trialed as described in Chapter 2 (2.3.1). Isoelectric point precipitation was employed as an example for milk fractionation via micelle disruption while centrifugation was considered as a good method to fractionate milk without disruption of the micelles. In the latter case, the possibility of entrapment of serum milk proteins with the micelle fraction was minimal (Fox, 2003).

The resulting fractions were analyzed using SDS-PAGE and western blotting techniques. The CB stained gels showed no difference between $TGmilk_h$ and WTmilk samples (Figure 13). The recombinant protein was detected by western blotting technique in CNF and CNM, traces were found in SF and no rhMBP was detected in WF (Figure 13).

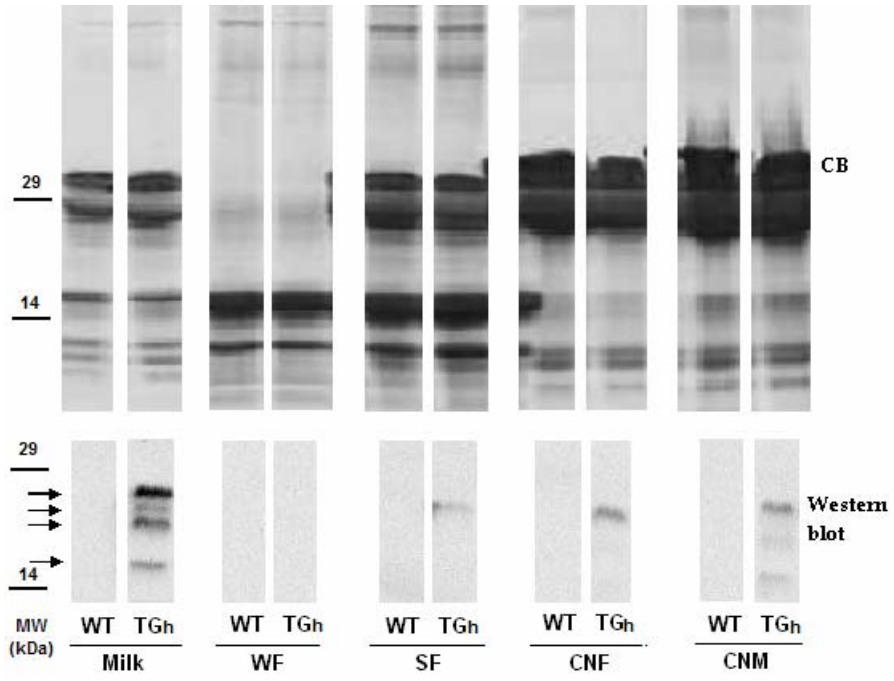

Figure 13: CB-stained gels (top) and western blots using anti-hMBP mAb (bottom) of WTmilk, of $TGmilk_h$ samples and fractions obtained from each type of milk upon centrifugation and isoelectric point precipitation of caseins. WF, whey fraction; SF, serum fraction; CNF, casein fraction and CNM, casein micelle fraction.

These results were clear evidence for the association of the rhMBP with the casein micellar phase. The faint response for rhMBP which was detected in the SF could be attributed to the rhMBP associated with small casein micelles which remained in solution at the centrifugation speed employed. Acid disruption of the casein micelles resulted in complete precipitation of the rhMBP in the casein pellet. A large excess of urea was necessary to disrupt the CNF and dissolve the rhMBP.

3.3 Design of the purification strategy

3.3.1 Direct capture of rhMBP from milk

The chromatographic recovery of recombinant proteins from crude feed stock is a known concept and a few examples have been reported in the literature (Thoemmes et al., 2001; Wlad, Ballagi, Bouakaz, Gu, & Janson, 2001). The applicability of the direct capture of endogenous milk basic proteins using cation exchanger resins has been reported also (J. S. Denman & Cole, 1995; Fee & Chand, 2006; Nuyens & VanVeen, 1999). However, this technique seems not to have been used for downstream purification of recombinant proteins expressed in milk. Clarification of milk samples prior to chromatographic processing has been a standard treatment as discussed in Chapter 1.

The isoelectric point of the rhMBP was calculated employing its amino acid sequence (Appendix I) and was found to be pI 10.5 (Bjellqvist et al., 1993). Based on this value, it could be expected that the recombinant protein will carry a net positive charge at the pH of milk (≈ pH 6.7). Cation exchange chromatography using SPBB could then be an ideal approach for the capture of the recombinant protein from milk. Taking into consideration that milk contains minute amounts of endogenous basic proteins (when compared to the total amounts of proteins in milk), a high purification factor could be expected upon using cation exchange chromatography.

The zwitterionic organic buffer (HEPES) was selected for testing the usefulness of SPBB for isolation of the rhMBP from TGmilk. It has a buffering region (pH 6.8 - 8.2) which spans that of milk and lacks interaction with calcium. Therefore the HEPES buffer

was expected to have a minimal effect on casein micelle integrity. Moreover, the low conductivity properties of HEPES made it an ideal choice for the screening of biological samples using electrophoretic techniques without extensive sample pre-treatment (Good et al., 1966; Hautala, Wiedmer, & Riekkola, 2005; Wiedmer, Jussila, Hakala, Pystynen, & Riekkola, 2005).

Preliminary experiments employing $TGmilk_h$ loaded directly onto a small disposable column (PD 10 - cv 5 ml) confirmed the excellent retention of the rhMBP on the SPBB resin and showed that elution with 1.0 M NaCl was sufficient to elute any specifically or non-specifically bound proteins from the column. These results indicated that the reported CIP protocols that were employed for the isolation of endogenous milk basic proteins (Fee & Chand, 2006) were applicable in the case of rhMBP. Once the TGmilk became available, modifications to the chromatographic system were carried out. A post-column bypass line was installed as described in Chapter 2 (2.2.1) in order to avoid problems associated with milk flowing through the flow cells of the detectors. Modifications of the built-in strategies of the Unicorn platform were carried out in order to maintain the automated capabilities of the chromatographic system.

A small column (Tricorn 10/100 – cv 8 ml) was packed with SPBB resin according to the manufacturer's guidelines. Milk samples were loaded directly to the column and elution was carried out using a linearly increasing NaCl concentration (0.0 - 1.0 M). The rhMBP was detected in fractions obtained over salt concentrations ranging from 0.15 M to 0.45 M using western blotting analysis. These results were in agreement with those obtained previously employing $TGmilk_h$ (Appendix I and II) showing that a linear gradient was unable to resolve the rhMBP from other endogenous milk proteins eluting below 0.5 M salt. A step elution was considered in order to obtain the rhMBP isoforms in one fraction. Direct capture of the rhMBP from TGmilk was carried out using two steps of the elution buffer containing 0.5 and 1.0 M NaCl (5 cv each) as shown in Figure 14-A. The collected fractions were analyzed using SDS-PAGE and western blotting analysis (Figure 14-B). No difference was noted in the CB-stained gels; however, multiple isoforms of the rhMBP of different apparent molecular weights were detected in 0.5 M salt fractions. The 1.0 M

fractions were found to contain LF which is one of the endogenous milk basic proteins, as will be discussed in more detail below.

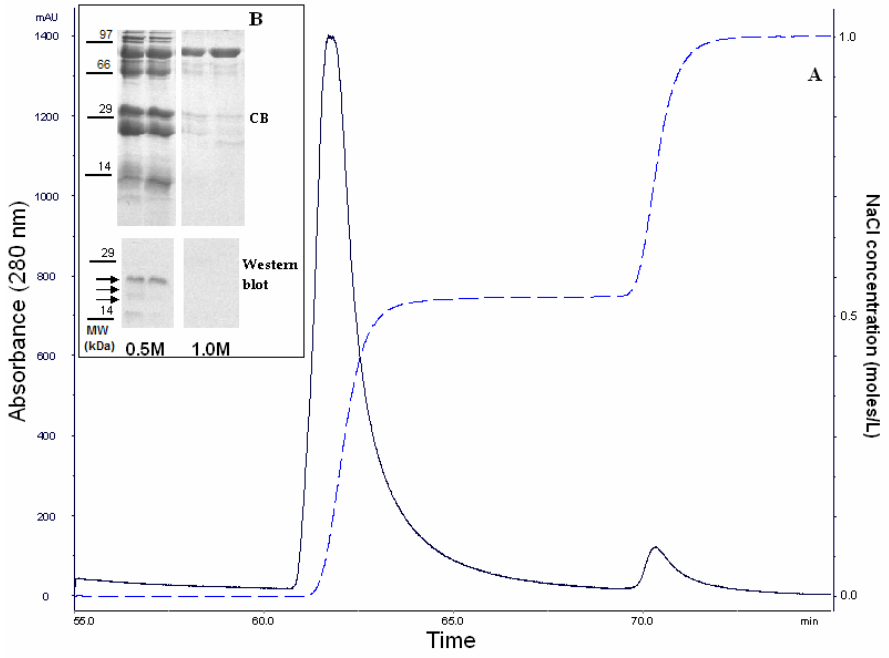

Figure 14: (A): Chromatogram showing the elution pattern of milk basic proteins from the cation exchanger column using a two-step elution (0.5 and 1.0 M NaCl). Solid line: UV trace at 280 nm (mAU) and dashed line: NaCl concentration in (M). (B): CB-stained gels (top) and western blots (bottom) of the fractions collected from the column at 0.5 and 1.0 M steps showing the elution of the rhMBP as multiple isoforms at 0.5 M NaCl. Column: Tricorn 10/100 – cv 8 ml, sample: 30 ml TGmilk loaded at 1.0 ml/min, elution flow rate: 5.0 ml/min, loading buffer: 50 mM HEPES (pH 7.0) and elution buffer: 50 mM HEPES (pH 7.0) - 1.0 M NaCl.

Contrary to what was expected from a highly basic protein with no ordered structure such as hMBP, the recombinant protein was found to elute from the cation exchanger resin at low salt concentration (< 0.5 M). The presence of multiple isoforms, eluting from the column over a wide salt concentration range (0.15 - 0.45 M) suggested that the rhMBP isoforms had different affinities to the cation exchanger resin. These isoforms are most likely rhMBP post-translationally modified to different degrees. A similar banding pattern was detected when the anti-His tag mAb was used in western blotting detection which

indicated that the smaller molecular weight bands were not due to proteolysis (Appendix I). Investigation of the nature of these isoforms will be discussed in detail in Chapters 5 - 6.

3.3.2 Affinity purification of rhMBP

Taking advantage of the N-terminal His tag of the rhMBP, the IMAC technique using Ni^{2+} Sepharose resins was employed for further purification. This method has the additional advantage that it does not add any animal-derived impurities to the final protein preparation such as antibody-based affinity chromatography techniques would. Again, a preliminary study using HisGravi columns (cv 1 ml) and $TGmilk_h$ was carried out to optimize the IMAC step using the pooled SPBB fractions containing the rhMBP as described above. A loading buffer of 50 mM HEPES buffer (pH 7.0) containing 0.5 M NaCl and 50 mM imidazole was found to provide good rhMBP retention and to minimize the non-specific binding of milk proteins whereas the increase of the imidazole concentration to 0.5 M resulted in the complete elution of the bound rhMBP.

A HisTrap HP column (cv 5 ml) was used in order to develop a column format purification step employing TGmilk samples. Fractions collected from the optimized cation exchange step (as described below) were adjusted to the loading buffer specification by adding imidazole to a final concentration of 50 mM. A gradient elution over 10 cv (50 - 500 mM imidazole) was employed and the rhMBP was detected in fractions collected at ≈ 0.4 - 0.5 M imidazole. A sharp gradient elution over 2 cv followed by 5 cv of elution buffer was used in order to obtain the rhMBP in concentrated fractions. The IMAC purification step resulted in elution of the recombinant product in high purity as shown from the CB-stained gels in (Figure 15). It resulted also in enrichment of the minor isoforms of the recombinant protein in one fraction as shown by the western blotting detection in Figure 15.

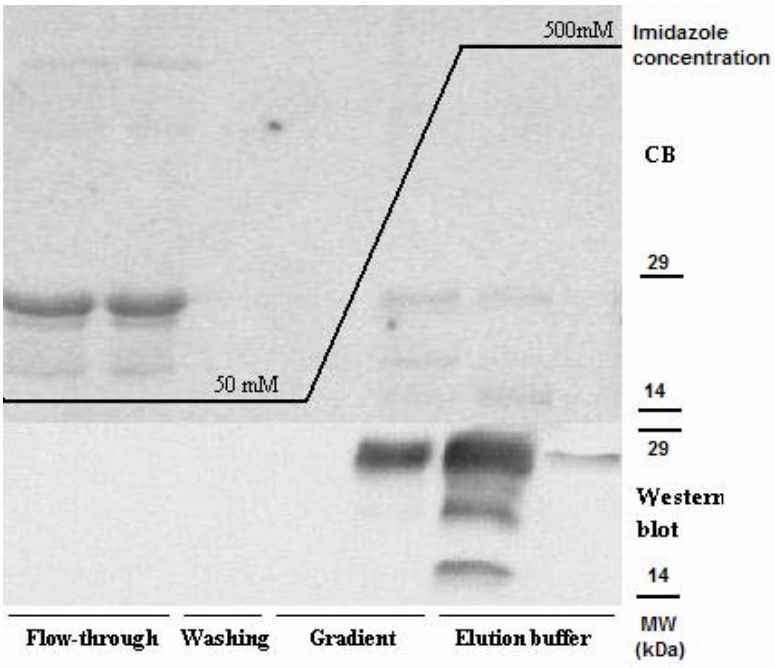

Figure 15: Fractions collected from an IMAC run analyzed by SDS-PAGE (top) and western blotting using anti-hMBP mAb (bottom) showing the elution pattern of rhMBP with varying imidazole concentrations. A diagram representing the imidazole concentration is overlaid. Column: HisTrap HP – cv 5 ml, sample: 50 ml pooled SPBB fractions loaded at 2.5 ml/min, elution flow rate: 5.0 ml/min, loading buffer: 50 mM HEPES - 0.5 M NaCl - 50 mM imidazole (pH 7.0) and elution buffer: 50 mM HEPES - 0.5 M NaCl - 500 mM imidazole (pH 7.0).

3.3.3 Short term stability of rhMBP

Several proteolytic enzymes are present in milk and proteolysis has been a key event that determines the textural characteristics of milk products in dairy industry. In order to obtain high yields of a recombinant protein expressed in milk, chances for proteolysis should be minimized (Fox & Brodkorb, 2008; Wilkins & Velander, 1992). In this study, a two-step purification protocol for downstream purification of rhMBP from milk is described. The stability of the product was studied throughout the time taken and the conditions employed before investing in optimization and scale-up of the downstream purification protocol. The short term stability of the rhMBP in milk, SPBB fractions, IMAC

fractions and rhMBP stock was studied over 24 h as described in Chapter 2 (2.3.4). Unexpectedly, the rhMBP was found to be highly stable in milk samples even at room temperature (Figure 16). In contrast, the rhMBP was no longer detectable in SPBB fractions following 24 h incubation at room temperature indicating complete degradation under such conditions. The rhMBP showed good stability in IMAC fractions. However, the rhMBP stock showed prominent degradation at room temperature within 12 h and partial degradation at 4 - 8 ^{o}C.

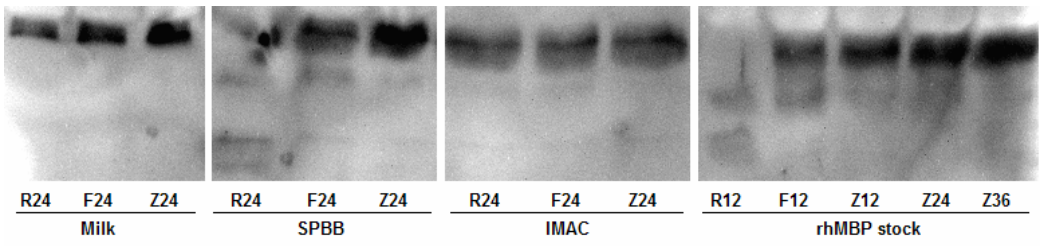

Figure 16: Western blotting analysis using anti-hMBP mAb of TGmilk samples and chromatography fractions incubated at different conditions. R: room temperature, F: 4 - 8 ^{o}C and Z: - 80 ^{o}C for different periods of time (12, 24 or 36 h).

These results were of extreme value since the milk sample is the one required to withstand the animal's body temperature as well as the early in-farm processing steps. The noted stability of the rhMBP in milk even at room temperature could be explained on the basis of the association of the recombinant protein with the micellar phase as discussed above. The relative instability of the rhMBP in the SPBB fractions when compared to the IMAC fractions (Figure 16) had a direct impact on the downstream purification strategy. Fractions obtained from SPBB have to be either processed to the next step as soon as they were collected or stored frozen until the next step. A possible explanation for the instability of rhMBP in SPBB fractions could be attributed to the non-specific retention of some of the proteolytic enzymes on the SPBB resin. In this experiment, preparation of the rhMBP stock was carried out at RT as described. In order to minimize any chances for degradation during these steps, the use of a refrigerated centrifuge was recommended for future

applications. The good stability of the rhMBP stock at 4 - 8 ^{o}C and - 80 ^{o}C was crucial for the product analysis steps.

In this stability study, western blotting analysis was used successfully to investigate the stability of the rhMBP in milk fractions throughout the conditions encountered during its purification. However, to obtain a quantitative evaluation of the stability of the rhMBP, a more reliable analytical technique which is capable of tracing minor changes in intact rhMBP amounts had to be employed. The development and optimization of such a testing protocol for the rhMBP will be discussed in detail in Chapter 4.

3.4 Optimization of the direct capture of rhMBP from milk

3.4.1 Premature breakthrough

The downstream purification protocol was considered successful with respect to the following: direct capture of intact rhMBP from milk with no denaturing additives, good purity and solubility of the product in the final preparation, and the ability to monitor the rhMBP throughout the purification steps. However, when milk samples were loaded onto the cation exchanger column, a premature breakthrough of rhMBP was noted in the flow-through fractions. Association of the rhMBP with milk caseins was suggested after studying the results obtained by centrifugation and isoelectric point precipitation of TGmilk samples. The relative stability of rhMBP in TGmilk samples supported this hypothesis. The amount of the rhMBP retained on the SPBB column, from the same volume of milk, was found to improve upon reducing the sample loading flow rate which indicated slow kinetics which controls the release of the rhMBP into serum. Investigation of the type of the molecular interaction between the rhMBP and other milk proteins was beyond the scope of this study but will be discussed in detail in Chapter 6.

3.4.2 Effect of endogenous milk basic proteins

The elution pattern of the rhMBP showed that it does not bind strongly to the resin as discussed earlier. The weak binding of the rhMBP to the resin could also contribute to the early breakthrough noted since milk contains other endogenous basic proteins which

compete with the rhMBP for the binding sites. Lactoferrin is one of the endogenous milk basic proteins which has a molecular weight of 77 kDa (Fox & Brodkorb, 2008). The direct capture of LF from milk has been previously reported employing SPBB, and LF was found to elute from the resin in a pure form at salt strength 0.9 - 1.0 M NaCl (Fee & Chand, 2006). While developing the cation exchange chromatography step, LF was detected in the 1.0 M fraction using SDS-PAGE by its molecular weight (Figure 14-B) and was considered as a marker for a strongly bound endogenous basic milk protein. In this experiment, the integrated peak area was employed as an estimate of the total amount of basic protein retained by the column and eluting with 0.5 and 1.0 M NaCl. A two fold increase in the volume of loaded TGmilk sample to the cation exchanger column (under the same experimental conditions) resulted in increase in integrated peak areas of 82% and 255% for 0.5 and 1.0 M fractions respectively (Figure 17-A).

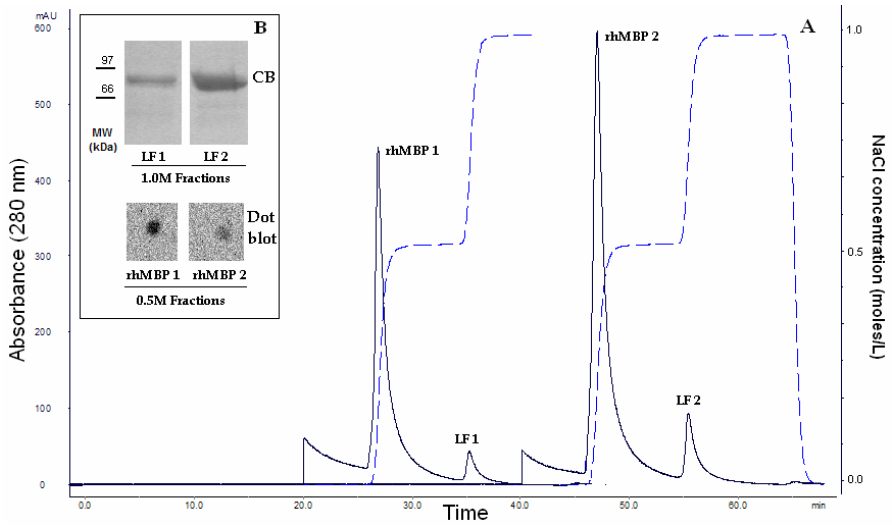

Figure 17: (A): Chromatograms showing the relative increase in peak height and peak area upon increasing the volume of milk sample loaded to the cation exchanger column from 10 to 20 ml. Solid line: UV trace at 280 nm (mAU) and dashed line: NaCl concentration in (M). (B): CB-stained gel (top) showing the increase in intensity of the LF band and dot blots using anti-hMBP mAb (bottom) showing the decrease in intensity of the rhMBP bands upon increasing the volume of milk loaded to the cation exchanger column. Column: Tricorn 10/100 – cv 8 ml, sample: 10 and 20 ml TGmilk loaded at 1.0 ml/min, elution flow rate: 5.0 ml/min, loading buffer: 50 mM HEPES (pH 7.0) and elution buffer: 50 mM HEPES (pH 7.0) - 1.0 M NaCl.

The band corresponding to LF in the latter case (CB-stained gel) was found to be more intense while that corresponding to the rhMBP (dot blotting) was found to be less intense upon increasing the milk volume loaded (Figure 17-B). These results indicated that LF has a higher affinity for the cation exchanger resin than rhMBP and thus the amount retained of LF was enriched on the expense of the weakly bound rhMBP. The competition between the rhMBP and endogenous milk basic proteins for the active sites of the resin did not favor rhMBP retention.

3.4.3 Effect of milk calcium

In a systematic study for evaluation of the influence of major components in milk on the chromatographic recovery of a target protein from milk, the effect of calcium was found to be significant. Milk calcium was found to compete for the adsorption sites of the resin leading to a significant reduction in the number of adsorption sites available for selective binding of milk basic proteins. The effect of calcium was found to be of higher significance than that of either casein micelles or lipid (Pampel et al., 2007). Milk contains approximately 30 mM of calcium with about 68% of it associated with caseins. Micellar calcium plays a key role in the maintenance of the structure and stability of casein micelles and it has been reported that it is in equilibrium with the soluble calcium fraction (Cross, Huq, Palamara, Perich, & Reynolds, 2005; Gaucheron, 2005).

The effect of reducing the milk sample ionic strength by dilution with MilliQ water on the retention behavior of rhMBP was studied. A four-fold dilution with water was found sufficient to bring the conductivity of the milk samples close to that of the loading buffer. The amounts of rhMBP retained on the column were determined using the developed dot blot assay for rhMBP. Dilution resulted in an increase in the amount of rhMBP that was retained on the column. However, the effect of dilution was found comparable to reducing the sample loading flow rate to the extent that kept the residence time of a sample in the column constant. It could be concluded from these results that the early breakthrough is mainly due to association of the rhMBP with the casein micelles. Alkaline earth metals in

milk reduce the dynamic capacity of the cation exchanger column as discussed above. Under such reduced capacity, increasing the milk volume loaded resulted in enrichment of the more strongly bound milk proteins over the weakly bound ones including the rhMBP. The effects of either reducing the sample loading flow rate or reducing the sample ionic strength are comparable. However, dilution does not release the rhMBP from the micelles and reducing the sample flow rate does not help reduce the effect of milk calcium. It could be suggested also that in order to enhance the recovery of the rhMBP from milk samples, gentle disruption of the casein micelles and reducing the effect of calcium in milk in a more efficient way than dilution, are the key parameters.

3.4.4 On-line casein micelle disruption

While developing this capture protocol using the PD-10 disposable columns, it was noted that the first few flow-through fractions always had an unusually transparent appearance. The total volume of these fractions was found to be larger than the void volume of the column. Casein micelle disruption during the loading step was then considered to be the main reason for the transparent flow-through. Additional investigations were carried out in order to evaluate the significance of this phenomenon on the retention capacity of SPBB resin towards the rhMBP.

A sample of TGmilk was loaded onto the column (Tricorn 10/100 – cv 8 ml) at 1.0 ml/min and the flow-through fractions were collected and analyzed using SDS-PAGE and dot blotting analysis. Figure 18 shows that the early flow-through fractions (F1 - F2) contain high molecular weight milk proteins only, which indicated that the column dead volume has been exceeded. Caseins were detected in the following flow-through fractions (F3 - F4) while the flow-through appearance was still transparent. This observation clearly showed that on-column casein micelle disruption had taken place. The on-line monitoring of the conductivity of the flow-through indicated that the conductivity of the transparent flow-through fractions was similar to that of the starting buffer.

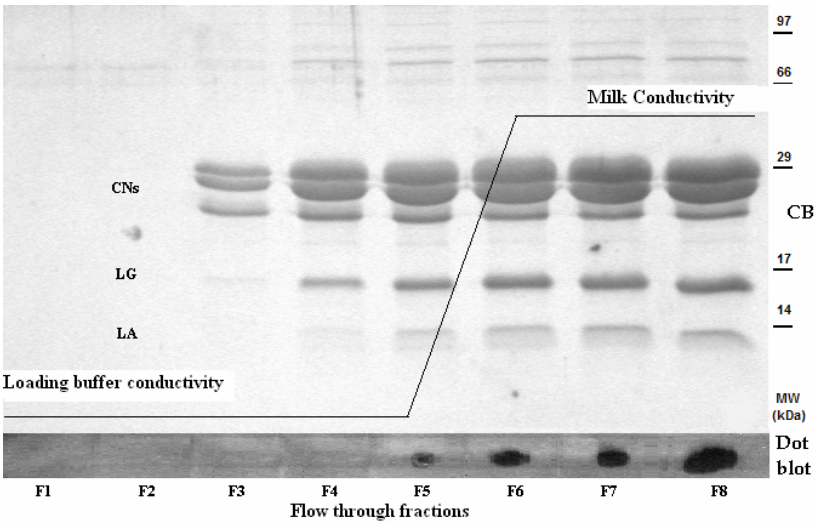

Figure 18: CB-stained gel (top) of the flow-through fractions collected upon loading TGmilk to the cation exchanger column and dot blot analysis using anti-hMBP antibody (bottom) for the same fractions showing that the rhMBP is detectable in the flow-through fractions F5 - F8. A diagrammatic representation of the change in ionic strength of the flow-through fractions is overlaid. Column: Tricorn 10/100 – cv 8 ml, sample: 25 ml TGmilk loaded at 1.0 ml/min, elution flow rate: 5.0 ml/min, loading buffer: 50 mM HEPES (pH 7.0) and elution buffer: 50 mM HEPES (pH 7.0) - 1.0 M NaCl.

The presence of the caseins in the flow-through without a milky appearance or an increase in the conductivity of the flow-through strongly suggested that disruption of the casein micelles was due to the adsorption of the calcium to the active sites of the resin. The dot blot screening of the transparent fractions showed no detectable rhMBP specific signal. When the flow-through started to look like milk, the conductivity of the flow-through was found to increase progressively and the rhMBP was detected in the flow-through fractions (F5 - F8). These results indicated that the appearance of the rhMBP in the flow-through is directly linked to the presence of intact casein micelles in the flow-through fractions.

3.4.5 The sequential sample loading approach

Based on the above results and taking into consideration the key role of calcium in maintaining casein micelle integrity it could be concluded that micelle disruption was a direct impact of calcium binding to the adsorption sites of the resin. Micelle disruption

during milk loading could provide a novel approach for the recovery of recombinant proteins expressed in milk and exclusively associated with the micellar phase, if the micelle disruption phase could be extended. In order to investigate this hypothesis, two TGmilk samples (25 ml) were loaded to the column, either as one aliquot (Figure 19) followed by a wash step or in five aliquots (Figure 20) with column washing in between.

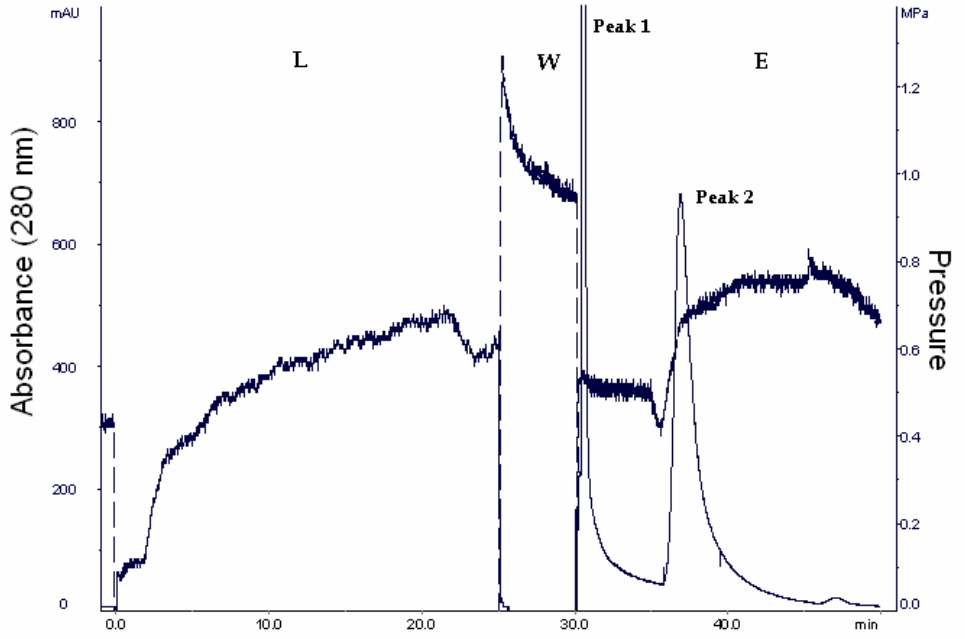

Figure 19: A chromatogram showing the elution pattern upon loading the milk sample as one aliquot. Left Y-axis: UV trace at 280 nm and right Y-axis: trans-column pressure. Peak 1: non-specifically retained proteins eluting during the wash step and peak 2: elution of the selectively retained proteins using 1.0 M NaCl. L: sample loading, W: column wash and E: elution step. Column: Tricorn 10/100 - cv 8 ml, sample: 25 ml TGmilk loaded at 1.0 ml/min, elution flow rate 5.0 ml/min, loading buffer: 50 mM HEPES (pH 7.0) and elution buffer: 50 mM HEPES (pH 7.0) - 1.0 M NaCl.

A wash step of 2 - 3 cv of the loading buffer was enough to reduce the conductivity of the flow-through to that of the loading buffer. A software modification to the Unicorn platform controlling the chromatography system was carried out in-house in order to maintain automation for the whole process and to integrate this function with the bypass function that had been developed. The flow-through and the column wash fractions were collected and elution was carried out in one step using 1.0 M NaCl.

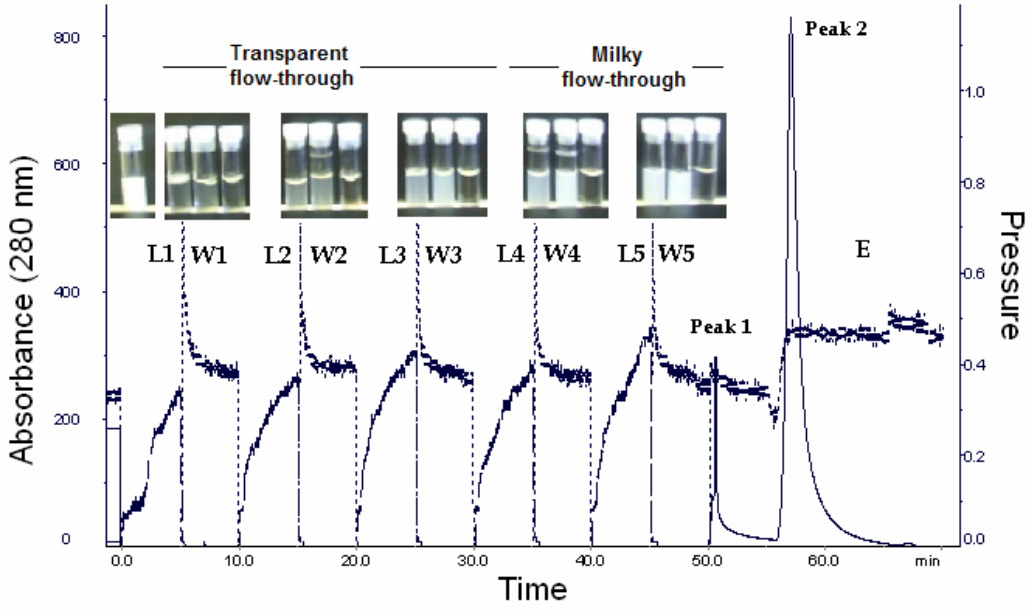

Figure 20: A chromatogram showing the elution pattern upon loading the milk sample in five aliquots and showing pictures for the flow-throw fractions collected. Left Y-axis: UV trace at 280 nm and the right Y-axis: trans-column pressure. Peak 1: non-specifically retained proteins eluting during the wash step and peak 2: elution of the selectively retained proteins using 1.0 M NaCl. L: sample loading, W: column wash and E: elution step. Column: Tricorn 10/100 - cv 8 ml, sample: 25 ml TGmilk loaded at 1.0 ml/min, elution flow rate 5.0 ml/min, loading buffer: 50 mM HEPES (pH 7.0) and elution buffer: 50 mM HEPES (pH 7.0) - 1.0 M NaCl.

The amount of non-specifically retained milk proteins (peak 1) was compared using the integrated peak area (A_1) obtained in each case. The peaks representing the selectively retained proteins (Peak 2) were compared with respect to peak height (h), width at half height ($W_{1/2}$) and integrated peak area (A_2). All results were expressed relative to those obtained by loading the milk sample in one aliquot and summarized in Table 4. The trans-column pressure build-up was monitored during the sample loading steps (sample pump) and throughout the run (main system pump). The dot blot assay was used to estimate the concentration of the rhMBP in eluted fractions.

Table 4: A comparison between the direct sample loading approach and the sequential loading approach showing the relative increase / decrease in the parameters studied.

Parameter	Direct loading method	Sequential loading method
A_1 (mAU*min)	677.99	80.30 (- 88.16%)[§]
A_2 (mAU*min)	811.78	1047.90 (+ 29.10%)[§]
h (mAU)	618.01	812.87 (+ 31.53%)[§]
$W_{1/2}$ (min)	1.15	0.98 (- 14.78%)[§]
rhMBP (µg/ml) [#]	16.0	20.0 (+ 25.0%)[§]

[§] **Relative to the corresponding values obtained using the direct loading method.**

 # Dot blot assay.

A relative decrease of 88.16% in A_1 which represented the amount of non-specifically retained proteins (peak 1) and a relative increase of 29.10% in A_2 and of 31.53% in h which represented the amount of selectively retained proteins (peak 2) was noted. A decrease in the $W_{1/2}$ of 14.78% of peak 2 was also noted when the sequential sample loading method was employed. These results demonstrated that the total amount of selectively retained protein on the column was significantly higher using the sequential method. Narrower peak width indicated the improvement in column dynamics when the milk samples were loaded in aliquots with column washing steps after each aliquot.

A notable decrease in the trans-column pressure during the sample loading, wash and elution steps was recorded which indicated an improvement in the hydrodynamic properties of the column when the sample was loaded in aliquots. This reduction in the trans-column pressure along with the profound decrease in A1 indicated the decrease in the amount of non-specifically adsorbed proteins, typically caseins and casein micelles on the column. The non-specifically adsorbed proteins were causing mass transfer limitations at the active sites of the cation exchanger resin, while casein micelles were physically blocking the small pores of the resin and thus responsible for the pressure build-up during the sample loading steps and the reduced dynamic capacity.

The flow-through was found to remain transparent over a much larger volume which indicated that the casein micelle disruption phase was extended when the sample was loaded in aliquots. This observation demonstrated that the calcium occupying the active sites of the resin was washed off the column by the loading buffer regenerating free adsorption sites for binding of additional rhMBP during the next loading step. Once most of the adsorption sites were again occupied, calcium could no longer bind and the micelles remained intact. Thus, the flow-through started to appear milky (Figure 20). This conclusion was confirmed by the observation that the dot blotting assay revealed a 25% increase in the amount of eluted rhMBP when the sequential loading approach was employed. Two to three sequential loadings of (≈ 0.64 cv each) were found to be the maximum volume of the loaded milk sample. Loading larger volumes of milk samples resulted in enrichment of other strongly bound endogenous milk basic proteins (such as LF) and thus premature elution of the rhMBP as discussed previously.

3.4.6 Scale-up of the direct capture step

A scale-up experiment (scaling factor 2.5) was carried out in order to evaluate the performance of the sequential loading approach at scale. A bigger column (XK 16/20 – cv 20 ml) was packed to a bed height of 10 cm using the same resin (SPBB). The performance of the XK column was compared to that of the Tricorn 10/100 (cv 8 ml) which was used for method development. The loading and elution steps were carried out at the same linear velocity and using the same number of column volumes. The milk samples were loaded in two aliquots while maintaining the ratio of milk volume per aliquot to the bed volume at 0.64 cv. A good overlap in elution profile over the time scale of the run indicated a successful scale-up experiment (Figure 21). The fractions containing the rhMBP were pooled together and further purification was carried out using the HisTrap HP column (cv 5 ml) as previously described. The total amount of the rhMBP in the starting TGmilk sample (≈ 2.56 mg) was compared to that of the pooled fractions after the SPBB (≈ 2.0 mg) and the IMAC steps (≈ 2.0 mg) employing the dot blotting assay and the cumulative recovery percentage was found to be ≈ 78%.

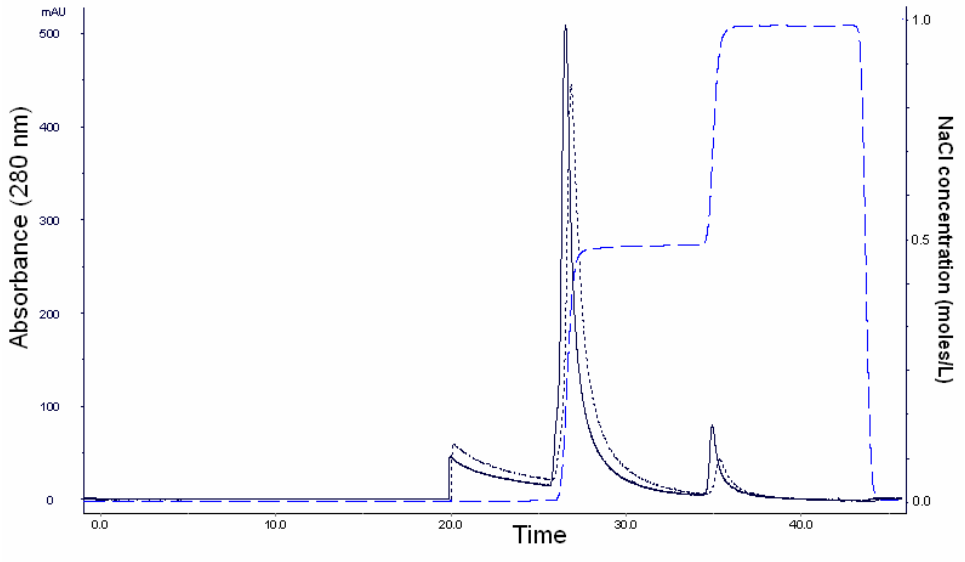

Figure 21: Chromatograms showing the overlap in elution patterns obtained from the columns used in the scale up experiment. Column 1: Tricorn 10/100– cv 8 ml (------), sample volume: 2x5 ml TGmilk loaded at 1.0 ml/min, elution flow rate: 5.0 ml/min. Column 2: XK 16/20 – cv 20 ml (——), sample volume 2 x 12.8 ml TGmilk loaded at 2.6 ml/min, elution flow rate 12.8 ml/min. Loading buffer: 50 mM HEPES (pH 7.0) and elution buffer: 50 mM HEPES (pH 7.0) - 1.0 M NaCl. Solid line: UV trace at 280 nm (mAU) and dashed line: NaCl concentration in (M).

3.5 Conclusion

In this chapter, a novel automated approach for the direct chromatographic capture of the model transgenic protein (rhMBP) was developed. The method should prove to be useful for other transgenic basic proteins which could be partially or completely associated with the milk micellar phase. The interaction between the micellar calcium and the adsorption sites of the cation exchanger resin was utilized in order to disrupt the micelles and liberate the target protein. Simultaneous product capture and on-line casein micelle disruption obviated the need for the inclusion of denaturing additives. The new approach was found to improve not only the retention properties of the target protein but also the hydrodynamic properties of the chromatographic matrix.

Chapter 4

4 Monitoring and Analysis of Recombinant Human Myelin Basic Protein

4.1 Introduction

A downstream purification protocol for the rhMBP was developed as described in Chapter 3. The purification protocol was considered successful with respect to the following: the ability to directly capture the rhMBP from milk without denaturing additives, the good purity and solubility of the purified rhMBP and the ability to monitor the rhMBP levels throughout the purification steps. The development of a more reliable, quantitative, high throughput testing protocol was of crucial importance. Any testing protocol for the rhMBP has to consider that the recombinant protein does not interact strongly with conventional protein stains and that the immunogenic activity is the only activity to trace.

In this study, a CZE total protein assay and a Bio-Plex immunoassay were developed and validated. A testing protocol employing both methods was employed to monitor the model biopharmaceutical protein in milk fractions and to optimize the purification protocol. Other applications have also been investigated including monitoring of the short term stability of rhMBP as well as fingerprinting of the expression levels in milk samples.

4.2 Preparation of in-house rhMBP reference standard

While developing the downstream purification protocol of the rhMBP, a commercially available hMBP standard was used for comparative purposes in the immunodetection applications. This hMBP standard is a mixture of various molecular weight isoforms, with one major isoform of molecular weight of 18.5 kDa, and many charge isoforms. The molecular weight isoforms arise from the alternative splicing of the primary mRNA transcript encoding for the hMBP. Differences in the post-translational modification patterns of each molecular weight isoform explain the large number of charge isoforms as discussed in Chapter 1 (1.5.3).

A hMBP standard of only one molecular weight isoform is available from recombinant E. coli. However, it lacks the post-translatonal modifications which are characteristic of mammalian proteins. The rhMBP used in this study is produced in the milk of transgenic cows and consists of the amino acid sequence of the 17.2 kDa isoform of hMBP with an N-terminal His tag as shown in Appendix I. Expression of the rhMBP in the mammary gland of the transgenic animals resulted in one major isoform (21 kDa) and several minor small molecular weight isoforms (18 – 20 kDa).

Development and validation of analytical methods require the availability of a reference standard of identical nature to the analyte and of known purity and concentration (FDA, 2001; Findlay et al., 2000). Therefore, an in-house rhMBP reference standard was prepared and characterized as described in Chapter 2 (2.3.5). Western blotting showed good stability of the rhMBP in the final preparation over three freeze / thaw cycles in 36 h (Figure 16). Since this standard is intended mainly for antibody-based applications, a dot blotting assay was used to estimate the concentration of the rhMBP in the final preparation (1.0 mg/ml), using an anti-hMBP monoclonal antibody and the hMBP as a reference standard. The rhMBP concentration, determined using the dot blotting assay, was compared to the total protein concentration, determined using the CZE assay. The purity in the final preparation was estimated to be ≈ 90% which was in agreement to the previously obtained estimate from the results of the SDS-PAGE analysis as mentioned above.

4.3 Determination of the total protein content using CZE

The rhMBP was found to interact weakly with conventional in-gel protein stains such as Comassie Blue. High sensitivity, fluorescent total protein stains such as Deep Purple and other selective stains for His-rich proteins (Brophy et al., 2005) resulted in minimal improvement in the detection sensitivity of the rhMBP. Based on these preliminary investigations, and since commonly used procedures for determination of protein concentration involve interaction between the protein and a reagent / dye (Planning, 2007), it was concluded that the reliability of such procedures could be of questionable value in the case of rhMBP.

A CZE method which does not involve an interaction between the rhMBP and a dye was developed in order to determine the total protein concentration in the rhMBP standard and chromatography fractions. Under CZE conditions, proteins migrate according to their charge and frictional forces. The apparent net charge carried out by a protein molecule depends on its pI, pH of the BGE employed and the native structure of the protein (Y.-F. Huang, Hsieh, Tseng, & Chang, 2006). The use of SDS in conjunction with reducing agents such as BME is a commonly used procedure for the preparation of protein samples for electrophoretic methods such as SDS-PAGE and capillary gel electrophoresis. This pre-treatment effectively imparts a negative charge on the protein molecules (proportional to the mass of the protein, ≈ 1.4 g SDS / g protein), which then migrate at the same speed under the effect of an applied electric field (Hu et al., 2002; Laemmli, 1970; Otzen, 2002; Parker & Song, 1992).

In this CZE method, the protein samples were incubated with SDS and a reducing agent (BME) then injected into a capillary which was pre-filled with a PEO solution as described in Chapter 2 (2.3.6). Such a procedure resulted in the stacking of all protein-SDS complexes as one band which enhanced the sensitivity of the UV detection and facilitated the quantitative analysis. The sensitivity of detection was further enhanced via the HSDC which physically increased the detection path length by more than 10 fold. Detection was carried out at 214 nm which relies on the light absorption by the peptide bonds of protein molecules (Planning, 2007). Thus, this protocol was considered also valid for determination of the total protein concentration in mixtures using a calibration curve developed using BSA standard solutions. The ability of the CZE technique to stack all charged protein-SDS complexes in one band eliminated the possibility of interference by any light absorbing additive that could be present in chromatography fractions. The spectral analysis function of the DAD integrated with the Agilent HP^{3D} CE was employed to confirm the identity of eluted peaks in these experiments.

4.3.1 Capillary pre-conditioning

HEPES buffer (pH 7.0), in which samples were obtained following the downstream purification protocol, was used as the BGE in order to minimize sample preparation time. Preconditioning of fused silica capillaries with a PEO polymer solution is a commonly used protocol as will be discussed in detail in Chapter 5. PEO forms a neutral dynamic coat on the capillary wall that suppresses the electroosmotic flow (EOF) and prevents the adsorption of the protein molecules to the FS capillary wall (Horvath & Dolnik, 2001; Lucy, MacDonald, & Gulcev, 2008). In this study, the efficiency of the preconditioning procedure was evaluated based on its ability to form a reproducible dynamic coat under the experimental conditions employed in the CZE assay. A short plug of a negatively charged marker was analysed as described above. The OG marker was found to migrate toward the anode which indicated the suppression of the EOF by the dynamic coat (Figure 22). A stable current trace of a constant value along the run time (30 min) and over different runs indicated that the dynamic coat is sufficiently stable.

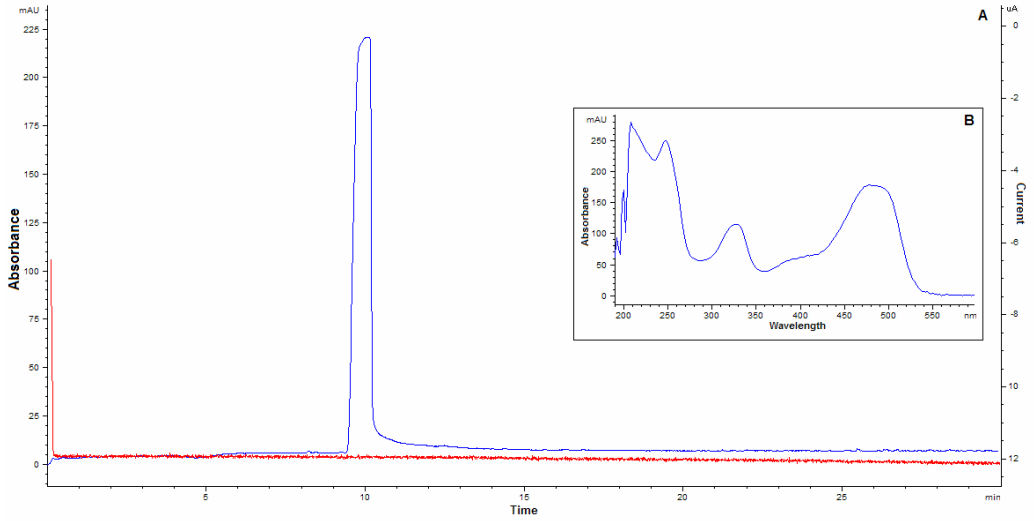

Figure 22: A: Electrophoregram and the current trace showing the migration behavior of the negatively charged orange G marker. B: The DAD absorption spectrum confirming the identity of the orange G marker. Fused silica capillary total / effective length: 72 cm / 63.5 cm x 75 µm I.D., voltage: - 30 kV, temperature: 25 ^{o}C, detection: UV at 214 nm, hydrodynamic injection: 50 mbar - 40 s and sample: 4% v/v OG in 50 mM HEPES buffer (pH 7.0).

While in the absence of the dynamic coat, the marker peak was found to migrate in the opposite direction, towards the cathode, under the effect of the EOF (Appendix III). The marker sample was analysed as described in Chapter 2 (2.3.6.1) over five consecutive runs within the same day and over two days. No significant difference (Alpha 0.05) using analysis of variance (ANOVA) in the migration time of the marker peak indicated good repeatability and reproducibility of the dynamic coat. When samples containing the BSA-SDS complexes were analyzed under the same experimental conditions, the negatively charged complexes were found to elute as a single, well resolved peak.

4.3.2 The effect of SDS concentration

The role of SDS in the sample preparation was discussed above. However, it has been reported that a large amount of protein secondary structures were detected in the presence of SDS (Parker & Song, 1992). It has been reported also that protein unfolding typically occurs above the critical micelle concentration (CMC) of SDS (< 4 mM in HEPES buffer) (Otzen, 2002; Thorsteinsson, Richter, Lee, & DePhillips, 2005).

In this experiment, the effect of SDS concentration on the performance of the method was investigated. Denatured and non-denatured BSA samples (1.0 mg/ml each) were prepared using different SDS concentrations (4.4 - 35.0 mM) and in the absence of SDS respectively. The BSA sample which was prepared in the absence of SDS showed a broad peak representing the heterogeneity of the native BSA molecules (Figure 23-E). Large differences in BSA peak shape and migration time were noted upon using different SDS concentrations for the preparation of the protein sample (Figure 23-A: D). Results showed that protein denaturation was crucial to obtaining good peak shape. The use of SDS concentration of 35 mM was employed for sample preparation in order to achieve good stacking of the BSA-SDS complexes and peak shape, thus facilitate protein quantitation. The delay in the migration time noted at high SDS concentration was attributed to formation of BSA-SDS micelles of larger size that migrate slower than the usual BSA-SDS complexes. This conclusion was confirmed via the analysis of the OG marker in the presence of different SDS concentrations and similar results were obtained (Appendix IV).

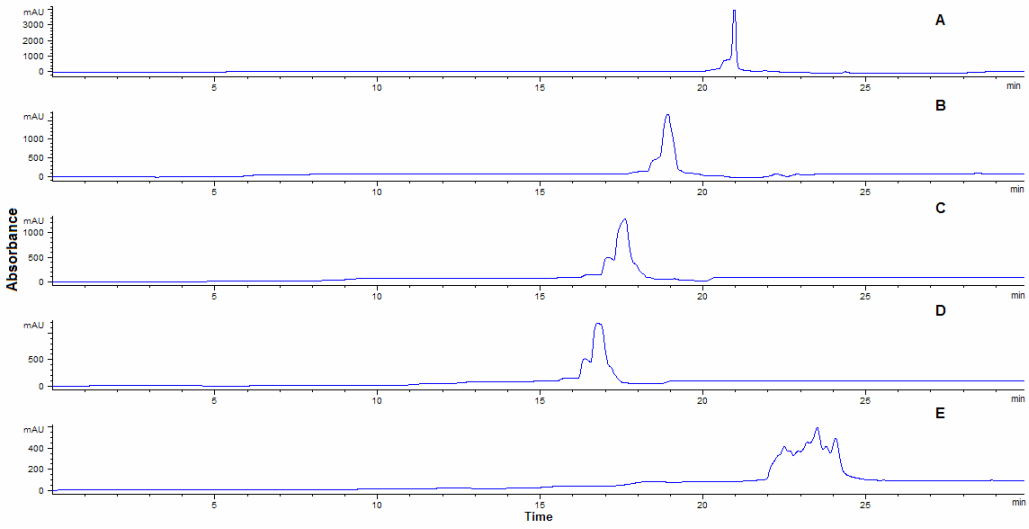

Figure 23: Electrophoregrams showing the UV traces obtained by analysis of denatured BSA samples using different SDS concentrations: (A: 35.0, B: 17.5, C: 8.8, D: 4.4 mM) and a non-denatured BSA sample (E). Fused silica capillary total / effective length: 72 cm / 63.5 cm x 75 µm I.D., voltage: - 30 kV, temperature: 25 °C, detection: UV at 214 nm, hydrodynamic injection: 50 mbar - 40 s and sample: 1.0 mg/ml BSA in the presence of different SDS concentrations.

4.3.3 Stacking conditions

The injection of the protein-SDS complexes into a capillary pre-filled with a PEO solution resulted in sample stacking at the interface between the sample plug and the PEO plug. This approach resulted in a significant improvement in the peak shape and the detection sensitivity which is the main limitation for protein analysis by CZE. In this experiment, the effect of the sample plug volume and length, relative to the capillary volume and length respectively, was investigated. BSA samples (1.0 mg/ml each) were analyzed using the above method employing injection times of 10 - 320 s, which corresponded to ≈ 1.8 - 47.0% of the capillary volume. A peak for the BSA was recorded even when the longest injection time was employed which indicated the stacking of the protein-SDS complexes at the interface between the sample plug and the PEO plug. An injection time of 40 s (7.6% of capillary volume and ≈ 9.0% of capillary length to the

detection window) was employed since very broad peaks with non-reproducible migration time were noted for injection times longer than that.

4.3.4 Calibration and validation

A series of BSA standards over a wide concentration range was analyzed employing an injection time of 40 s. The mean migration time was found to be (21.8 ± 0.5 min) which indicated good reproducibility of the migration time. The migration time-corrected integrated peak area was utilized in order to further improve the reproducibility of the response (Goodall, Williams, & Lloyd, 1991). The PA values were plotted vs BSA concentration and a linear relationship was obtained over a BSA concentration range of 8.49 - 135.87 μg/ml. The regression equation was calculated (Y = 2.8737 X – 6.026); where Y is the PA and X is the concentration (μg/ml) of the BSA standard solutions. A correlation coefficient (R^2) of 0.996 and random distribution of the residuals showed good linearity of the calibration curve over this concentration range. The standard deviation of the intercept and the slope of the calibration curve were used to calculate the limit of detection (LOD) and lower limit of quantitation (LLOQ) (ICH, 2005). The calculated LOD (0.26 μg/ml) was found to be in good agreement with the visually determined one. However, the predictability of the calibration curve below the calculated LLOQ (0.97 μg/ml) was found to be highly variable. Thus, the lower limit of the linear range of the calibration range (8.49 μg/ml) was considered as the LLOQ.

The accuracy of the method was evaluated via analysis of a series of BSA standard samples over five concentration levels covering the linear range of the calibration curve. The predicted concentrations were compared to the actual values using ANOVA and no significant difference (Alpha 0.05) indicated good accuracy of the method. The same set of standards was analyzed within the same day and over two days and the lack of any significant difference in PA suggested good repeatability and reproducibility. The concentration of the BSA validation samples was determined using a reference method (Bradford assay). The results were compared to those determined using the CZE method, no significant difference suggested good predictability of the CZE method.

4.3.5 Application to chromatographic fractions and salt effect

Salts are common additives in protein chromatography owing to their role in the differential screening of the interactions between protein molecules and the adsorption sites of the chromatographic resins. However, salts are known to have deleterious effects on electrophoretic analytical methods and desalting is a common practice for samples intended for CE analysis. In addition, the changes in the sample ionic strength has been reported to affect protein - SDS interaction (Otzen, 2002). The CZE method described above was successfully employed for the determination of the total protein content in desalted chromatographic samples. The protein-SDS complexes were found to elute as a single peak at a migration time similar to that obtained for the BSA standard. This observation confirmed that all proteins in the sample were of equal m/z ratio after the suggested pre-treatment. In contrast, non desalted chromatography fractions containing 0.5 M NaCl and 0.5 M imidazole were found to give poor responses. However, a good peak shape was obtained when these samples were diluted before analysis with the BGE (Appendix IV).

The effect of salt was studied in more detail in order to ensure the robustness of the method and to determine the limit for the concentration of salt in the samples. A series of BSA samples over a wide range of concentration (0.5 – 10.0 mg/ml) was prepared in the presence of 0.5 M NaCl. Samples were analysed before and after a two-fold dilution with the BGE. The effect of dilution was found to be critical to obtaining a well resolved peak for the protein-SDS complexes, especially at the lower protein concentration range (Figure 24). These results indicated that the loss of good peak shape is mainly due to the disruption of the protein-SDS complexes under the effect of salt.

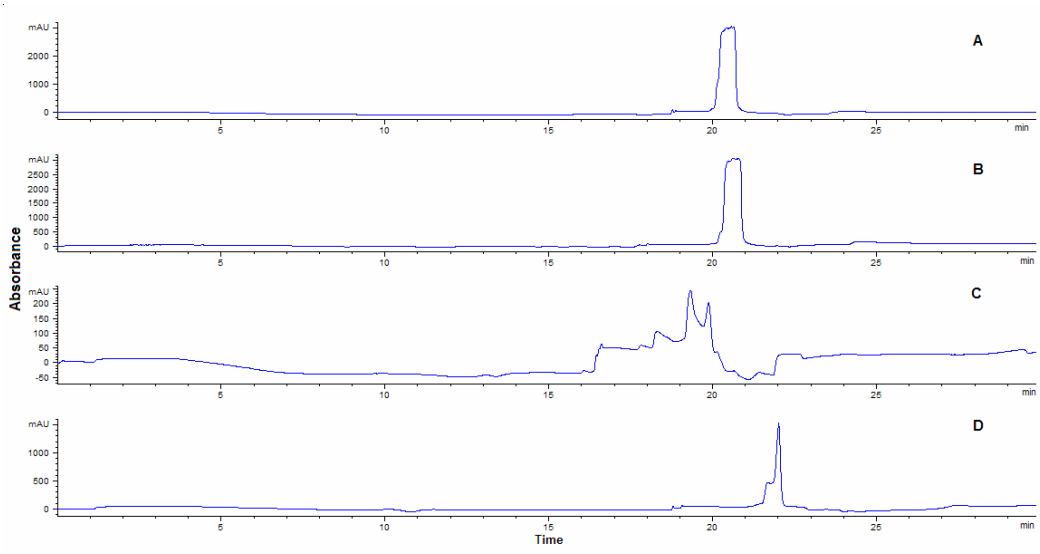

Figure 24: Electrophoregrams showing the UV traces obtained by analysis of two BSA standard samples containing 0.5 M NaCl before and after two-fold dilution with 50 mM HEPES buffer (pH 7.0). A and B: 10.0 mg/ml BSA before and after dilution respectively, C and D: 0.5 mg/ml BSA before and after dilution respectively. Fused silica capillary total / effective length: 72 cm / 63.5 cm x 75 µm I.D., voltage: - 30 kV, temperature: 25 ^{o}C, detection: UV at 214 nm and hydrodynamic injection: 50 mbar - 40 s.

In order to accurately evaluate the effect of salt on the predictability of the developed method, three BSA standard solutions covering the calibration range of the method were prepared. Each standard sample was prepared in triplicate containing variable amounts of NaCl (0 – 200 mM). All samples were analysed using the optimized method. The BSA concentrations were then determined from the calibration curve and compared to their nominal values. No significant difference between the actual and predicted protein concentrations (Alpha 0.05) was noted over salt concentration up to 50 mM. For future applications, the proposed method was used to analyze the protein content in chromatography fractions either after desalting or after dilution to a salt concentration less than 50 mM.

4.4 Determination of rhMBP using Bio-Plex immunoassay

Immunodetection of the rhMBP by western blotting analysis using an anti-hMBP mAb was carried out as previously discussed in Chapter 3. This method provided a highly sensitive, qualitative tool for probing the target protein in milk samples and throughout the downstream purification protocol. However, it is a laborious technique and is reliable only for screening purposes of a limited number of samples per run. The dot blot analysis on the other hand is suitable for the analysis of a larger number of samples in a much shorter time. Dot blotting analysis provided a good estimate of the quantity of the rhMBP but was unable to differentiate intact and degraded rhMBP molecules.

The high specificity and sensitivity of immunoassays account for their indispensable role in quality control protocols. Sandwich-type enzyme linked immunosorbant assay (ELISA) has been the standard for quantitative protein immunoassays. ELISA is specific and reproducible yet time consuming, sample volume demanding and can not determine more than one analyte per run. On the other hand, advances in particle encoding technologies have provided valuable tools for the development of semi-automated, multiplexed immunoassays (Hanley, Xing, & Cheng, 2007; Nolan & Mandy, 2006).

Luminex Corporation has developed an array of one hundred different types of color-coded beads. Each of these labeled bead types can be used to probe an analyte on its surface using the sandwich assembly characteristic for ELISA. Detection is carried out by monitoring of the fluorescence generated by a reporter molecule bound to the second primary antibody. Provided that a specific antibody pair is available for each analyte, simultaneous analysis of up to one hundred different analytes can be achieved with no extra sample volume required. The Bio-Plex Suspension Array System utilizes the xMAP technology which was originally developed by Lumenix in order to differentiate these beads. Detection of the fluorescence generated by the reporter molecule bound to the antibody sandwich can then be used to measure the quantity of each analyte. Since this approach utilizes the same essence of ELISA, high levels of specificity are retained.

Moreover, coupling of the capture antibodies to the surface of the beads can be carried out in a separate step since antibody-coupled beads are stable for at least six months. This advantage resulted in a significant reduction of the analysis time when compared to that required for an ELISA run (Hanley et al., 2007; Kellar & Iannone, 2002; Nolan & Mandy, 2006; Vignali, 2000). Several examples for Bio-Plex applications covering a wide variety of analytes in different matrices have been reported in the literature (Bossart et al., 2007; Fitzgerald et al., 2007; Flagella et al., 2006; Fulton, McDade, Smith, Kienker, & Kettman Jr, 1997; Nolan & Mandy, 2006; Prabhakar, Eirikis, & Davis, 2002; Taylor et al., 2001; van Gageldonk, van Schaijk, van der Klis, & Berbers, 2008). However, to the best of our knowledge, the applicability of this technique for the analysis of milk components or the analysis of biopharmaceuticals produced in the milk of Tg animals has not been explored yet.

In this section, the development of a sandwich-type immunoassay on the surface of the fluorescent beads is described for the analysis of the rhMBP. A mouse anti-hMBP antibody, which detects an epitope very close to the C-terminus of the recombinant protein, was immobilized to the surface of one type of the fluorescent beads. The detection of the captured antigen on the surface of the beads was achieved using a biotin conjugated anti-His tag antibody. The well characterized interaction between the biotin label and the fluorescent marker SA-PE was used to detect the antibody sandwich using the Bio-Plex system. Taking into consideration that this matched antibody pair detects two epitopes at the opposite ends of the rhMBP molecule, it could be concluded that only full length rhMBP molecules will be detected. In addition, this immunoassay was considered as an *in-vitro* activity indicating assay for the rhMBP since the immunogenic activity of the full length rhMBP has been reported to be higher than its proteolytic fragments (Oettinger et al., 1993).

4.4.1 Bio-Plex method development and optimization

Three aliquots of the mouse anti-hMBP antibodies were coupled to three aliquots of an equal number of beads. The amount of anti-hMBP antibody coupled to the bead surface in each case was determined using a biotin-labeled anti-mouse antibody. An amount of

1.8 µg anti-hMBP antibody was found to be the optimal amount for the coupling reaction. The functionality of the coupled beads was investigated via the analysis of a set of the rhMBP standard samples. An equivalent set of WTcontrol samples was included for comparative purposes. Blank samples (buffer only) were included also in order to evaluate the background fluorescence signal. In this experiment, different concentrations of the detection antibody were trialed in order to optimize the detection step. The obtained MFI indicated that the selected antibody pair was able to probe the rhMBP in the samples. The control samples gave a MFI comparable to that of the blank samples (Figure 25) which indicated that any impurities remaining in the standard did not interfere with the assay. A low background signal suggested that the washing protocol employed had successfully removed excess reagents. An anti-His tag antibody dilution of 1:1000 was selected since the MFI obtained using this dilution was comparable to that obtained from the more concentrated antibody preparations as shown in Figure 25.

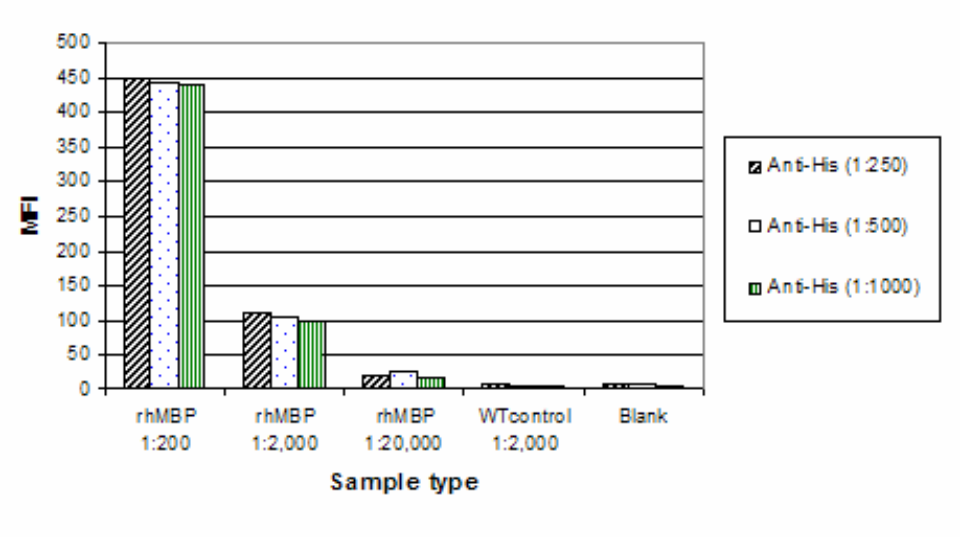

Figure 25: A plot of the MFI obtained by analyzing diluted samples of the rhMBP standard 1.0 mg/ml (1:200, 1:2,000 and 1:20,000), WTcontrol sample (1:2,000) and blank samples using three anti-His tag antibody concentrations (1:250, 1:500 and 1:1000).

4.4.2 Assay specificity

The ability of the immunoassay to differentiate between the recombinant protein and its human counterpart was investigated. A set of the hMBP standards equivalent to the rhMBP standard series, used to optimize the anti-His tag antibody concentration was prepared and analyzed. The obtained responses from the hMBP series were comparable to that of the blank and WTcontrol samples (Figure 26). Lack of any specific response from the hMBP standard provided good evidence that the assay is specific to the (His tagged) rhMBP only. It could be concluded also that product-related impurities (degraded protein molecules which lack the His tag) will not interfere. Since all rhMBP isoforms were His tagged, the Bio-Plex method can be considered as a total activity and stability indicating assay for the rhMBP.

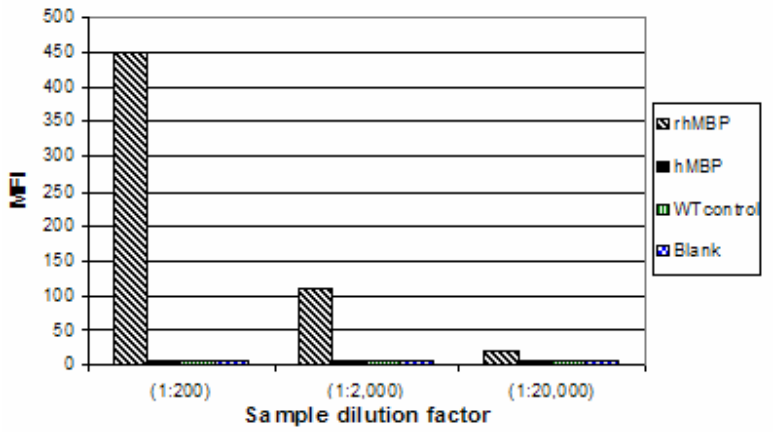

Figure 26: A plot of the MFI obtained by analyzing diluted samples (1:200, 1:2,000 and 1:20,000) of the rhMBP standard (1.0 mg/ml), hMBP standard (1.0 mg/ml), WTcontrol and blank samples using the Bio-Plex method showing the specificity of the method and lack of any interference by milk proteins.

4.4.3 Calibration, sensitivity and range of the Bio-Plex method

Serial dilution of the rhMBP standard, WTcontrol samples and blank samples were prepared and analyzed using the optimized protocol. The obtained MFI was plotted against the log of the rhMBP concentration and the characteristic sigmoid shape concentration-response relationship was obtained. The non-linear, four-parameter logistic regression

(4-PL) model was found to be the best fitting model (R^2 0.998) (Figure 27) (Findlay & Dillard, 2007; Findlay et al., 2000). The fit was found not to improve upon using the 5-PL model which indicated that the response was symmetric across the inflection point of the calibration curve. The resulting regression equation was used to back predict the concentrations of the reference standards used to generate the model. The average recovery percent at Alpha 0.05 (observed / predicted *100) was found to be 100.53 ± 1.01 The LOD was calculated from the standard deviation of the background MFI (blank response n = 12) and was found to be (6.04 ng/ml). The LLOQ and the upper limit of quantitation (ULOQ) were obtained so that the calculated percent relative error meets an intra-assay precision of ≤ 15% and inter-assay precision of ≤ 20%. The assay range was found to be (9.77 - 10,000.00 ng/ml). The predicted concentrations of the standards were compared to the actual ones and no significant differences (Alpha 0.10) were found indicating good predictability of the model.

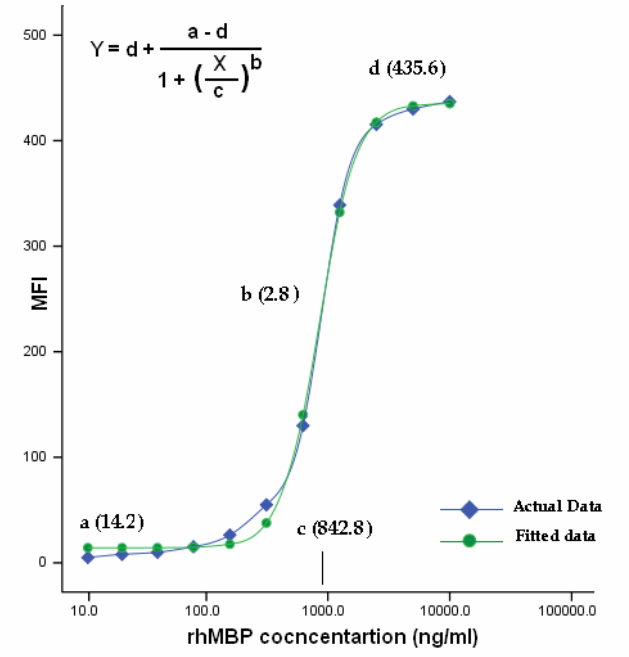

Figure 27: Calibration curve for the Bio-Plex immunoassay with the actual and fitted data (predicted) using the 4-PL regression model. The equation representing the model and the estimated values of the parameters were overlaid. MFI: median fluorescence intensity.

4.4.4 Assay accuracy and precision

A series of validation samples covering the assay range was prepared from the rhMBP standard and was analyzed in triplicate. The predicted concentrations were compared to the actual concentrations in order to evaluate the accuracy of the method. Intra-assay variability (within a plate and between plates within the same day) was carried out by comparing the MFI obtained at each concentration level. The same procedure was repeated over two different days and the inter-assay variability was investigated in a similar manner. Statistical comparisons were carried out using ANOVA (Alpha 0.10) and no significant difference indicated good repeatability and reproducibility of the method.

4.4.5 Applications of the Bio-Plex method

4.4.5.1 Determination of the rhMBP concentration in milk samples

The effect of remaining impurities in the final recombinant protein preparation was evaluated by analysis of the WTcontrol sample as described above. Lack of any specific response indicated that the sample matrix has no significant effect on the assay performance. A strong interaction between the rhMBP and other milk proteins has been demonstrated and confirmed earlier (Chapter 3). Thorough investigation of possible matrix effects was essential in order to evaluate the applicability of the method for determination of the rhMBP concentration in various milk fractions.

A sample of the WTmilk was processed using the optimized downstream purification protocol as described in Chapter 2 (2.3.3). Samples of the WTmilk and of each of the chromatography fractions (after each step; WT-SPBB and WT-IMAC) were obtained and equal amounts of the rhMBP were spiked in each sample. A serial dilution of each of the spiked samples was prepared in 50 mM HEPES (pH 7.0) and analyzed using the optimized method. The MFI obtained from each set at each concentration level was compared to that obtained from an equivalent set of the rhMBP standard prepared in the assay buffer (Figure 28). No significant difference (ANOVA at Alpha 0.10) was obtained between the rhMBP standard series and that of the spiked chromatography fractions (WT-SPBB and WT-IMAC).

This observation suggested that any endogenous milk proteins remaining after the first and the second chromatography steps do not interfere with the assay performance. On the other hand, the responses from the spiked WTmilk samples were much lower than that of the corresponding responses obtained from the equivalent standard series (Figure 28). Even though, the responses of the spiked WTmilk samples showed a good dependence on the rhMBP concentration. It could be concluded from these results that the method is still applicable for determination of the rhMBP concentration in milk samples yet another calibration curve should be generated using standard samples prepared in the same matrix. The decrease in the MFI could be attributed to the non-specific interference from the relatively large amounts of endogenous milk proteins in the sample.

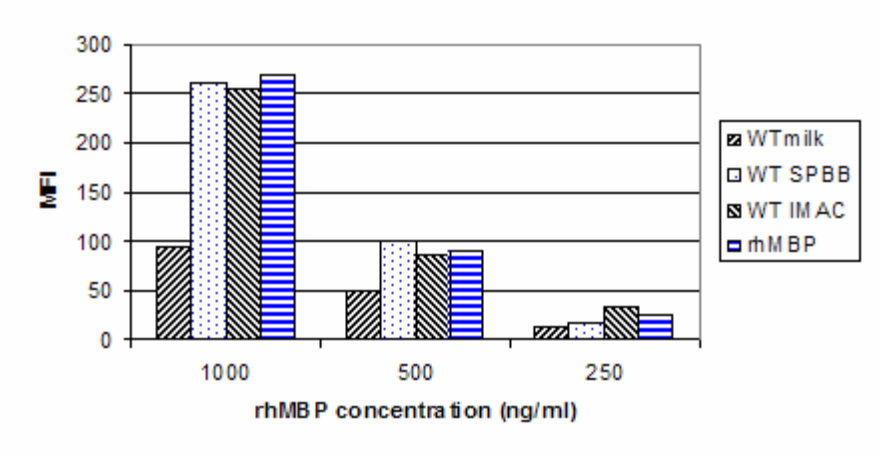

Figure 28: A plot showing the MFI obtained by spiking of three different concentrations of rhMBP (1000, 500 and 250 ng/ml) into various control milk matrices (WTmilk, WT-SPBB and WT-IMAC) compared to that obtained from an equivalent rhMBP standard solutions.

When a serial dilution of a TGmilk sample was prepared in 50 mM HEPES (pH 7.0) and analyzed along with the spiked WTmilk samples (in the same plate) as described above, the MFI obtained from the TGmilk series was found to increase first with dilution then decrease. This observation supported our hypothesis about the association between the rhMBP and other milk components. Expression of the rhMBP in the milk of transgenic cows resulted in the association of the rhMBP with the casein micelles to the extent that it

is not available in milk serum. Spiking of the rhMBP in the WTmilk samples did not lead to a similar effect and a good dependence of the response on the dilution factor was noted. This observation indicated that the rhMBP was available for the anti-hMBP antibody-coupled beads for detection. Based on the above results, it was concluded that the concentration of the rhMBP in milk can not be determined from a calibration curve generated using spiked WTmilk samples with the recombinant protein. However, monitoring of the expression levels of the rhMBP in TGmilk samples was still possible provided that the correct dilution factor was used and the results obtained can be used mainly for fingerprinting of the expression levels. The Bio-Plex method could not differentiate the rhMBP isoforms, thus it can not be used for monitoring of the isoforms pattern in milk samples and western blotting analysis has to be employed.

4.4.5.2 Monitoring of the elution of rhMBP in chromatography fractions

The rhMBP is a "silent" protein that has no traceable enzymatic activity and is difficult to detect by SDS-PAGE using conventional protein stains. Immunodetection by western blotting and dot blotting have been successful in monitoring of the elution pattern / level of the recombinant protein respectively, as discussed previously. A transgenic milk sample was processed using the optimized purification protocol and the Bio-Plex immunoassay was used to trace the rhMBP in the chromatography fractions collected from the second chromatography step (IMAC). Aliquots of the loaded sample (pooled SPBB fractions), the flow-through fractions and the eluted fractions (IMAC fractions) were analyzed using the optimized method. The MFI obtained from each fraction was plotted vs the fraction number (Figure 29). The responses recorded indicated a similar elution pattern of the recombinant protein to that obtained previously by western blotting analysis. These results confirmed that the Bio-Plex method is suitable for in-process qualitative and quantitative monitoring of the rhMBP throughout the downstream purification protocol.

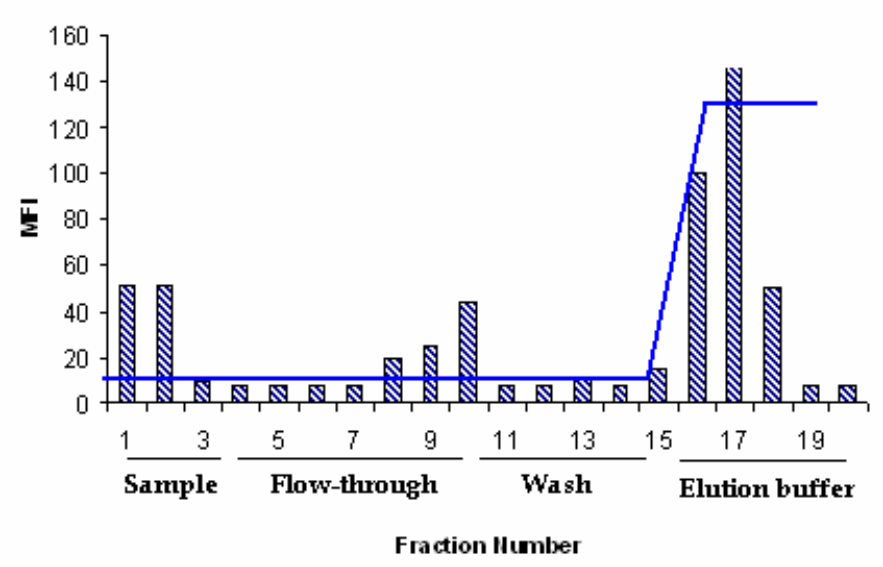

Figure 29: A plot of the MFI obtained from fractions collected throughout a chromatography experiment for the purification of the rhMBP. The X-axis represents the fraction numbers collected throughout the run, 1 - 2: starting sample, 3 - 10: flow-through, 11 - 14: column wash, 15 - 16: gradient elution (50 – 500 mM imidazole) and 17 - 19: eluted fractions (500 mM imidazole). Column: HisTrap HP – 5 ml, sample: 50 ml pooled SPBB fractions loaded at 2.5 ml/min, elution flow rate: 5.0 ml/min, loading buffer: 50 mM HEPES - 0.5 M NaCl - 50 mM imidazole (pH 7.0) and elution buffer: 50 mM HEPES - 0.5 M NaCl - 500 mM imidazole (pH 7.0). MFI: median fluorescence intensity.

4.4.5.3 Monitoring of the stability of the rhMBP

SDS-PAGE followed by western blotting analysis was used successfully to evaluate the stability of the rhMBP in different chromatographic fractions over the time and the conditions encountered during the downstream purification. In this stability study, we focused on studying the stability of the rhMBP in the final preparation. Suitably diluted aliquots of the rhMBP reference standard were incubated at room temperature and at 4 - 8 ^{o}C. The samples were taken after 0, 1, 4, 8 and 24 h and immediately frozen. All fractions were analyzed using the optimized Bio-plex immunoassay employing a calibration curve generated on the same day. The concentration of the rhMBP in each sample was determined from the calibration curve and was plotted vs the incubation time (Figure 30).

The results showed the good stability of the rhMBP reference standard at 4 - 8 ^{o}C for up 24 h and at RT for up to 4 h which was in agreement to the previously reported results using western blotting analysis. Results confirmed the ability of the immunoassay to detect small changes in the rhMBP concentration with time. Thus the Bio-plex assay was considered suitable for studying the stability of the rhMBP in future work since it can provide a good estimate of the intact rhMBP remaining. The relative stability of the rhMBP at 4 - 8 ^{o}C indicated that the use of a refrigerated centrifuge for preparation of the rhMBP stock was essential as previously discussed in Chapter 3 (3.3.3).

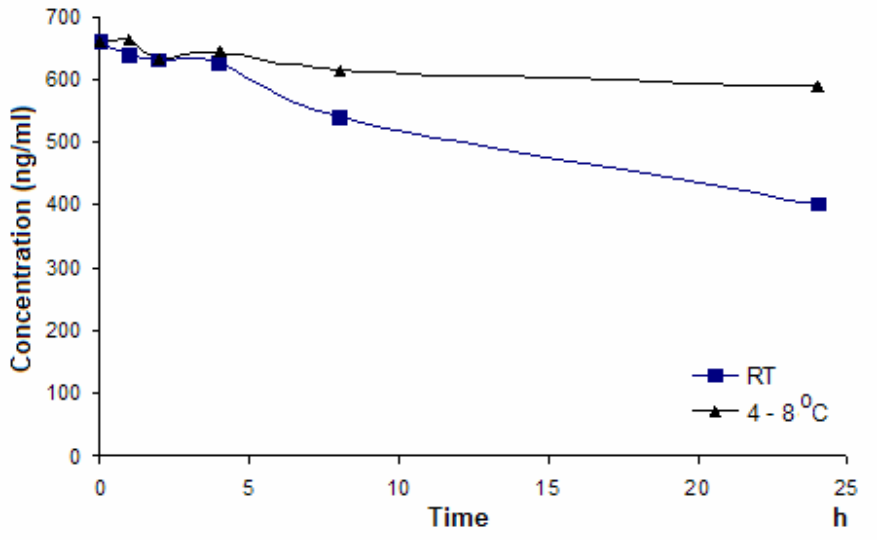

Figure 30: A plot representing the change in the concentration of two rhMBP standard samples incubated at 4 - 8 ^{o}C and room temperature over 24 h showing the ability of the Bio-Plex assay to determine small changes in the rhMBP concentration.

4.5 Conclusion

In this study, a CZE with an on-line sample stacking protocol was developed in order to determine the total protein concentration in chromatography fractions. The CZE assay provided a good alternative for the determination of total protein concentration without the need for using protein stains. A sandwich type, semi-automated immunoassay was developed for monitoring of the expression levels of the rhMBP in transgenic milk and milk fractions using the Bio-Plex system. The assay was considered as a total activity and stability indicating method since it determined the total amount of the intact rhMBP isoforms. The method was used successfully for monitoring of the elution pattern of the recombinant protein in the fractions obtained by column chromatography. Fingerprinting of the expression levels of the rhMBP in transgenic milk samples from each animal at different stages of the lactation cycle / over different lactation cycles can be achieved in minimal time. Theoretically, a large number of applications could be achieved employing the multiplexing capabilities of the Bio-Plex assay such as monitoring of impurities of different sources (process-related, product-related and host-related) and possibly monitoring of markers for the health condition of each animal using the same assay. Both the CZE and the Bio-plex methods formed a good testing protocol which is particularly useful for analysis of structural protein biopharmaceuticals which lack traceable enzymatic activity.

Chapter 5

5 Capillary Isoelectric Focusing of Milk Samples

5.1 Introduction

Capillary isoelectric focusing is the automated version of conventional gel isoelectric focusing (IEF) technique where separation of a mixture of peptides or proteins is carried out according to their isoelectric points. CIEF combines the high sensitivity and high resolving power of IEF with the instrumental capabilities of CE. The capillary format allows faster separation under higher voltages, since efficient dissipation of the Joule heat generated during the electrophoresis separation is feasible (Dolnik, 2006; Mazzeo & Krull, 1991; Righetti, Gelfi, & Conti, 1997; Strelec et al., 2002).

The traditional two-step CIEF in coated capillaries was first introduced by Hjerten and co-workers (Hjerten, 1985). They believed that the use of covalently coated capillaries was necessary to eliminate the EOF in order to obtain successful focusing of the proteins and to prevent adsorption of the analytes to the charged capillary surface, thus improve the reproducibility of separations. Lack of hydrolytic stability of the covalent coat and the expensive price of coated capillaries has limited the use of CIEF to research purposes only (Hjerten & Zhu, 1985; Horvath & Dolnik, 2001; Mazzeo & Krull, 1991; Yeung, Atwal, & Zhang, 2003).

The formation of an electrical double layer is a general phenomenon observed when an electrolyte comes in contact with a charged surface. In the presence of an electric field, this electrical double layer is responsible for the bulk flow of liquid in the capillary, known as EOF, which is generally beneficial in CE. It helps mobilize bands past the detector window without contributing to zone dispersion. The use of buffer additives to establish a dynamic coat on the wall of the FS capillaries has been in use in CE applications. This approach overcomes the batch-to-batch and run-to-run variability associated with the covalently coated capillaries, enables the use of the relatively cheap uncoated FS capillaries in protein analysis applications and provides a simple tool to tune the magnitude and the direction of the EOF. Several trials have been reported to adapt this approach to CIEF however low resolution, incomplete suppression of the EOF as well as differences in the

magnitude of the EOF along the pH gradient formed along the capillary, were the main limitations to obtaining high resolution and reproducible results (Dolnik, 2006; Horvath & Dolnik, 2001; T.-L. Huang & Richards, 1997; Righetti, 2004; Tang & Lee, 1997).

The rhMBP has a relatively high isoelectric point (pI ≈ 10.5) and milk contains very few basic proteins as discussed in Chapter 2 and shown in Table 2. In this study, a CIEF protocol in dynamically coated capillaries was developed for the screening of the TGmilk and the chromatographic fractions for the presence of rhMBP via its pI. Under these conditions, the ability of the CIEF technique to separate proteins according to their isoelectric points was considered a novel tool to identify peaks corresponding to the rhMBP. At first, a "one-step" CIEF protocol in dynamically coated capillaries was developed and compared to the conventional "two-step" CIEF protocol in coated capillaries. The one-step protocol was then employed in order to investigate various factors affecting the reproducibility and resolution of CIEF in dynamically coated capillaries.

5.2 Reference CIEF method

A mixture of four standard proteins was analyzed employing coated capillaries and a two-step CIEF protocol as described in the CIEF kit supplier's manual and summarized in Chapter 2 (2.3.8.1). The electrophoregrams showed a successful separation of the four standard proteins while a typical current trace for a CIEF run was obtained as shown in Figure 31 - A. Upon application of the electric field, the current was found to initially increase (≈ 5 μA), rapidly decrease and level off (< 1 μA) after approximately 6 min. A sharp change in the current was noted at 6 min which corresponded to the onset of the change of the applied voltage from 15 kV "focusing voltage" to 21 kV "mobilization voltage" and the onset of application of the hydraulic pressure (35 mbar). This hydraulic pressure was used to mobilize the protein bands past the detection window over 55 min. During the last five minutes of the run time, the current was noted to increase again (Figure 31 - A).

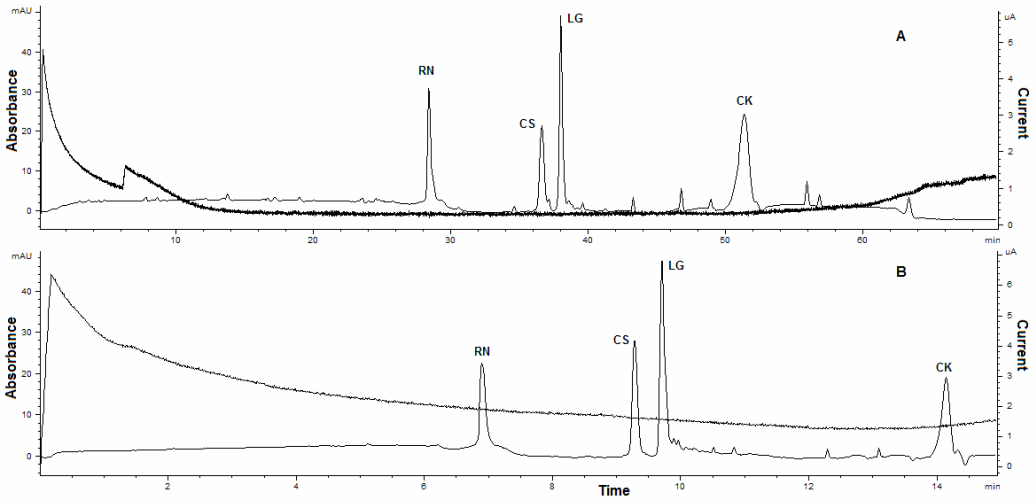

Figure 31: Electrophoregrams and current traces obtained using covalently coated capillaries (A) and dynamically coated capillaries (B). A: eCAP neutral capillary, total / effective length: 33 cm / 24.5 cm x 50 µm I.D., anolyte: 91 mM H_3PO_4 in CIEF gel, catholyte: 20 mM NaOH, focusing: 15 kV - 6 min, mobilization: 21 kV - 35 mbar (after 6 min), temperature: 25 ^oC and detection: 280 nm. (B): Dynamically coated fused silica capillary total / effective length: 33 cm / 24.5 cm x 50 µm I.D., anolyte: 91 mM H_3PO_4 in CIEF gel, catholyte: 20 mM NaOH, focusing and mobilization: 15 kV - 35 mbar (after 6 min), temperature: 25 ^oC, hydrodynamic injection: 950 mbar - 2 min and detection: 280 nm. Sample: mixture of four standard proteins: ribonuclease A (RN), carbonic anhydrase II (CS), β-lactoglobulin (LG) and cholecystokinin peptide (CK).

The initial increase in the current was attributed to the rapid migration of the CA and to lesser extent the protein molecules during the focusing step. After each protein had reached a position in the capillary where the pH is equal to its pI value, nothing moves inside the capillary and equilibrium was established (i.e. focusing is complete). Then the mobilization of the focused protein bands past the detection window was carried out while the electric field was maintained. The current recorded after the focusing is complete, the "residual current", was attributed to the conductivity of the pH gradient formed by the CA as previously reported (Mosher & Thormann, 2002; Stoyanov, Das, Fredrickson, & Fan, 2005). The increase in the current before the end of the run indicated the gradual decrease in the resistance of the capillary contents, according to Ohm's law, due to the partial filling of the capillary lumen with the anolyte solution under the effect of the applied hydraulic

pressure. In this two-step protocol, the CIEF gel, which has been previously described as a "PEO solution" (T.-L. Huang & Richards, 1997), was added to both the sample and the anolyte solutions. This could be explained by the ability of the PEO polymer to coat any exposed silanol groups on the wall of the coated capillary and thus overcome the poor reproducibility associated with the manufacture of coated capillaries.

5.3 Development of the one-step CIEF protocol

Initially, the two-step CIEF protocol was adapted for the analysis of the same standard mixture but in bare FS coated capillaries. The previously reported protocols for flushing of the new FS capillaries and for pre-conditioning of the capillary surface every morning and before each run were employed as described in Chapter 2 (2.3.6.1) (NaOH then MilliQ water) (Busnel et al., 2005; Gomez & Sandoval, 2008). Subsequently, a one-step CIEF protocol that involved simultaneous focusing and mobilization of protein bands using 15 kV and a hydraulic pressure applied after 6 min of run (Figure 31 - B) was employed. The good resolution that had been achieved within much shorter time (15 min) indicated the successful focusing and mobilization of the protein molecules. The current trace showed the same basic features (as discussed above) with the following differences: i:) a higher current value at the maxima (≈ 6 μA), ii) the equilibrium was not established except for a very short period of time (less than 2 min) and iii) higher value of the residual current.

Several combinations of the voltage and the hydraulic pressure, applied after 6 min, were trialed (Appendix V). The acidic protein standard (CK, pI 3.6) was not detected at all in the absence of a hydraulic pressure. This could be attributed to the negligible magnitude of the residual EOF (after the dynamic coat) at the acidic part of the pH gradient. Thus, the hydraulic pressure was considered critical for mobilizing the focused protein bands, in particular, those of the acidic proteins. The basic protein standard (RN, pI 9.5) was found to elute with approximately the same migration time (tm_{RN} 7.0 ± 0.4 min) even in the absence of an applied pressure which indicated that mobilization at the basic part of the pH gradient was exclusively due to the residual EOF.

In order to simplify the modelling of the combined effects of the experimental conditions, a pressure of 35 mbar was applied from the beginning of the run with a ramp time equal to that employed for the voltage (6 s). Thus, a homogeneous effect of the pressure on the migration time of all protein standards was achieved. These results indicated that the addition of the PEO polymer during sample preparation and to the anolyte solution resulted in formation of a dynamic coat on the capillary wall. This dynamic coat suppressed the EOF to the extent that good focusing of protein bands was achieved. The combined effects of the residual EOF and the applied hydraulic pressure resulted in elution of protein bands in less than 15 min.

The role of the CIEF gel which has been added to the anolyte solution was not clear and its role has not been reported in the literature. The one-step CIEF protocol was repeated under the same experimental conditions except for the anolyte composition. An anolyte solution of the same concentration (91 mM) was prepared in MilliQ water without the addition of the PEO polymer. Results showed an identical electrophoregram and current trace to that obtained in Figure 31 - B which indicated that the inclusion of the PEO polymer in the sample only was sufficient to form a stable dynamic coat. Thus the addition of the CIEF gel to the anolyte solutions was discontinued in future applications. This one-step CIEF protocol was employed in future experiments to optimize the capillary conditioning procedures and the functionality of BGE additives. The current trace provided a novel tool to determine the stop time of the run in order to prevent the complete filling of the capillary with the anolyte solution and thus prevent excessive contamination of the catholyte solution with the anolyte solution.

5.3.1 Capillary conditioning

Most of the capillaries used in CE are made of FS externally coated with a polyimide coat for mechanical strength. Under the effect of the high temperatures involved in the manufacture of the FS capillaries (up to 2000 ^{o}C), the silica surface undergoes complete de-hydroxylation. During capillary storage and in the presence of atmospheric oxygen, the capillary surface becomes hydroxylated to a varying degree (Figure 32).

An irreversible surface treatment is generally carried out before using new capillaries via flushing of the capillaries with 1.0 M NaOH for periods of time ranging from few minutes up to about 1 h. A diagrammatic representation of the irreversible and reversible effects of strong bases and acids on the FS capillary surface is shown in Figure 32 (Gomez & Sandoval, 2008; Pallandre, de Lambert, Attia, Jonas, & Viovy, 2006).

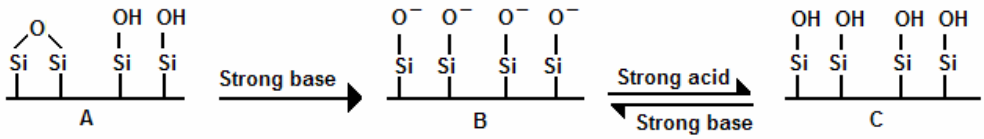

Figure 32: A diagrammatic representation of the fused silica capillary surface of new capillaries (A) and after conditioning with a strong base (B) and a strong acid (C).

The silica surface has been modelled as a polyprotic acid (Figure 32 - C) where adjacent silanol groups have pKa values ranging from 2 to 9 (mean pKa ≈ 6.3). Since the EOF originates from the ionized silanol groups when they come in contact with an electrolyte in the presence of an electric field, it is essential to regenerate the surface between successive runs in order to obtain a reproducible population of charged silanol groups. The pH hysteresis is another factor that complicates the reproducibility of separations in FS capillaries. Briefly, the magnitude of the EOF at a certain pH value depends on how this pH is reached (Horvath & Dolnik, 2001; Strelec et al., 2002).

Measuring the residual EOF in dynamically coated capillaries under CIEF conditions is technically difficult. The CA form a pH gradient that spans the average pKa value of the silanol group and thus, a wide range of residual EOF magnitudes are expected to exist along the capillary length (according to the pH at each point). In this study, the ability to achieve the typical current trace of CIEF applications as well as the reproducibility of migration times of the protein standards was employed to investigate the reproducibility of surface regeneration protocols using the one-step CIEF protocol.

The effect of flushing new FS capillaries from two manufacturers, before the first run and every morning with NaOH solutions of different strengths and for different periods of time was investigated. Results showed that: i) flushing of new capillaries before the first run and every morning with 0.1 M NaOH then MilliQ water for 10 min each, and ii) filling of the capillaries with MilliQ water when not in use was sufficient to achieve good reproducibility. A good run-to-run reproducibility was obtained when the capillaries were pre-conditioned with base followed by acid of the same strength for two minutes each and MilliQ water for at least five minutes. When water was used for flushing the capillaries for periods of time less than four minutes, the typical current trace characteristic for CIEF was not achieved. These results indicated that water helps overcome the pH hysteresis phenomenon reported earlier by the washing-off any remaining traces of the electrolytes used in the preconditioning steps. Water could be involved also in the stabilization of the protonated form of the silanol groups on the surface of the FS capillaries obtained after pre-conditioning the capillaries with acid. These observations were in agreement with what has been reported before that silanol groups must be fully protonated in order to achieve good coating characteristics (Horvath & Dolnik, 2001).

5.3.2 Concentration of the anolyte and catholyte solutions

Five combinations of anolyte / catholyte concentrations were studied over a concentration range of 50 - 200 mM H_3PO_4 and 10 - 40 mM NaOH for the anolyte and catholyte respectively as described in Chapter 2 (2.3.8.4). The electrophoregrams obtained showed a good resolution in all cases with differences in peak shapes and migration times of the standard proteins (Appendix V). These results were in agreement with the previously reported role of the BGE in CIEF that is to mainly prevent pH gradient drift in either direction. A pair of anolyte and catholyte solutions of 100 mM and 20 mM concentration respectively was chosen for future applications.

5.3.3 Functionality of CA

CA are small amphoteric organic amines covering a wide pI range, mixed together in a certain ratio so that the desired pH gradient can be achieved. The exact composition of the commercially available CA preparations is propriety information but it is estimated that they contain several hundred ampholytes per pH unit. Additives such as urea, glycerol and surfactants are often included to help prevent protein precipitation at their pI. It has been reported also that CA can be used to control the EOF, stop protein-wall interaction and as a BGE in CZE applications (Horka, Ruzicka, Horky, Hola, & Slais, 2006; Righetti et al., 1997; Tang & Lee, 1997; C.-X. Zhang et al., 2000).

In this study, two sets of control samples were prepared in order to investigate the role of CA in CIEF separation. Samples were analyzed using the one-step CIEF protocol as described in Chapter 2 (2.3.8.5). The first set was prepared using three protein standards: RN, CS and CK in three different sample matrices and analyzed under the same conditions. Results indicated that CA are certainly essential for the separation but were not enough by themselves to establish an efficient dynamic coat under the experimental conditions employed (Figure 33).

A typical CIEF current profile and good resolution were obtained for samples prepared using both CA and PEO polymer solution (Figure 33 - A). Samples containing CA and no PEO polymer gave separation in less than 2 min (Figure 33 - B) while those prepared using CIEF gel and no CA gave poor results and the typical current trace for CIEF that indicates successful focusing of the protein bands, was not achieved (Figure 33 - C). These results indicated that CA are essential for CIEF separation and are involved in the prevention of protein–wall interaction. The fast onset of the sharp increase in the current that indicates the filling of the capillary with the anolyte solution was noted with samples containing no polymer. These results suggested a role for the sample viscosity in obtaining good resolution.

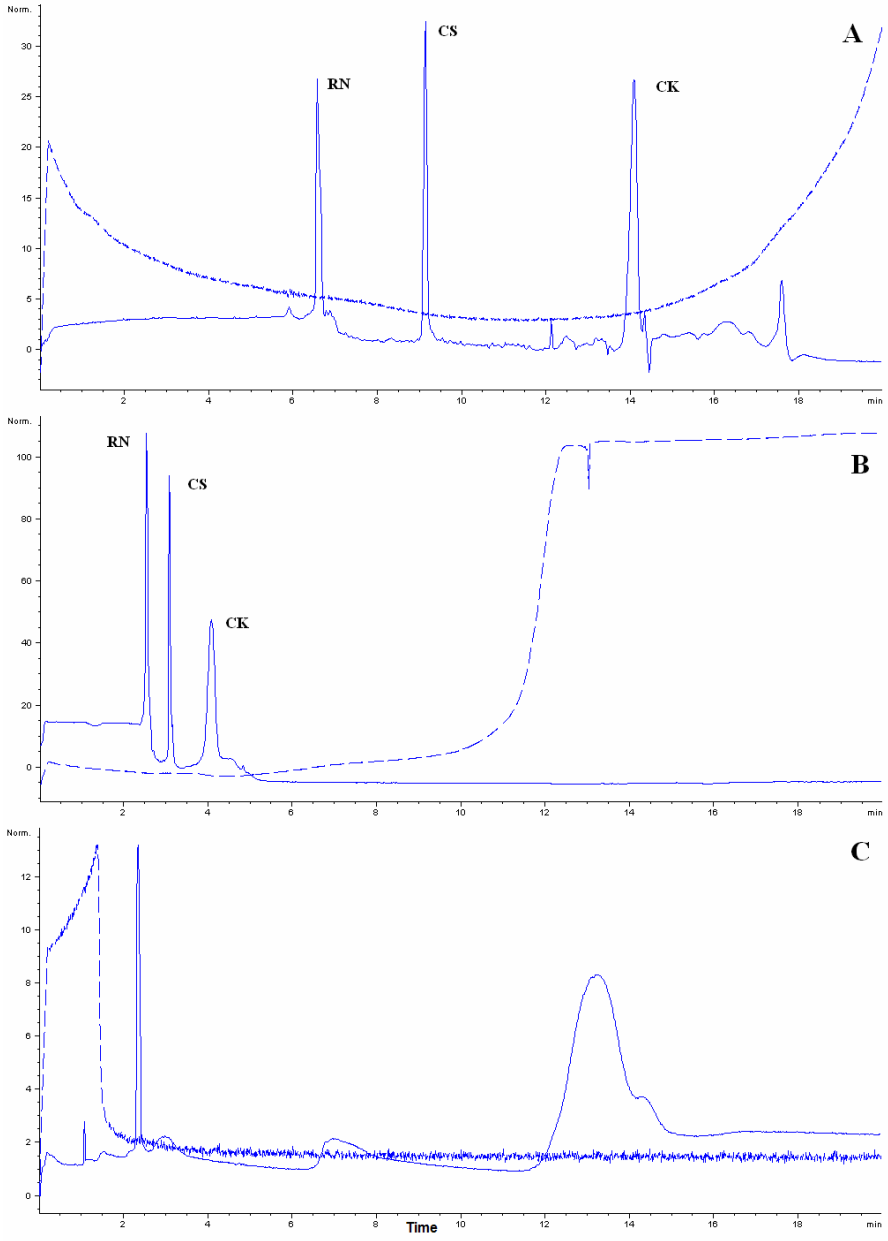

Figure 33: Electrophoregrams (solid lines) and current traces (dashed lines) plotted as normalized responses (Y-axis) of the control samples containing three standard proteins (RN, CS and CK) in 2% CA / polymer solution (A), 2% CA / MilliQ water (B) and 2% MilliQ water / polymer solution (C). Capillary: dynamically coated fused silica of total / effective length: 33 cm / 24.5 cm x 50 µm I.D., anolyte: 100 mM H_3PO_4, catholyte: 20 mM NaOH, focusing and mobilization: 15 kV - 35 mbar, temperature: 25 ^{o}C, hydrodynamic injection: 950 mbar - 2 min and detection: 280 nm.

The role of the CA and the PEO polymer in the suppression of the EOF was investigated further. The second set of control samples containing no protein standards but different concentrations of CA (1 - 3%) prepared in either MilliQ water or polymer solution was analyzed and the current traces were compared. All samples gave the current profile characteristic of CIEF experiments (Figure 34). The recorded values of the current maxima at each CA concentration level were found to be higher (by a factor of 20 - 30%) in the absence of the PEO polymer. These results indicated the key role of the PEO polymer in formation of the dynamic coat and thus suppression of the current. The equilibrium state was reached much faster with samples prepared using CA in water, which confirmed the role of sample viscosity.

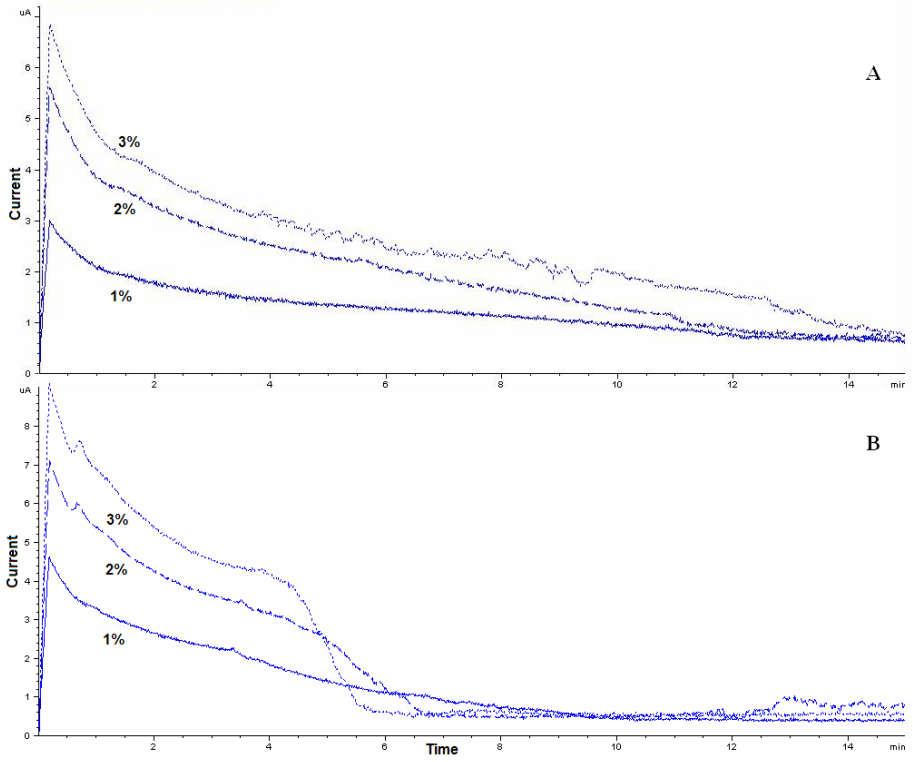

Figure 34: Current traces obtained from the second set of control samples prepared using 1 - 3% CA in either PEO polymer solution (A) or MilliQ water (B). Capillary: dynamically coated fused silica of total / effective length: 33 cm / 24.5 cm x 50 µm I.D., anolyte: 100 mM H_3PO_4, catholyte: 20 mM NaOH, focusing and mobilization: 15 kV - 35 mbar, hydrodynamic injection: 950 mbar - 2 min and temperature: 25 ^{o}C.

5.3.4 Functionality of PEO polymer

Polyethylene oxide is a linear, neutral, hydrophilic polymer which has surface coating properties. PEO is available in a series of molecular weights and the viscosity of PEO solutions depends on both the concentration and the molecular weight of the PEO polymer employed. High molecular weight PEO polymers and co-polymers have been used as sieving matrices in capillary gel electrophoresis of proteins and nucleotides. While low molecular weight ones were used for dynamic coating of the capillary wall to reduce protein and microbial adhesion and in sample stacking applications in CZE (Chang, Chiu, & Chang, 2006; Horka et al., 2006; Horvath & Dolnik, 2001; Y.-F. Huang, Hsieh et al., 2006; Y.-F. Huang, Huang, Hu, & Chang, 2006; Kuo, Chiou, & Wu, 2006; Lupi et al., 2000; Miksik et al., 2006).

Preliminary investigations of the role of the PEO polymer in the suppression of the EOF were carried out using the commercial PEO, marketed by Beckman (USA) under a trade name of "CIEF gel". Deriving conclusions about its role or the optimum conditions was difficult since the composition of the CIEF gel is propriety information. Moreover, the use of such ready-made PEO preparation resulted in more than a ten-fold dilution of the sample while the use of a PEO polymer from a stock solution of a known molecular weight and concentration provided a good alternative to analyze samples under minimum dilution conditions as well as investigate its role in the dynamic coat formation.

A set of control samples containing the most basic protein standard (RN, pI 9.5) and the most acidic protein standard (CK, pI 3.6) was prepared employing different concentrations (0.1, 0.5 and 1.0%) and molecular weight of PEO polymers (100, 300 and 900 kDa) as described in Chapter 2 (2.3.8.6). Samples were analyzed using the one-step CIEF protocol under a wide variety of voltage and hydraulic pressure combinations. The effects of the PEO concentration and molecular weight were investigated at 15 kV and 35 mbar. Results showed that the protein standard migrated faster, under the same experimental conditions, in the presence of 0.1% of the polymer when compared to the 1.0% concentration as shown in Figure 35.

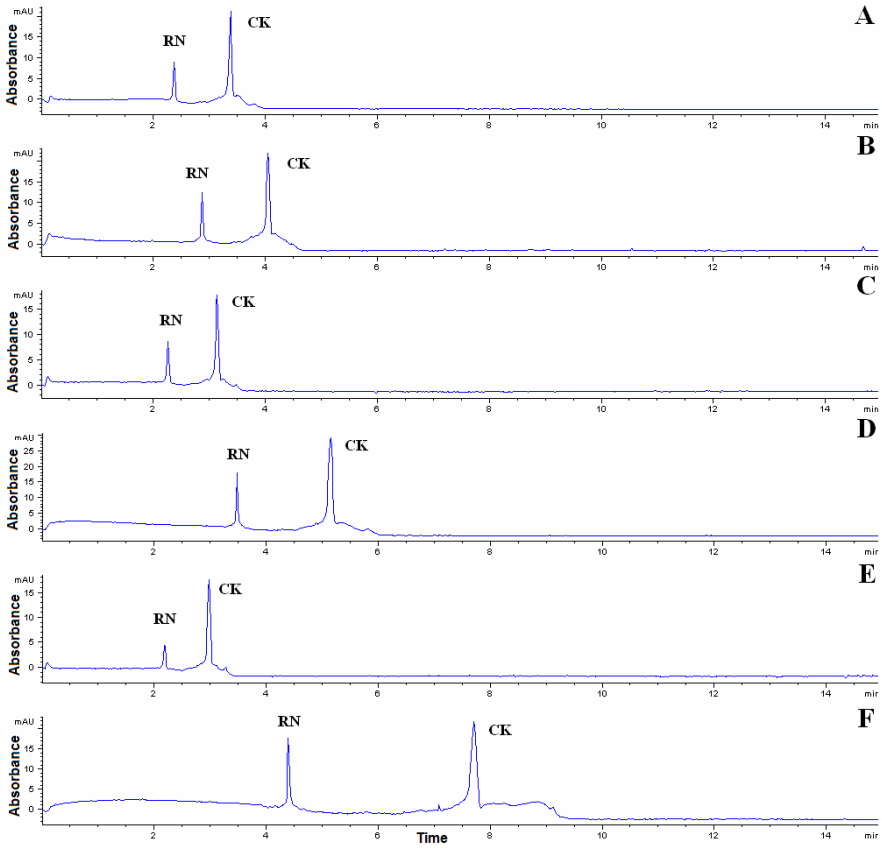

Figure 35: Electrophoregrams obtained from a set of control samples containing two standard proteins (RN and CK) in 2% CA / polymer solution. A: 0.1% PEO 100, B: 1% PEO 100, C: 0.1% PEO 300, D: 1% PEO 300, E: 0.1% PEO 600 and F: 1% PEO 600. Capillary: dynamically coated fused silica of total / effective length: 33 cm / 24.5 cm x 50 µm I.D., anolyte: 100 mM H_3PO_4, catholyte: 20 mM NaOH, focusing and mobilization: 15 kV - 35 mbar, temperature: 25 °C, hydrodynamic injection: 950 mbar - 2 min and detection: 280 nm.

The Δtm between tm_{RN} and tm_{CK} were found to be approximately the same at 0.1% concentration (95% confidence limit), regardless of the polymer molecular weight (Figure 35 - A, C and E) while at 1.0% concentration of each polymer, the Δtm was found to be directly proportional to the molecular weight of the polymer employed (Figure 35 - B, D and F). This could be attributed to either the higher viscosity of the 1.0% PEO solutions in comparison to the 0.1% solutions or the ability of the high molecular weight polymer solutions to form a more efficient dynamic coat at this concentration level and thus affect greater suppression of the EOF.

Lack of differences between the Δtm at 0.1% of each polymer solution was investigated further in the following experiment. Samples prepared using 0.1% of each polymer were analyzed in the absence of an applied hydraulic pressure at 15 kV (Figure 36).

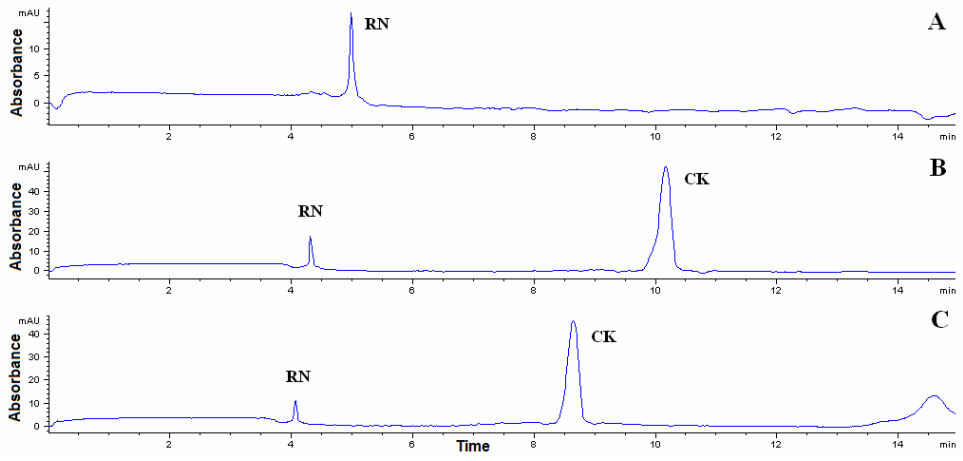

Figure 36: Electrophoregrams showing the effect of PEO molecular weight on residual EOF (0.1% polymer solution, 15kV and 0 mbar). A: PEO 100, B: PEO 300 and C: PEO 600. Capillary: dynamically coated fused silica of total / effective length: 33 cm / 24.5 cm x 50 µm I.D., anolyte: 100 mM H_3PO_4, catholyte: 20 mM NaOH, focusing and mobilization: 15 kV - 35 mbar, temperature: 25 °C, hydrodynamic injection: 950 mbar - 2 min detection: 280 nm.

Both protein standards (RN and CK) were found to migrate faster when the PEO molecular weight was increased from 100 to 600 kDa. The CK protein standard was not detected when 0.1% PEO 100 was used (Figure 36 - A) whereas it was detected as broad peaks when the higher molecular weight polymers were utilized (Figure 36 - B and C). Since the only mobilizing force that exists in the absence of a hydraulic pressure is the residual EOF, it could be concluded that the efficiency of the PEO polymer in forming a dynamic coat is in the order of 100 > 300 > 600 kDa. When the same standard mixture was analyzed in the presence of 0.1% PEO (100 kDa) at 15 kV but in the presence of an increasing hydraulic pressure (Appendix V), the protein standards were found to migrate faster (shorter elution time) and the CK peak size was found to get smaller (shorter residence time at the detector window).

These observations confirmed that the lack of the difference in Δtm noted above (Figure 35) was due to the effect of the hydraulic pressure (35 mbar) which demolished the effect of viscosity at the low polymer concentration range (0.1%).

5.3.5 Factorial design analysis

All the previously obtained results showed that the relationship between the studied variables is complex. Visual comparison of the results presented above (Figure 35 and Figure 36) showed that, it is hard to determine which variable has a statistically significant effect, which variable has more significance than the others or what the interaction between these variables is. The comparison suggested that a more systematic statistical analysis procedure was required in order to determine the relationship between the studied variables. Two full factorial design experiments (3^3) were carried out to study the effects of PEO concentration, molecular weight and voltage at constant pressure (35 mbar) or the effect of pressure at constant voltage (15 kV). The migration time of each marker (tm_{RN} and tm_{CK}) as well as the difference in migration time between the two markers (Δtm) were used as the response variables in the statistical analysis.

Statistical analysis of the results obtained by varying the pressure as well as PEO concentration and molecular weight at 15 kV showed that the effects of pressure and polymer concentration significantly affect the three response variables. The effect of PEO molecular weight was found to have a significant effect on tm_{CK} and Δtm only. A significant interaction between the PEO concentration and molecular weight was noted in case of tm_{CK} only. On the other hand, varying the voltage, PEO concentration and molecular weight at 35 mbar showed that PEO concentration and molecular weight have significant effects on the three response variables while the voltage has a significant effect on tm_{RN} and tm_{CK} but not Δtm. The interaction between the PEO concentration and molecular weight was found to significantly affect the three response variables.

From the above results as well as the P values obtained it could be concluded that the PEO molecular weight has the least significance within the studied variables. The order of significance of the factors studied was in the following order: pressure > PEO concentration > voltage > PEO molecular weight. These results indicated that the nature of interaction between the PEO molecules and the wall of the FS capillaries is basically the same over the molecular weight range studied. The significant interaction between the PEO concentration and molecular weight could be explained in terms of the polymer solution viscosity. In order to achieve good method performance under a certain set of experimental conditions, a certain polymer solution viscosity has to be reached regardless which polymer molecular weight is used. On the other hand, the pressure effect was found to be of more significance than that of the voltage, as long as the voltage is strong enough to establish the focusing. The migration time of the acidic protein marker (tm_{CK}) was found to be more sensitive to changes in the experimental variables, which was in agreement to the previously obtained results.

5.4 Prediction of protein isoelectric point

Determination of the pI of a protein is one of the most important objectives of protein chemists working to develop characterization techniques. It has been previously reported that the accuracy in determination of protein pI using CIEF is only reliable down to the first decimal place and "if you feel like Superman, give them to the second decimal digit, but at your own risk!" (Righetti, 2004). Direct comparison of the pI values determined using the CIEF technique to those obtained using the conventional gel IEF technique is of questionable value for the following reasons: i) pI values are determined using gel IEF under denaturing conditions, ii) heterogeneity in the pH gradient formed by the CA, iii) the non-linear relationship between the migration times and the pI values and iv) interpolation is only valid over small pH ranges and between markers of known pI values (Kundu & Fenters, 1995; Lee, 1997; Righetti, 2004; Rodriguez-Diaz et al., 1997; Shimura, Zhi, Matsumoto, & Kasai, 2000).

5.4.1 Regression model

The mathematical extraction of an empirical relationship between the migration time and the nominal pI values of the standard proteins (under the experimental conditions studied) was carried out. The one-step CIEF protocol and two sets of validation samples were employed as described in Chapter 2 (2.3.8.8). A representative electrophoregram and a current trace for the standard mixture is shown in Figure 37.

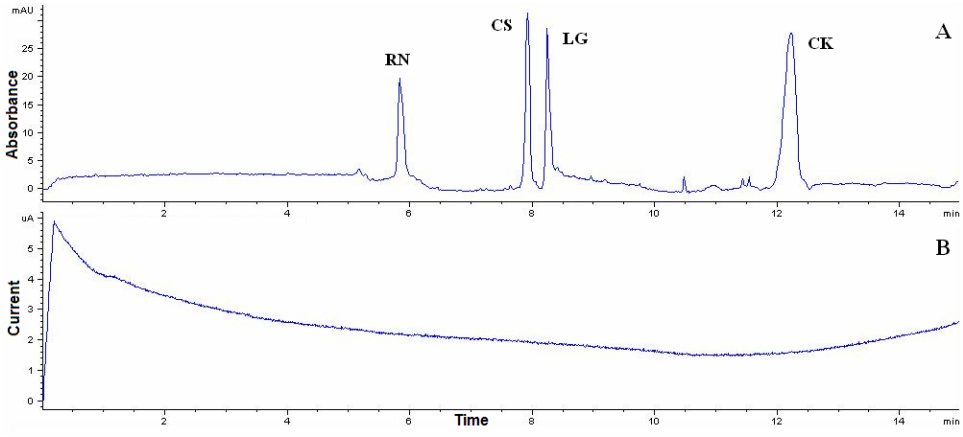

Figure 37: Electrophoregram (A) and current trace (B) obtained using the one-step CIEF protocol. Dynamically coated fused silica capillary total / effective length: 33 cm / 24.5 cm x 50 µm I.D., anolyte: 100 mM H_3PO_4, catholyte: 20 mM NaOH, focusing and mobilization: 15 kV - 35 mbar, temperature: 25 ^oC and hydrodynamic injection: 950 mbar - 2 min and detection: 280 nm. Sample: mixture of four standard proteins: ribonuclease A (RN, pI 9.5), carbonic anhydrase II (CS, pI 5.9), β-lactoglobulin (LG, pI 5.1) and cholecystokinin peptide (CK, pI 3.6).

The migration time of the protein standards in both data sets were compared as shown in Table 5 and no significant difference (ANOVA at Alpha 0.05) was obtained. The data from both sets were pooled together and the pooled mean migration time of each protein standard was plotted vs its nominal pI value (Figure 38). Several models were trialed (linear, polynomial and exponential) since it was not clear from the theoretical understanding which model could be applicable under the current experimental conditions. The correlation coefficient, the average value of the residuals as well as the shape of residuals plot of each protein vs the sample number was used to evaluate the models.

Results were compared to the commonly used linear model (Table 6). The high correlation coefficient, the small value of the average of the residuals as well as the random distribution of the residuals suggested that the second order polynomial was the best fitting model under the experimental conditions employed.

Table 5: Statistical comparison of the reproducibility of the migration time of the four standard proteins in the two data sets.

	Validation set 1				Validation set 2			
	RN	**CS**	**LG**	**CK**	**RN**	**CS**	**LG**	**CK**
Mean*	5.65	7.59	7.94	12.67	5.72	7.75	8.07	12.18
Standard error	0.068	0.109	0.125	0.210	0.038	0.060	0.062	0.090
Confidence level (95.0%)	0.15	0.25	0.28	0.47	0.09	0.14	0.14	0.20

*** Average of ten determinations**

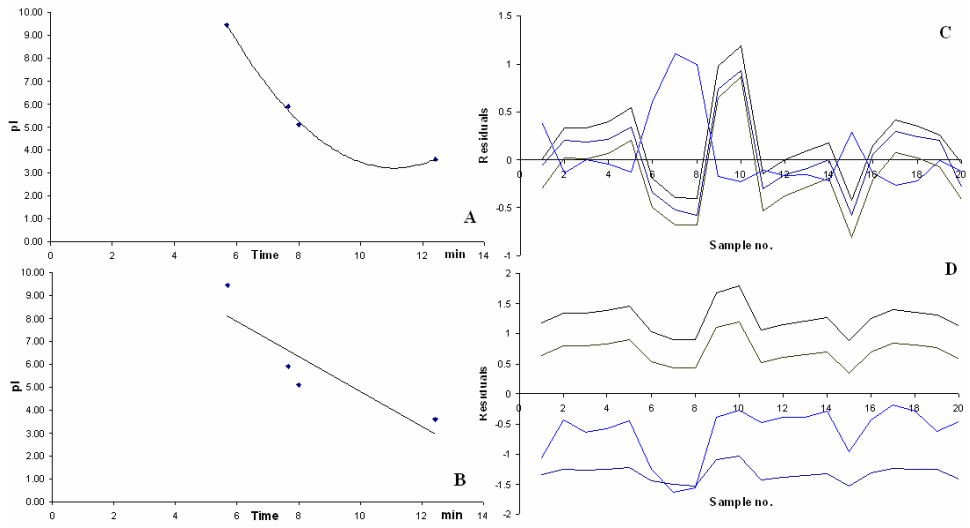

Figure 38: Regression models (A and B) and residuals plots (C and D) using a set of twenty mixtures showing the good fit to the second order polynomial model under the employed experimental conditions.

Table 6: Statistical comparison of the regression models derived using the pooled data set.

	Linear				Polynomial			
Regression equation	y = -0.7668 x + 12.488				y = 0.2141 x^2 - 4.7489 x + 29.552			
R^2	0.771				0.997			
Average residuals*	**RN**	**CS**	**LG**	**CK**	**RN**	**CS**	**LG**	**CK**
	-1.32	0.71	1.25	-0.64	0.02	-0.16	0.18	0.06

*** Average of twenty determinations.**

5.4.2 Cross validation

Cross validation was carried out to evaluate the predictive capability of the second order polynomial regression model. A regression equation was generated for each data set and then the regression equation derived from the first set of data was used to predict the pI values of the standard proteins in the second set of data and vice versa. The mean pI, standard error as well as the confidence level (95.0%) were calculated and compared (Table 7). No significant difference between the results obtained from each set of data suggested good predictability of the second order polynomial regression model.

5.4.3 Reproducibility of the migration time

FS capillaries from two manufacturers, different sets of BGE and samples were analysed within the same day and over two days to investigate the repeatability and the reproducibility of the one-step CIEF protocol respectively. No significant difference (at Alpha 0.05) was found with respect to the mean migration time as well as in integrated peak area suggesting good repeatability, reproducibility and robustness.

Table 7 : Statistical comparison of the results obtained using cross-validation employing the second order polynomial regression model.

	Validation set 1				Validation set 2			
Regression equation	$y = 0.2132x^2 - 4.7429x + 29.457$				$y = 0.2127x^2 - 4.7163x + 29.486$			
R^2	0.997				0.996			
Cross prediction	RN	CS	LG	CK	RN	CS	LG	CK
pI*	9.64	5.97	5.48	3.96	9.30	5.52	5.08	3.33
Standard error	0.157	0.164	0.168	0.158	0.088	0.085	0.079	0.048
Confidence level (95.0%)	0.35	0.37	0.38	0.36	0.20	0.19	0.18	0.11

*** Average of 10 determinations.**

5.5 Application to milk samples

The validated one-step CIEF protocol was used for the screening of the transgenic milk samples for the presence of the rhMBP. The TGmilk samples and milk fractions obtained by centrifugation (CNM and SF) as described in Chapter 2 (2.3.1) were analyzed. Results showed good resolution of the major milk proteins (Figure 39), as confirmed by the analysis of spiked TGmilk samples with protein standards. A good agreement between the electrophoregrams and the expected composition of the milk fractions confirmed the identity of these protein bands. Results were compared to those obtained from an equivalent set of WTmilk samples and fractions (Figure 40). The basic part (tm 1 - 6 min) of the pH gradient in the case of TGmilk and TG-CNM showed several minor peaks of relatively higher intensity than those detected with the corresponding WTmilk fractions.

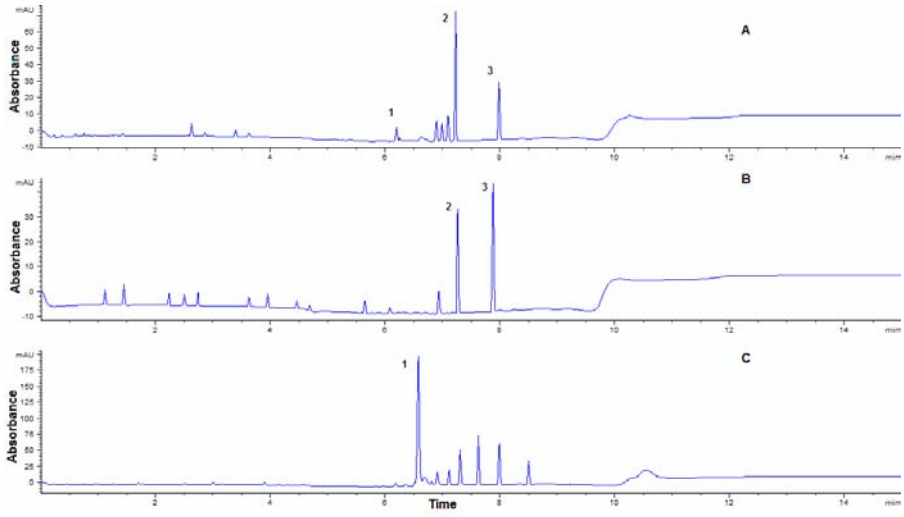

Figure 39: Electrophoregrams showing the protein composition of TGmilk (A), CNM (B) and SF (C) using the one-step CIEF protocol. Dynamically coated fused silica capillary total / effective length: 33 cm / 24.5 cm x 50 µm I.D., anolyte: 100 mM H_3PO_4, catholyte: 20 mM NaOH, focusing and mobilization: 15 kV - 35 mbar, temperature: 25 °C, hydrodynamic injection: 950 mbar - 2 min and detection: 280 nm. (1: LG, 2: β-CN and 3: α_s-CN).

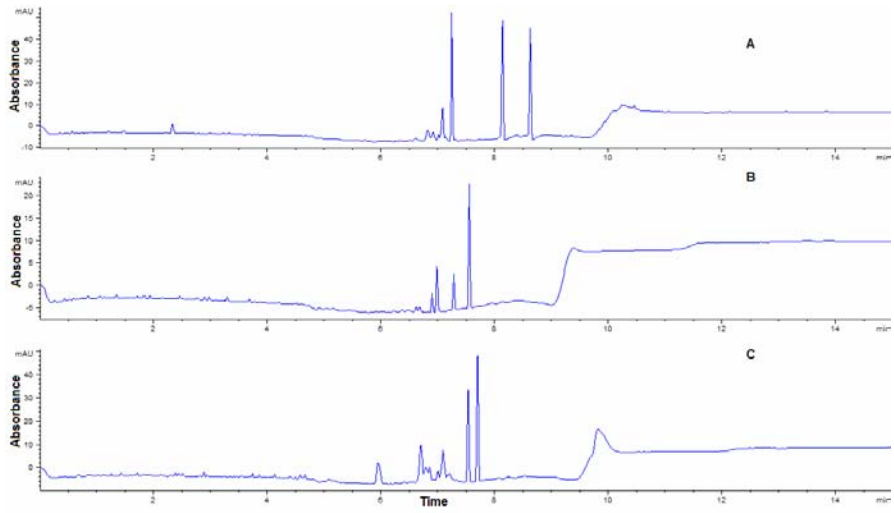

Figure 40: Electrophoregrams showing the protein composition of WTmilk (A), CNM (B) and SF (C) using the one-step CIEF protocol. Dynamically coated fused silica capillary total / effective length: 33 cm / 24.5 cm x 50 µm I.D., anolyte: 100 mM H_3PO_4, catholyte: 20 mM NaOH, focusing and mobilization: 15 kV - 35 mbar, temperature: 25 °C, hydrodynamic injection: 950 mbar - 2 min and detection: 280 nm.

The chromatographic fractions (SPBB and IMAC fractions) that were obtained from the downstream purification protocol as described above (Chapter 2) were analyzed using the one-step CIEF protocol (Figure 41). The peaks corresponding to caseins were still detectable while other proteins eluting between 6 - 9 min were found to be enriched. The casein peaks were detected at longer migration times, which indicated an entire shift in the pH gradient. This could be attributed to the presence of traces of salts in the chromatographic fractions. Owing to this shift, the accurate determination of isoelectric points of the peaks was not feasible using the previously modeled second order polynomial.

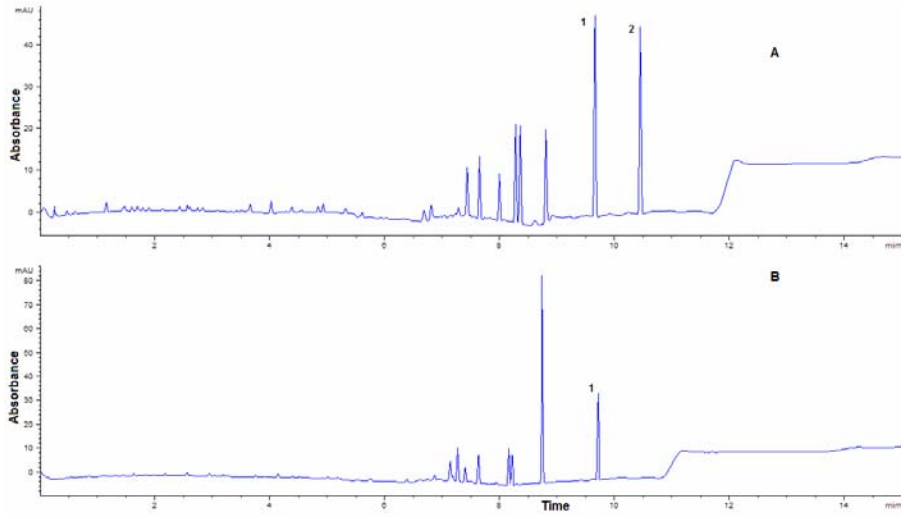

Figure 41: Electrophoregrams showing the protein composition of TGmilk chromatographic fractions: SPBB (A) and IMAC (B) using the one-step CIEF protocol. Dynamically coated fused silica capillary total / effective length: 33 cm / 24.5 cm x 50 µm I.D., anolyte: 100 mM H_3PO_4, catholyte: 20 mM NaOH, focusing and mobilization: 15 kV - 35 mbar, temperature: 25 °C, hydrodynamic injection: 950 mbar - 2 min and detection: 280 nm. (1: β-CN, 2: α_s-CN).

Results obtained from the IMAC fractions confirmed that the peaks previously detected at the basic end of the gradient (Figure 39) do not correspond to rhMBP. The IMAC fractions analyzed in these experiments were shown before to contain the rhMBP isoforms as discussed in Chapter 3 (Figure 15). The absence of peaks which could correspond to highly basic proteins in the IMAC fraction indicated that the rhMBP isoforms have lower isoelectric points than the calculated one (pI 10.5). This observation

supported the assumptions suggested earlier about the nature of the rhMBP isoforms and the effect of the PTM on the physicochemical characteristics of the rhMBP. However, the identity of the detected protein bands can not be confirmed from using UV detection, the CIEF protocol provided an efficient tool to fingerprint the expression pattern of the rhMBP isoforms in TGmilk samples. Further confirmation of the nature of these extra peaks is required via mass spectrometry to confirm that they are not proteolysis products.

5.6 Conclusion

A robust and reproducible one-step CIEF protocol employing economical dynamically coated capillaries was developed. Various separation conditions were investigated in order to determine their effects on the method performance. The effect of long preconditioning steps of the FS capillaries using MilliQ water was found critical for method performance in order to overcome the pH hysteresis phenomenon and thus achieve a reproducible dynamic coat. The catholyte and anolyte concentrations were found not to be critical factors as long as their pH is high / low enough to prevent the pH gradient drift. The effect of PEO polymer concentration was found to have a more significant effect than that of the PEO molecular weight, which indicated that the nature of interaction between the PEO polymer and the FS capillary wall is not sensitive to the PEO chain length. The significant effect of the interaction between the PEO molecular weight and concentration suggested a role for sample viscosity on the resolution. The analysis of transgenic milk samples and chromatographic fractions indicated that the isoelectric points of the rhMBP isoforms do not agree with the theoretical values. Due to the overlap between the isoelectric point of rhMBP isoforms and those of endogenous milk proteins, mass spectrometry was deemed necessary to confirm the identity of the detected bands. Despite this, the one-step CIEF protocol is still applicable for the fingerprinting of the expression pattern of rhMBP in various milk fractions.

Chapter 6

6 Probing the Interaction of rhMBP with Milk Caseins

6.1 Introduction

Milk caseins are examples of intrinsically unstructured / natively unfolded proteins. They form 76 - 86% of total milk proteins and exist in milk as large aggregates or "micelles" of an average radius of 100 nm. Although the size and the protein composition may vary across species, the general structure of the casein micelle is thought to be the same. In the micelles, caseins are held together and organized by a variety of non-covalent forces: hydrophobic interaction, electrostatic interaction, hydrogen bonding and specific calcium-mediated interaction (between phosphoserine residues). A homogeneous network of caseins interlocked by calcium phosphate nanoclusters has become the most accepted model for the casein micelle structure (De Kruif, 1999; Horne, 2002, 2006; McMahon & Oommen, 2008; Swaisgood, 2003).

The rhMBP used in this study was produced in the milk of transgenic cows and was shown to be exclusively associated with the milk micellar phase, as discussed in Chapters 3 and 4. Partial entrapment of recombinant proteins into the milk micellar phase has been previously reported as one of the problems associated with the production of therapeutic proteins in the milk of transgenic animals (Nikolov & Woodard, 2004; Wilkins & Velander, 1992; C. Zhang & Van Cott, 2007). However, complete entrapment of a recombinant protein into the casein micellar phase has not been reported before. The interaction between the rhMBP and milk caseins could be attributed partly to an electrostatic interaction between the numerous basic residues of rhMBP (positively charged at milk pH) and the negatively charged acidic and phosphorylated residues of caseins. However, the noted deviation of the rhMBP behavior from that of a "classic" highly basic, natively unfolded protein (Chapters 3 and 5) suggested that the rhMBP has been modified during its expression. In this study, assumptions explaining the possible mechanisms of the interaction between rhMBP and various milk caseins were investigated. The interaction between the rhMBP and major bovine milk caseins: α_s-CN (α_{s1} and α_{s2}-caseins in a 4:1 ratio), β-CN and κ-CN was studied employing the SPR technique. The interaction patterns were compared to those noted between caseins and the hMBP under the same experimental

conditions. Diffusing wave spectroscopy was employed in order to probe the effects of association of the rhMBP with the casein micelles of transgenic milk.

6.2 Gel electrophoresis and western blotting

At first, differences between the TGmilk and the WTmilk samples were established using SDS-PAGE employing three in-gel protein stains with different affinities (CB, DP and PQ) and western blotting using anti-hMBP antibody as described in Chapter 2 (2.3.11). The three protein stains showed no extra bands corresponding to the rhMBP isoforms in TGmilk when compared to WTmilk as shown in Figure 42.

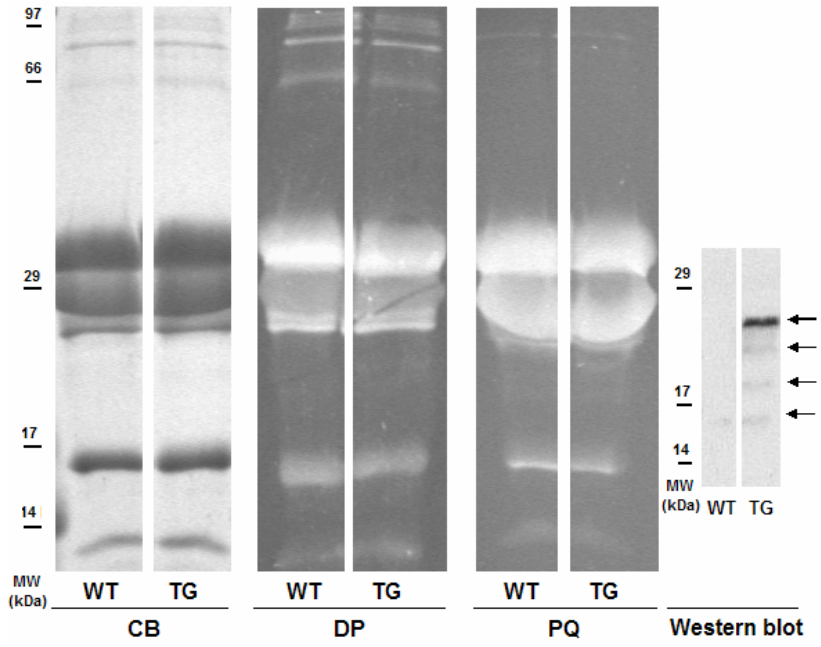

Figure 42: Comparison of milk proteins in WTmilk and TGmilk samples analysed using three different protein stains (left). CB: Comassie Blue, DP: Deep Purple and PQ; ProQ Diamond protein stain. Western blots using anti-hMBP antibody (right) showing the multiple banding pattern with the molecular weight markers highlighted.

Western blotting on the other hand showed bands corresponding to the rhMBP major isoform as well as several minor isoforms of smaller apparent molecular weights

(Figure 42). The position of the band that corresponded to the major isoform of rhMBP relative to those of the marker bands (14 - 29 kDa) indicated an overlap between the apparent molecular weight of the rhMBP major isoform and casein bands. This observation along with the previously reported low levels of expression of rhMBP in TGmilk (2 - 3 mg/ml) relative to the large amounts of caseins in milk (30 - 35 mg/ml), explained the lack of visual differences between the milk samples. When $TGmilk_h$ samples were included in such a comparison (Appendix II) differences were noted with the DP and PQ protein stains. Several bands, which may correspond to the small molecular weight, minor isoforms of the rhMBP were detected. This observation supported the above conclusion about an overlap in molecular weight between the rhMBP major isoform and milk caseins.

The minor isoforms were more abundant in $TGmilk_h$ when compared to TGmilk samples, as indicated by the western blotting analysis (Appendix II). Taking into consideration the ability of the PQ stain to indicate the presence of these isoforms, it could be concluded that the rhMBP isoforms are phosphorylated to different degrees and thus migrated at different velocities under the conditions of SDS-PAGE. Further investigations of the rhMBP isoforms in $TGmilk_h$ are required in order to prove this assumption. Such investigations and why this observation was noted with only the $TGmilk_h$ samples are beyond the scope of this study and will need to be investigated in future work.

6.3 Surface plasmon resonance

The SPR technique is a novel tool for studying protein-protein interaction in real time using a label-free assay format. Immobilization of one protein (ligand) to the surface of a biosensor chip is carried out either directly (hydrophobic or covalent attachment) or indirectly (via immobilization of a capture molecule). The interaction between the immobilized ligand and other proteins (analytes) can be then investigated by flowing samples containing the analyte over the surface of the sensor chip. As analytes bind to the ligand, a change in the SPR response is detected which is proportional to the change in mass at the sensor surface (Boozer, Kim, Cong, Guan, & Londergan, 2006; Myszka & Rich, 2000; Rebecca L. Rich & Myszka, 2000).

Several applications of this technique have been reported in the literature covering drug discovery (Myszka & Rich, 2000; Saefsten, Klakamp, Drake, Karlsson, & Myszka, 2006), biopharmaceutical quality control (Kelner & Bhalgat, 2007) and immunodetection and immunoassay development (Haasnoot, Smits, Kemmers-Voncken, & Bremer, 2004; Muller-Renaud, Dupont, & Dulieu, 2004, 2005; Yang et al., 2005). The SPR technique was previously utilized to study casein-casein interaction employing a different experimental set-up (Marchesseau et al., 2002). In this study, the interaction between the rhMBP and caseins was investigated at the molecular level as described in Chapter 2 (2.3.9).

6.3.1 Experimental design

Two different ligand molecules (rhMBP / hMBP) were immobilized to the surface of the sensor chip using a specific capture molecule (anti-hMBP mAb). The interaction between the immobilized ligand and various caseins was then investigated in the presence of different NaCl / $CaCl_2$ concentrations. The capture approach was considered superior to direct immobilization of ligand molecules to the sensor surface in this study. It enabled comparison of the interaction patterns of either the rhMBP or the hMBP with milk caseins using the same sensor chip. Ligand capture allowed further purification of the rhMBP before studying its interaction with caseins. Thus, non-specific responses which may originate from casein impurities in the rhMBP preparation were avoided.

6.3.2 Method development

The surface of the CM5 sensor chip was prepared as described in Chapter 2 (2.3.9.1). An acetate buffer of pH 4.5 was employed for the preparation of the anti-hMBP mAb solution. At this pH, the antibody molecules carry a net positive charge (pH < pI) while the carboxymethylated sensor surface is negatively charged (pH > 3.5). Under these conditions, pre-concentration of the antibody at the sensor surface, via electrostatic interaction, thus high levels of covalently-bound antibodies were achieved.

The surface of the sensor chip in Fc-2 was activated by injection of a freshly prepared mixture of NHS:EDC then the antibody solution was injected in sequential pulses until the target immobilization level was achieved (10,000 RU). Subsequently, an EtA solution was injected in order to deactivate the residual active sites in the CM dextran matrix. An increase in the SPR response of approximately 10,000 RU corresponded to the baseline after the coupling step was noted (Figure 43). A similar protocol but without the antibody was employed in order to deactivate the sensor surface in Fc-1. In all future experiments, samples were injected simultaneously into both flow cells and the difference in the SPR signals (RU_{Fc-2} - RU_{Fc-1}) was considered as the SPR response. This manipulation allowed the correction for non-specific binding to the sensor matrix as well as for the shifts in the baseline due to differences in refractive index of injected samples (due to the presence of salts).

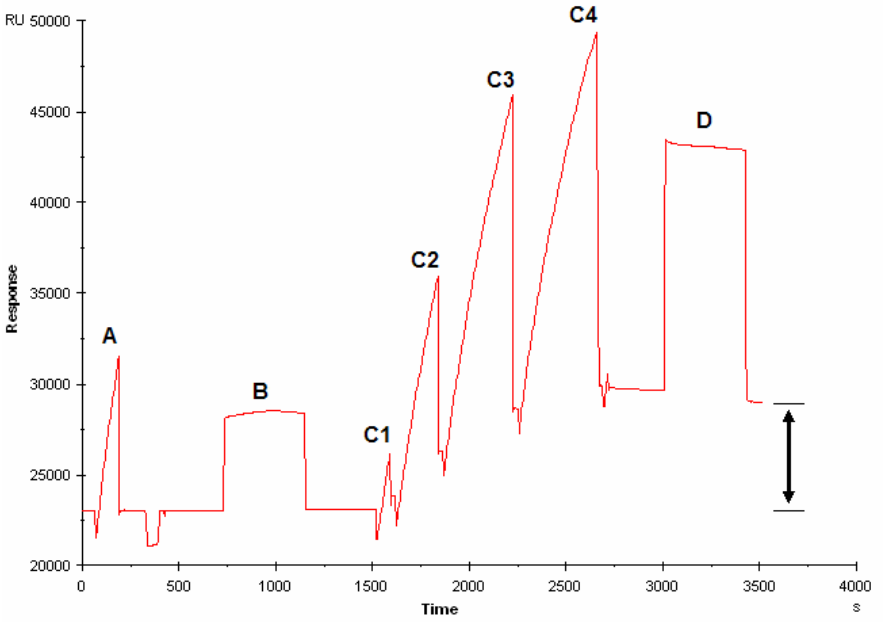

Figure 43: A sensogram representing the change in the SPR response (RU) during various steps of CM5 sensor surface preparation. A: a test of the electrostatic binding of the anti-hMBP antibody to the surface, B: surface activation step using NHS / EDC mixture, C1 - C4: covalent attachment of the anti-hMBP antibody and D: surface deactivation using EtA solution. The double arrow indicates the increase in the SPR response caused by the covalently immobilized antibody.

A preliminary experiment for testing the ability of the imunosensor chip to bind the rhMBP was carried out using a standard series of the recombinant protein over a wide concentration range. Samples were injected sequentially allowing a dissociation time of 200 s between injections. An increasing cumulative response was noted upon analyzing the standard series without surface regeneration between injections (Figure 44).

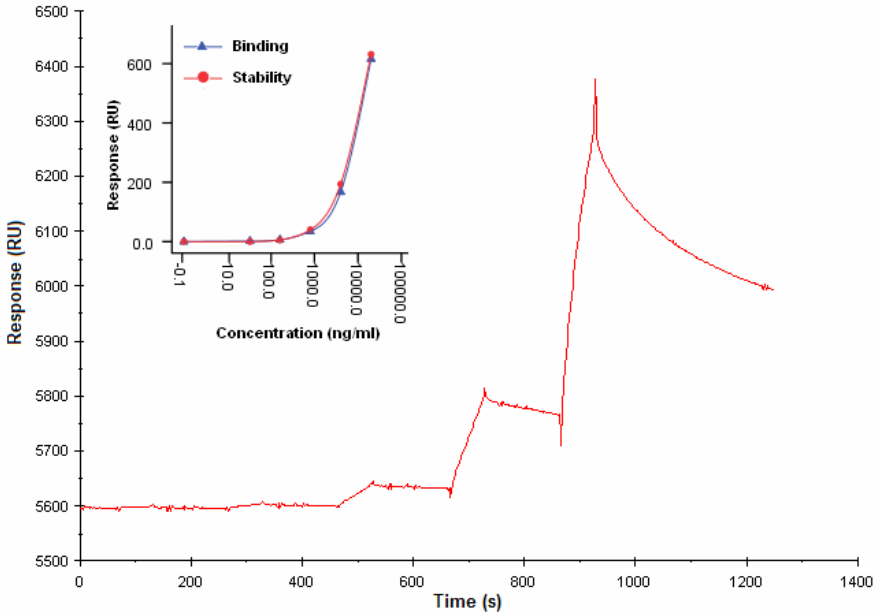

Figure 44: Sensogram representing the change in SPR response over the run time showing the cumulative response upon sequential injection of five standard solutions of rhMBP (32.0 ng/ml – 20.0 µg/ml). A plot of the binding and stability responses vs rhMBP concentration overlaid. Sensor: CM5 with covalently immobilized anti-hMBP monoclonal antibody, running buffer: HEPES-EP buffer, flow rate: 10 µl/min, binding time (injection time): 60s, dissociation time: 200s and sample: rhMBP standard in HEPES-EP buffer. The binding and stability responses were recorded after 50s and 20s respectively of the start of the corresponding step.

Results showed an agreement between the binding and the stability responses after each injection cycle, which indicated the ability of the antibody-bound sensor surface to retain rhMBP while the running buffer is flowing (dissociation phase). The high binding stability was reflected on the sensogram by an increase in the baseline after each injection cycle. The relatively large drop in response during the dissociation phase of the highest

standard concentration, suggested multilayered binding of rhMBP to the surface. These results showed clearly that the anti-hMBP mAb is suitable for studying the interaction between rhMBP and milk caseins.

A 10.0 µg/ml rhMBP standard solution was prepared in 10 mM HEPES buffer - pH 7.0 (HEPES-1) and employed to optimize a surface regeneration strategy that can effectively remove any bound ligand molecules without affecting the covalently immobilized capture molecules (anti-hMBP antibody). A series of glycine-HCl buffers (pH 3.0 – 2.0) was prepared and brief pulses of each buffer were tested in order of decreasing pH. A good reproducibility of both the binding responses and base line responses at pH 2.0 confirmed that surface regeneration has been successfully achieved using this buffer without denaturing the capture antibody. The optimized protocol was employed for the analysis of blank (running buffer, HEPES-1), WTcontrol (negative control), rhMBP and hMBP samples as described above (Figure 45). Lack of any binding response from either the blank or WTcontrol samples showed no matrix interference. The good reproducibility of the binding responses (over triplicate runs) with both rhMBP and hMBP samples confirmed the suitability of the regeneration protocol for both ligands.

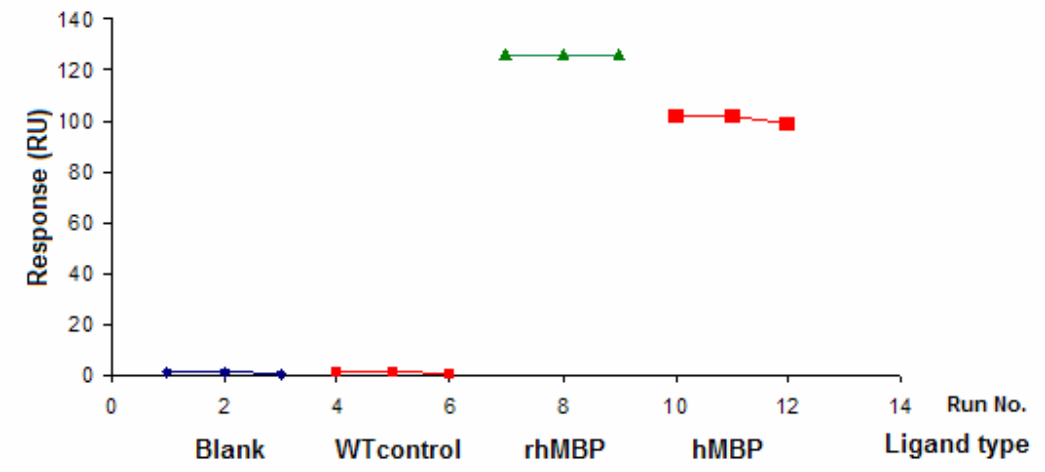

Figure 45: A plot of the binding responses (triplicate) of blank, WTcontrol, rhMBP standard (2.0 µg/ml) and hMBP standard (1.0 µg/ml) showing lack of matrix interference and good reproducibility of the SPR signals.

6.3.3 Concentration measurements

Preliminary experiments showed that the immobilized anti-hMBP antibody reacts with the hMBP and cross reacts with the rhMBP with sufficient stability. However, binding responses obtained in the case of the hMBP standards were significantly higher than those obtained when equivalent concentrations of the rhMBP were employed. This difference was attributed to host-related differences in the PTM of each protein. Such effects on protein-protein interactions in general and on antigen-antibody interaction in particular have been reported before (Meri & Baumann, 2001; Robinson, 2006; Sims & Reinberg, 2008). These differences supported our hypothesis attributing the unexpected behaviour of the recombinant protein discussed in the previous chapters to differences in PTM. A different experimental set-up is required in order to compare the binding affinities of both ligands to the anti-hMBP antibody and needs to be investigated in future work.

In this study, we focused on the comparison of the interaction between either rhMBP or hMBP and milk caseins. In order to ensure a valid comparison, an equivalent amount of either the rhMBP or the hMBP was bound to the sensor surface. Next, the casein solutions were flowed over the surface and the interaction patterns were studied under different experimental conditions. Two sets of standard solutions of the rhMBP and of the hMBP were prepared, analysed as described and the concentration-response curves were generated (Figure 46). Since the SPR response depends on the amount of protein bound to the surface, two concentrations of the rhMBP (3.03 μg/ml) and of the hMBP (1.67 μg/ml) were selected so that approximately the same SPR response is achieved.

The response plots were found to fit to the 4-PL regression model and thus could be employed in an independent SPR immunoassay for the rhMBP employing either hMBP or rhMBP standards in order to generate a calibration curve. The SPR assay is particularly useful for the determination of the rhMBP concentration after the removal of the His tag in future product development stages. While the Bio-Plex assay is superior during the downstream purification stages, it can determine full length rhMBP only. A comparison between the SPR immunoassay and the Bio-Plex immunoassay is described below (Appendix IV - Table 9).

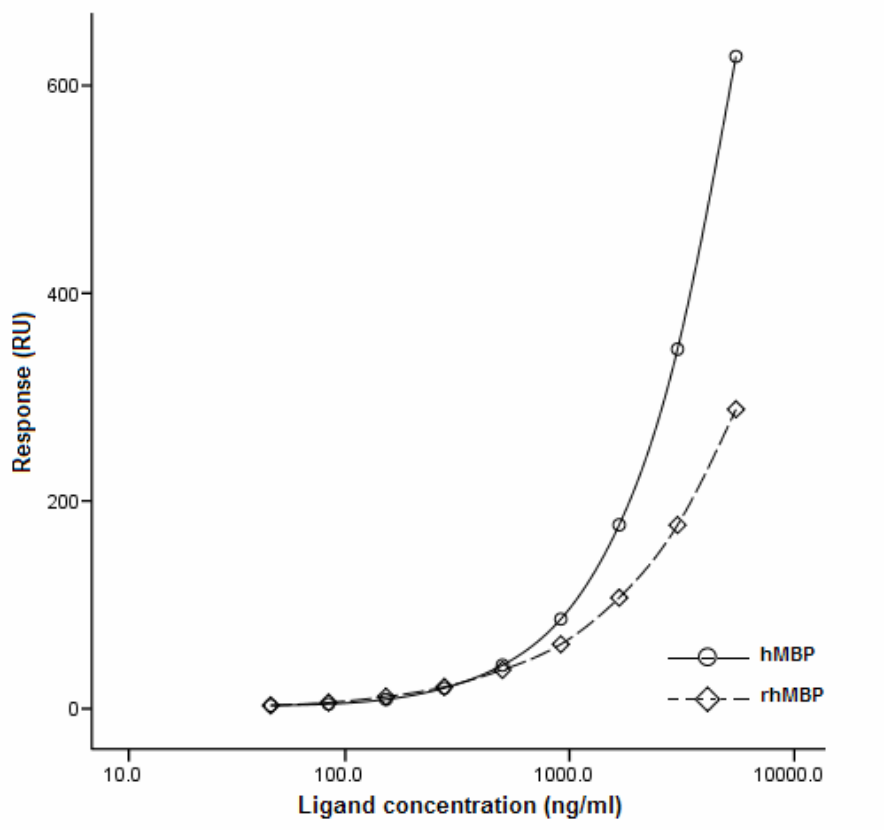

Figure 46: Two plots of the SPR response (RU) vs the concentration (ng/ml) of either the rhMBP or the hMBP showing a difference in the binding patterns of both proteins to the immobilized anti-hMBP antibody under the same experimental conditions.

6.3.4 Interaction analysis

All experiments were carried out using 10 mM HEPES - pH 7.4 as the running buffer and for the preparation of ligand solutions. At this pH, both hMBP and rhMBP showed good binding and stability responses to the immobilized capture molecule (anti-hMBP antibody). Moreover, the multimerization state of all caseins was previously studied at this pH and α_s- and β-CN were found mostly monomeric (≈ 70% and 80 - 90% respectively) while κ-CN was found to form aggregates (> 100 kDa) at this pH and over a wide pH range (Marchesseau et al., 2002). Subsequently, the interaction between rhMBP / hMBP and milk caseins was investigated using a set of HEPES based buffers as described above and in Table 3 (Chapter 2).

No interaction was noted between rhMBP / hMBP and various caseins in the absence of either NaCl or $CaCl_2$ (Figure 47). This could be attributed to electrostatic repulsion between caseins and the ligand molecules. Both ligands showed notable increases in the binding response with caseins in the presence of 150 mM NaCl following the order of κ- > β- > α_s-CN. The effect of NaCl could be attributed to the screening of the charges carried by both casein and ligand molecules allowing binding to occur (H. M. Farrell, Jr., Kumosinski, Malin, & Brown, 2002; Marchesseau et al., 2002). Both of the rhMBP and the hMBP showed the same order but with slightly higher responses in the case of hMBP (Figure 47).

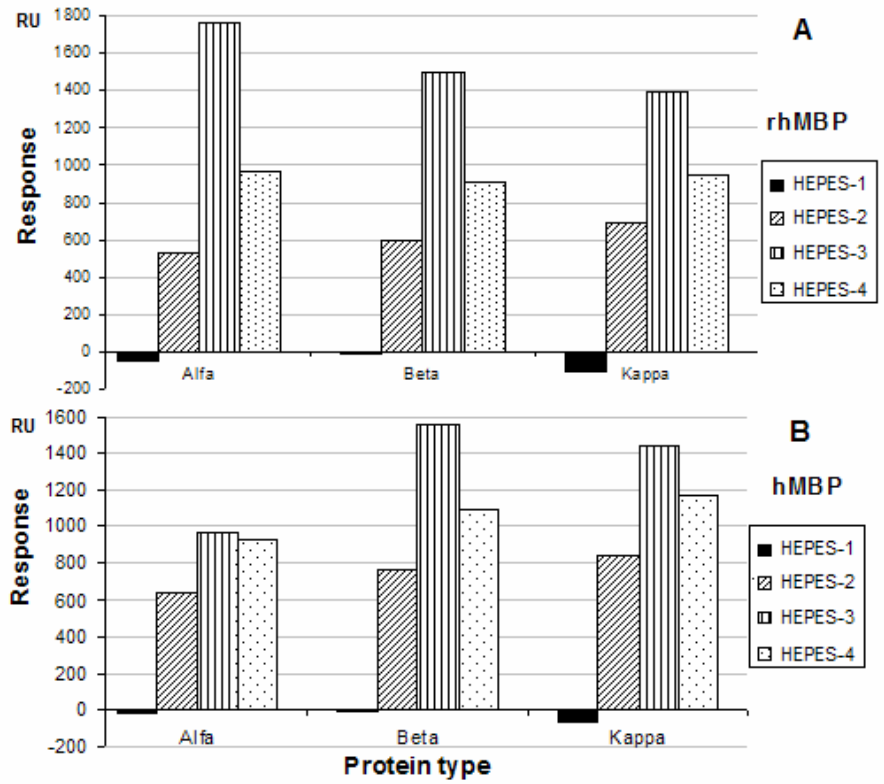

Figure 47: The impact of salt on the interaction responses between rhMBP (A) and hMBP (B) and different caseins. All buffers contain 10 mM HEPES, pH 7.4 with different salt composition: HEPES-1; no added salt, HEPES-2; 150 mM NaCl, HEPES-3; 10 mM $CaCl_2$, HEPES-4; 150 mM NaCl and 10 mM $CaCl_2$.

In the presence of 10 mM $CaCl_2$ that is close to the concentration of soluble calcium concentration in milk (Gaucheron, 2005), notable increases in binding response were observed in the case of rhMBP (Figure 47 - A) with an order of α_s- > β- > κ-CN (directly proportional to the number of phosphorylated residues on caseins). This increase in binding responses (especially with α_s-CN) as well as the order of the binding values suggested a calcium-mediated interaction between rhMBP and caseins. Such calcium mediated interaction has been previously reported, under similar experimental conditions, using the same technique when the interaction between different caseins was investigated (Marchesseau et al., 2002).

The interaction pattern between the rhMBP and caseins was very similar to that observed between immobilized α_s-CN and other caseins in the presence of calcium (Marchesseau et al., 2002). This interaction was explained on the basis of formation of calcium bridges between the negatively charged residues (mainly the phosphorylated residues) on casein molecules. The same explanation could be valid in the case of the interaction between the rhMBP and caseins. Although hMBP showed an increase in the binding values with all caseins (relative to those obtained in the presence of NaCl), it did not show a similar trend of interaction (β- > κ- > α_s-CN) to that obtained with rhMBP. Such a trend could be explained on the basis of the hydrophobicity of caseins. In the presence of calcium, self association between caseins (neutralization of the effect of the negatively charged residues) is possible giving a chance for other intermolecular forces to be established, mainly hydrophobic forces. Differences in the interaction patterns between the rhMBP and hMBP confirm our hypothesis suggesting differences between both molecules (Figure 47). The calcium dependent interaction between rhMBP and caseins and the order noted suggested that these differences were due to phosphorylation of the recombinant protein by the mammary gland.

Upon analysing the same calcium-containing samples but in the presence of NaCl, the effect of calcium was significantly attenuated by the presence of NaCl. These results were in agreement to those reported for the interaction between caseins in presence of calcium and different concentrations of NaCl as studied by SPR (Marchesseau et al., 2002).

Moreover, this agrees with the previous reports on the behaviour of micellar calcium upon addition of NaCl to milk samples (Gaucheron, 2005; Holt, 1992). In the case of rhMBP, the binding levels were all reduced to approximately the same value which indicated that the interaction noted in the presence of calcium was due to calcium bridging while with hMBP, the reduction in response ($RU_{CaCl2} - RU_{CaCl2/NaCl}$) showed the order κ- > β- > α_s-CN. This observation confirmed the role of calcium in the screening the effect of phosphorylated residues of caseins as discussed above.

The calcium-mediated interaction between the rhMBP and α_s-CN was investigated in more detail in the presence of different types and concentrations of salts as follows: i) no added salts, ii) NaCl (75, 150 and 300 mM), iii) $CaCl_2$ (5, 10 and 20 mM) and iv) 10 mM $CaCl_2$ in the presence of increasing concentrations of NaCl (75, 150 and 300 mM). Again no interaction was observed in the absence of either NaCl or $CaCl_2$ as discussed above (Figure 48 – run 1).

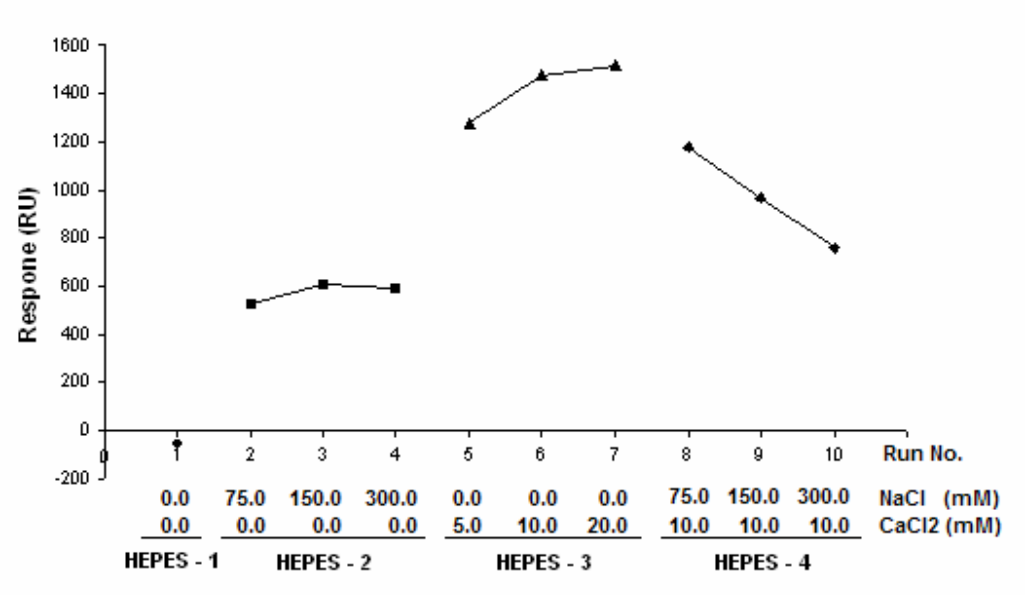

Figure 48: The effect of buffer composition on the interaction between the rhMBP and α_s-CN. All buffers contains 10 mM HEPES, pH 7.4 with different salt composition. HEPES-1: no added salt, HEPES-2: 75 - 300 mM NaCl, HEPES-3: 5 - 20 mM $CaCl_2$, HEPES-4: 75 – 300 mM NaCl and 10 mM $CaCl_2$.

The effects of NaCl and $CaCl_2$ were in agreement to what have been described above. Upon increasing the NaCl concentration, the interaction between the rhMBP and α_s-CN was found to increase (Figure 48 - runs 2 - 4). Such a trend confirmed the effect NaCl has on improving the interaction via the screening of the charges on both molecules, which is the prevalent effect at low salt concentrations. On the other hand, the interaction between the rhMBP and α_s-CN in the presence of different concentrations of $CaCl_2$ showed a notable increase upon increasing the concentration from 5 – 20 mM. The binding response approached a plateau between 10 – 20 mM $CaCl_2$ (Figure 48 – runs 5 - 7) which suggested that all negative sites of both molecules have been cross linked via calcium bridges. The effect of an increasing concentration of NaCl (0.0 – 300.0 mM) in the presence of 10 mM calcium showed a linear drop in the binding response (Figure 48 – run 6 and 8 - 10), approaching that obtained in the presence of NaCl only (Figure 48 - runs 2 - 5). These results were in agreement with the previously reported results of the interaction between α_s- / α_s-CN under similar experimental conditions (Marchesseau et al., 2002).

6.4 DWS investigations of the micelle properties

In this section, the effects of the noted interaction between the rhMBP and caseins on milk physical properties were investigated employing a non-invasive light scattering technique. The DWS is very similar to the traditional dynamic light scattering since both techniques follow fluctuations in intensity of scattered light over the time scale (correlation function). Conventional dynamic light scattering requires the sample to be highly diluted which severely restricts its relevance to real systems. On the other hand, DWS is based on the detection of photons that have been subjected to many scattering events and thus requires highly concentrated systems. In such a situation, light propagates in a diffusive manner gathering information not only on the dynamics of the scatterers (measure of the time dependence of MSD) but also the static properties of the system (changes in the structure of scatterers through measuring photon transport mean free path length l^*) (Corredig & Alexander, 2008; Donato et al., 2007).

6.4.1 Casein micelle size

In this experiment, DWS was utilized to compare the average casein micelle size in TGmilk to that of WTmilk samples as described in Chapter 2 (2.3.10). The extracted average micelle radius for WTmilk and TGmilk were (108 ± 8 nm) and (100 ± 20 nm) respectively (95% confidence limits), demonstrating that within experimental uncertainties there is no difference between the average micelle size in both milks (Figure 49).

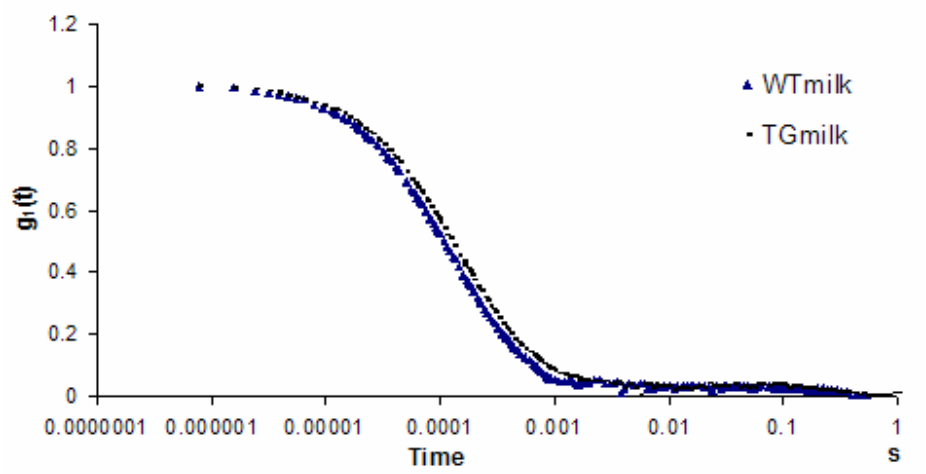

Figure 49: The autocorrelation functions obtained upon analyzing the TGmilk and WTmilk samples showing an overlap in casein micelle dynamics and indicating a close average micelle size in both milks.

Taking into consideration the wide distribution of casein micelle radius (50 – 500 nm - average of ≈ 100 nm), the dependence of the results on the technique employed (De Kruif & Holt, 2003; Fox, 2003; Holt, 1992) and the low level of expression of the recombinant protein (2 - 3 mg/ml), it could be understood why a small variation in casein micelle composition could have a negligible effect on the average micelle size. Other genetic manipulations which resulted in notable differences in the concentration of caseins in milk showed significant changes in micelle average radius and smaller micelles were formed upon either disruption (elimination) of the β-CN gene (Kumar et al., 1994) or significantly increasing the level of expression of the κ-CN gene (Brophy et al., 2003; Gutierrez-Adan et al., 1996; Laible & Wells, 2007).

6.4.2 Casein micelle stability

Casein micelles are believed to be surrounded by a "hairy layer" or a "salted brush" formed by the κ-CN providing a steric and electrostatic stabilization. The hydrophilic part of κ-CN (glycomacropeptide, residues 106 - 169) carries the glycosylated sites as well as approximately 14 acidic groups which are deprotonated at physiological pH. The rest of the molecule (para κ-CN, residues 1 - 105) is very hydrophobic and thus interacts with other caseins in the internal micelle network (Swaisgood, 2003).

Acidification of milk is a complex process which leads to aggregation and gelation of the casein micelles at pH ≈ 4.9. As the pH of milk decreases from its normal value of ≈ 6.7, micellar calcium phosphate gradually dissolves until it becomes soluble at pH near 5.2. Subsequently a collapse of the κ-CN layer is observed upon decreasing the pH of milk to ≈ 4.9 (Holland, Deeth, & Alewood, 2004) resulting in the loss of micelle stability and gel formation. It has been reported that the stability of casein micelles and hence the onset of acid gelation is sensitive to micelle surface charges and milk serum composition. This was demonstrated by the change in the onset of acid gelation of pre-heated milk as well as non pre-heated milk which has been spiked with denatured (heated) serum proteins (Marcela Alexander & Dalgleish, 2004; Corredig & Alexander, 2008; Holt, 1992). Such changes were attributed to the interaction between denatured serum proteins and the casein micelle surface.

In this experiment, the acid gelation behavior of the TGmilk was compared to that of the WTmilk and the effect of the presence of rhMBP on micelle stability was investigated. Analysis was carried out as described in Chapter 2 (2.3.10) and the MSD slope was plotted vs pH of milk. Changes in MSD slope versus time function have been used previously to observe the acid-induced gelation of milk (Marcela Alexander & Dalgleish, 2004; M. Alexander et al., 2002; Corredig & Alexander, 2008; Dalgleish, Alexander, & Corredig, 2004). In particular, the slope of the MSD versus time data is used as an indicator of the type of network formed. As gel formation upon acidification of milk is clearly dependent not only on the micelle size but also its charged state, it was considered that performing such an experiment with TGmilk would reveal if the recombinant protein

had a significant effect on the surface charge distribution and / or the nature within the micelle. Results showed that after slow acidification with GDL, a viscous medium was still found as indicated by a slope close to 1 down to ≈ pH 5.0 (a signature of a viscous solution where micelles are freely diffusing) as shown in Figure 50. Subsequently, below pH 5.0, the MSD slope started to decrease approaching a value of 0.5 which represented formation of a flexible network.

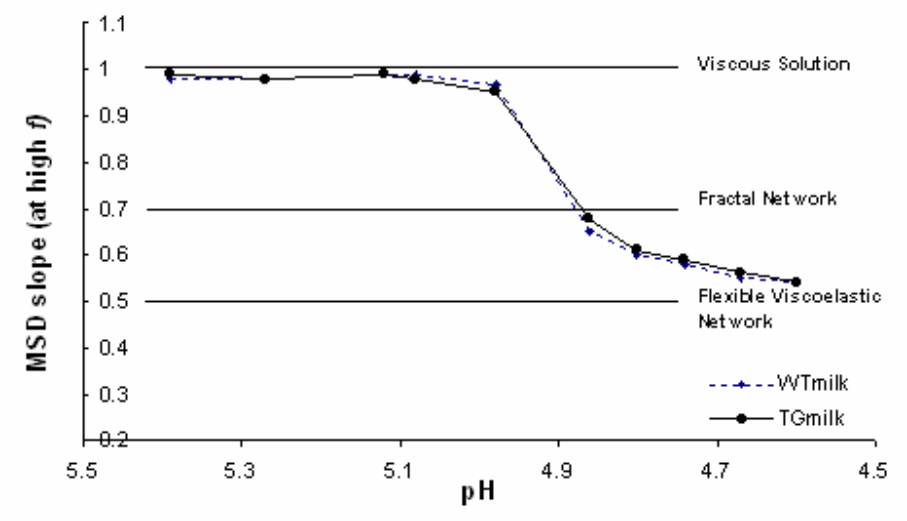

Figure 50: A plot representing the change in MSD slope at high frequency with pH of milk sample showing the change in the nature of milk sample upon acidification from "viscous solution": slope ≈ 1.0 to "flexible viscoelastic network": slope ≈ 0.5.

These results clearly showed that the way in which the MSD slope changed as acidification proceeds was indistinguishable between the WTmilk and TGmilk which suggested the lack of any effect of the rhMBP on micelle surface charge. These results supported our hypothesis that the rhMBP is deeply entrapped within the micelles and not adsorbed electrostatically at the negatively charged micelle surface. These results provide further evidence that the relatively small expression levels of the transgenic protein are insufficient to significantly alter the main physiochemical characteristics of the micelles.

6.5 Conclusion

The behaviour of the model recombinant human biopharmaceutical protein (rhMBP) expressed in milk of Tg animals has been investigated using SPR and DWS techniques. Binding experiments carried out using SPR technology revealed that the rhMBP can interact with milk caseins under different conditions and specifically with α_s-CN through calcium bridging. The interaction patterns between the rhMBP and various milk caseins were found to be different from those obtained when the hMBP was employed under the same experimental conditions. Such differences were attributed to host-related differences in the PTM patterns of both proteins. Results obtained from DWS experiments showed that at these low expression levels, the rhMBP did not alter the average size of the micelle or its stability towards acids. Further investigations are required in order to investigate if association of the recombinant protein with the micelle controlled the rate of its expression in a similar way to milk caseins.

Chapter 7

7 General Discussion and Future Directions

7.1 Recombinant hMBP: the “fifth casein” hypothesis

The rhMBP was produced in the milk of transgenic cows as a model for production of biopharmaceutical proteins in farm animals. An automated downstream purification protocol which tackled the association between the rhMBP and casein micelles was successfully developed. An orthogonal testing protocol that employed electrophoretic techniques along with immunodetection was developed and integrated with the purification protocol. The CIEF protocol and the Bio-Plex immunoassay were able to determine the expression patterns and levels of the rhMBP in milk respectively while the SPR immunoassay was suitable for the analysis of the recombinant protein even after the removal of the His tag. The CZE method was able to quantify the rhMBP in milk and in the chromatography fractions.

Milk fractionation showed that the rhMBP was exclusively associated with the casein micellar phase. The selective precipitation of caseins using CAP showed a tendency of the rhMBP to associate with calcium. Although this high degree of association between the rhMBP and casein micelles was not expected, it explained the following observations: i) the slow kinetics controlling the release of rhMBP from the micelles, ii) the high stability of the rhMBP in TGmilk samples, when compared to that in chromatography fractions (after micelle disruption) and iii) the non availability of the rhMBP to interact with the anti-hMBP antibody-coupled beads when a Bio-Plex assay was utilized for the quantitative determination of the rhMBP in TGmilk.

The noted microheterogeneity of the rhMBP was attributed to the presence of charge isoforms of the rhMBP due to PTM during expression. Several observations supported this conclusion: i) the recombinant protein was found to elute from the cation exchange resin with salt strength less than 0.5 M NaCl, contrary to what would be expected for a highly basic, natively unfolded protein, ii) the rhMBP was detected in fractions collected over a broad NaCl concentration range (0.15 - 0.45 M) which indicated that these

isoforms exhibit different affinities for the cation exchange resin and iii) CIEF analysis of milk samples did not reveal the presence of highly basic proteins in TGmilk.

Differences in the interaction patterns between the rhMBP and either monoclonal anti-hMBP antibody or milk caseins, when compared to those obtained employing the hMBP revealed host-related differences. These differences were attributed to differences in PTM patterns of both proteins, typically phosphorylation. This conclusion was supported by the following: i) the rhMBP contains residues that can be phosphorylated and the mammary gland has the required machinery to achieve this, ii) the charge isoforms and the interaction with calcium (CAP) have always been associated with phosphorylated proteins, iii) the weak interaction between the rhMBP and the negatively charged adsorption sites of the cation exchanger resin and iv) the calcium-mediated interaction between the rhMBP and phosphorylated caseins. The effect of phosphorylation on the isoelectric point of the rhMBP was mathematically predicted (Bjellqvist et al., 1993) employing its amino acid sequence (Figure 51). Such a decrease in the isoelectric point of the rhMBP upon phosphorylation explained the presence of the extra peaks that could correspond to rhMBP isoforms when CIEF was employed for the analysis of the transgenic milk fractions.

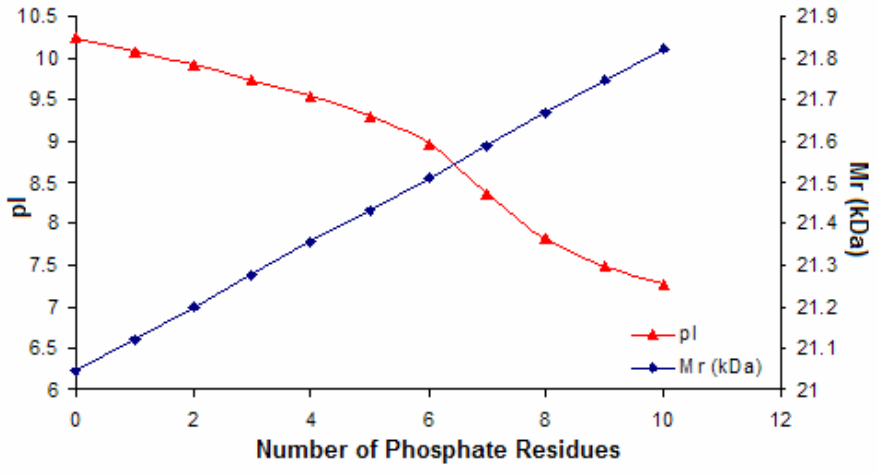

Figure 51: The effect of phosphorylation on the isoelectric point and the molecular weight of the rhMBP. Values were mathematically predicted based on the amino acid sequence of the rhMBP (Appendix I) employing ExPASy software.

Results of our investigations along with those reported in the literature formed a solid base for the hypothesis about the interaction between the rhMBP and milk caseins. The rhMBP has been modified during its expression by the mammary gland. Such modifications were different from those carried out by the human machinery and resulted in formation of a casein-like protein, "fifth casein". Several factors were thought to play a role in the interaction between rhMBP and caseins: i) the structural similarity between caseins and hMBP (flexibility – intrinsically unstructured – Pro rich) as well as the high tendency to associate with other molecules, ii) the electrostatic interaction between the positively charged residues of rhMBP and the negatively charged residues of caseins, iii) the formation of calcium bridges between the negatively charged phosphorylated residues of caseins and those of the rhMBP , and iv) the co-expression of the rhMBP along with caseins allowed interaction on the molecular level at early stages of micelle formation, which is a known event in milk biosynthesis (Boisgard, Chanat, Lavialle, Pauloin, & Ollivier-Bousquet, 2001; De Kruif, 1999; H. M. Farrell, Jr. et al., 2002; H. M. Farrell, Malin, Brown, & Qi, 2006).

Several examples have been reported in the literature where transgenic tools were able to alter the composition of the casein micelles. Three examples are reported here: i) over expression of caseins (β-CN and κ-CN) in the milk of transgenic cows resulted in a substantial increase in the amounts and the relative abundance of caseins (8 - 20% more β-CN and 100% more κ-CN), the extra copies of these caseins were successfully incorporated into the micelles and resulted in stable micelles of smaller size (Brophy et al., 2003; Laible & Wells, 2007), ii) the expression of bovine β-CN in the milk of transgenic mice resulted in a fully phosphorylated β-CN that was able to integrate successfully into casein micelles (Hitchin, Stevenson, Clark, McClenaghan, & Leaver, 1996) and iii) the β-CN is entirely dispensable in casein micelles while α_{s1}-CN is crucial for milking due its key role in the early micelle assembly stages (Chanat, Martin, & Ollivier-Bousquet, 1999; Kumar et al., 1994).

The results obtained in this study along with the supporting evidence from the literature indicated that it is possible to form casein micelles with altered casein balance or even with a non-endogenous milk protein as long as it has the right structural attributes and it is present during early micelle formation stages. It could be concluded also that the casein micelle has no specific molecular recognition pathway for its formation and it has an outstanding ability to accommodate other proteins in its assembly as long as they carry the right attributes. The presence of heterologous proteins in the micelles does not affect its physicochemical properties unless they are present in significantly high concentrations.

7.2 Future directions

Biopharmaceuticals are inherently heterogeneous and complex in nature since they have been produced in heterologous systems. Comparison of the recombinant products to their human counterparts is essential in order to ensure activity and safety. A battery of orthogonal testing methods is required. Each of these methods clearly defines some of the quality attributes of the product. Other attributes can be implied until they are confirmed using other techniques (Kelner & Bhalgat, 2007; Sadick, 2002).

In this study, several assumptions have been postulated and investigated. The results generated more questions that need to be investigated in-depth. In order to answer the new questions, the following investigations have to be carried out:

- Mass spectrometric analysis of the amino acid sequence and the PTM pattern of the rhMBP isoforms.
- Quantitative evaluation of the effect of the rhMBP expression on the rate of expression of other endogenous milk proteins.
- Investigation of the nature and the abundance of the rhMBP minor isoforms in $TGmilk_h$.
- Evaluation of the electrophoretic migration patterns of rhMBP isoforms before and after an incubation step with a phosphatase enzyme.
- The ability to extend the Bio-Plex method for the determination of other endogenous milk proteins as well as markers of the animal health.
- Comparison of the kinetics of interaction of anti-hMBP antibody with rhMBP and hMBP in order to establish a correction factor to employ in the development of a quantitative SPR assay for the rhMBP.
- Confirmation of the identity of the extra peaks noted in CIEF analysis via the development of a CIEF-MS protocol.
- Investigation of the mobilization modality noted with the zwitterionic HEPES buffer.

References

References

Alexander, M., & Dalgleish, D. G. (2004). Application of transmission diffusing wave spectroscopy to the study of gelation of milk by acidification and rennet. *Colloids and Surfaces, B: Biointerfaces, 38*(1-2), 83-90.

Alexander, M., Rojas-Ochoa, L. F., Leser, M., & Schurtenberger, P. (2002). Structure, dynamics, and optical properties of concentrated milk suspensions: An analogy to hard-sphere liquids. *Journal of Colloid and Interface Science, 253*(1), 35-46.

Arakawa, T., & Philo, J. S. (2002). Biophysical and biochemical analysis of recombinant proteins: Structure and analysis of proteins. In D. J. Crommelin & R. D. Sindelar (Eds.), *Pharmaceutical Biotechnology* (2nd ed., pp. 25-103): Taylor and Francis Group.

Beniac, D. R., Luckevich, M. D., Czarnota, G. J., Tompkins, T. A., Ridsdale, R. A., Ottensmeyer, F. P., et al. (1997). Three-dimensional structure of myelin basic protein. I. Reconstruction via angular reconstitution of randomly oriented single particles. *Journal of Biological Chemistry, 272*(7), 4261-4268.

Bizzozero, O. A., Odykirk, T. S., McGarry, J. F., & Lees, M. B. (1989). Separation of the major proteins of central and peripheral nervous system myelin using reversed-phase high-performance liquid chromatography. *Analytical Biochemistry, 180*(1), 59-65.

Bjellqvist, B., Hughes, G. J., Pasquali, C., Paquet, N., Ravier, F., Sanchez, J. C., et al. (1993). The focusing positions of polypeptides in immobilized pH gradients can be predicted from their amino acid sequences. *Electrophoresis, 14*(1), 1023-1031.

Boggs, J. M., Rangaraj, G., Gao, W., & Heng, Y. M. (2006). Effect of phosphorylation of myelin basic protein by MAPK on its interactions with actin and actin binding to a lipid membrane in vitro. *Biochemistry, 45*(2), 391-401.

Boisgard, R., Chanat, E., Lavialle, F., Pauloin, A., & Ollivier-Bousquet, M. (2001). Roads taken by milk proteins in mammary epithelial cells. *Livestock Production Science, 70*(1-2), 49-61.

Boozer, C., Kim, G., Cong, S., Guan, H., & Londergan, T. (2006). Looking towards label-free biomolecular interaction analysis in a high-throughput format: A review of new surface plasmon resonance technologies. *Current Opinion in Biotechnology, 17*(4), 400-405.

Bossart, K. N., McEachern, J. A., Hickey, A. C., Choudhry, V., Dimitrov, D. S., Eaton, B. T., et al. (2007). Neutralization assays for differential henipavirus serology using Bio-Plex Protein Array Systems. *Journal of Virological Methods, 142*(1-2), 29-40.

Brophy, B., Dines, M., Olifent, M., Piedrahita, J., Wells, D., & Laible, G. (2005). Purification of human myelin basic protein produced in transgenic cows. AgResearch Ltd, Ruakura Research Centre, Hamilton, New Zealand (Unpublished work).

Brophy, B., Smolenski, G., Wheeler, T., Wells, D., L'Huillier, P., & Laible, G. (2003). Cloned transgenic cattle produce milk with higher levels of beta-casein and kappa-casein. *Nature Biotechnology, 21*(2), 157-162.

Busnel, J.-M., Varenne, A., Descroix, S., Peltre, G., Gohon, Y., & Gareil, P. (2005). Evaluation of capillary isoelectric focusing in glycerol-water media with a view to hydrophobic protein applications. *Electrophoresis, 26*(17), 3369-3379.

Chanat, E., Martin, P., & Ollivier-Bousquet, M. (1999). alfa-S1-Casein is required for the efficient transport of beta- and kappa-casein from the endoplasmic reticulum to the Golgi apparatus of mammary epithelial cells. *Journal of Cell Science, 112*(19), 3399-3412.

Chang, P.-L., Chiu, T.-C., & Chang, H.-T. (2006). Stacking, derivatization, and separation by capillary electrophoresis of amino acids from cerebrospinal fluids. *Electrophoresis, 27*(10), 1922-1931.

Chantry, A., & Glynn, P. (1986). Two-dimensional electrophoretic characterization of microheterogenous myelin basic protein fragments. *Analytical Biochemistry, 159*(1), 29-34.

Cheifetz, S., Moscarello, M. A., & Deber, C. M. (1984). NMR investigation of the charge isomers of bovine myelin basic protein. *Archives of Biochemistry and Biophysics, 233*(1), 151-160.

Clark, A. J. (1998). The mammary gland as a bioreactor: Expression, processing, and production of recombinant proteins. *Journal of Mammary Gland Biology and Neoplasia, 3*(3), 337-350.

Corredig, M., & Alexander, M. (2008). Food emulsions studied by DWS: Recent advances. *Trends in Food Science & Technology, 19*(2), 67-75.

Cross, K. J., Huq, N. L., Palamara, J. E., Perich, J. W., & Reynolds, E. C. (2005). Physicochemical characterization of casein phosphopeptide-amorphous calcium phosphate nanocomplexes. *Journal of Biological Chemistry, 280*(15), 15362-15369.

Cruz, T. F., & Moscarello, M. A. (1983). Identification of the major sites of enzymic glycosylation of myelin basic protein. *Biochimica et Biophysica Acta, General Subjects, 760*(3), 403-410.

Dalgleish, D., Alexander, M., & Corredig, M. (2004). Studies of the acid gelation of milk using ultrasonic spectroscopy and diffusing wave spectroscopy. *Food Hydrocolloids, 18*(5), 747-755.

De Kruif, C. G. (1999). Casein micelle interactions. *International Dairy Journal, 9*(3/6), 183-188.

De Kruif, C. G., & Holt, C. (2003). Casein micelle structure, functions and interactions. In P. F. Fox & P. L. H. McSweeney (Eds.), *Advanced Dairy Chemistry* (Vol. 1, pp. 233-276): Academic/Plenum Publisher.

Deibler, G. E., Martenson, R. E., & Kies, M. W. (1972). Large scale preparation of myelin basic protein from central nervous tissue of several mammalian species. *Preparative Biochemistry, 2*(2), 139-165.

Denman, J., Hayes, M., O'Day, C., Edmunds, T., Bartlett, C., Hirani, S., et al. (1991). Transgenic expression of a variant of human tissue-type plasminogen activator in goat milk: purification and characterization of the recombinant enzyme. *Bio/Technology, 9*(9), 839-843.

Denman, J. S., & Cole, E. S. (1995). *Isolation of components of interest from milk*.

Doblhoff-Dier, O., & Bliem, R. (1999). Quality control and assurance from the development to the production of biopharmaceuticals. *Trends in Biotechnology, 17*(7), 266-270.

Dolnik, V. (2006). Capillary electrophoresis of proteins 2003 - 2005. *Electrophoresis, 27*(1), 126-141.

Donato, L., Alexander, M., & Dalgleish, D. G. (2007). Acid gelation in heated and unheated milks: Interactions between serum protein complexes and the surfaces of casein micelles. *Journal of Agricultural and Food Chemistry, 55*(10), 4160-4168.

Echelard, Y., Meade, H. M., & Ziomek, C. A. (2005). The first biopharmaceutical from transgenic animals: ATryn. In J. Knaeblein (Ed.), *Modern Biopharmaceuticals* (Vol. 3, pp. 995-1020): WILEY-VCH Verlag GmbH & Co.

Eylar, E. H. (1970). Amino acid sequence of the basic protein of the myelin membrane. *Proceedings of the National Academy of Sciences of the United States of America, 67*(3), 1425-1431.

Farrell, H. M., Jr., Kumosinski, T. F., Malin, E. L., & Brown, E. M. (2002). The caseins of milk as calcium-binding proteins. In H. J. Vogel (Ed.), *Methods in Molecular Biology* (Vol. 172, pp. 97-140): Humana Press.

Farrell, H. M., Malin, E. L., Brown, E. M., & Qi, P. X. (2006). Casein micelle structure: What can be learned from milk synthesis and structural biology? *Current Opinion in Colloid & Interface Science, 11*(2,3), 135-147.

FDA, Guidance for industry: Bioanalytical method validation, US Food & Drug Adminstration, (2001).

Fee, C. J., & Chand, A. (2006). Capture of lactoferrin and lactoperoxidase from raw whole milk by cation exchange chromatography. *Separation and Purification Technology, 48*(2), 143-149.

Findlay, J. W. A., & Dillard, R. F. (2007). Appropriate calibration curve fitting in ligand binding assays. *The AAPS Journal, 9*(2), 260-267.

Findlay, J. W. A., Smith, W. C., Lee, J. W., Nordblom, G. D., Das, I., DeSilva, B. S., et al. (2000). Validation of immunoassays for bioanalysis: A pharmaceutical industry perspective. *Journal of Pharmaceutical and Biomedical Analysis, 21*(6), 1249-1273.

Fitzgerald, C., Collins, M., van Duyne, S., Mikoleit, M., Brown, T., & Fields, P. (2007). Multiplex, bead-based suspension array for molecular determination of common Salmonella serogroups. *Journal of Clinical Microbiology, 45*(10), 3323-3334.

Flagella, M., Bui, S., Zheng, Z., Nguyen, C. T., Zhang, A., Pastor, L., et al. (2006). A multiplex branched DNA assay for parallel quantitative gene expression profiling. *Analytical Biochemistry, 352*(1), 50-60.

Fox, P. F. (2003). Milk proteins: General and historical aspects. In P. F. Fox & P. L. H. McSweeney (Eds.), *Advanced Dairy Chemistry* (Vol. 1, pp. 1-48): Academic/Plenum Publishers.

Fox, P. F., & Brodkorb, A. (2008). The casein micelle: Historical aspects, current concepts and significance. *International Dairy Journal, 18*(7), 677-684.

Fulton, R. J., McDade, R. L., Smith, P. L., Kienker, L. J., & Kettman Jr, J. R. (1997). Advanced multiplexed analysis with the FlowMetrix(TM) system. *Clinical Chemistry, 43*(9), 1749-1756.

Gaucheron, F. (2005). The minerals of milk. *Reproduction, Nutrition, Development, 45*(4), 473-483.

Gavin, W. G. (2001). The future of transgenics. *Regulatory Affairs Focus, May*, 13-18.

Gomez, J. E., & Sandoval, J. E. (2008). The effect of conditioning of fused-silica capillaries on their electrophoretic performance. *Electrophoresis, 29*(2), 381-392.

Good, N. E., Winget, G. D., Winter, W., Connolly, T. N., Izawa, S., & Singh, R. M. M. (1966). Hydrogen ion buffers for biological research. *Biochemistry, 5*(2), 467-477.

Goodall, D. M., Williams, S. J., & Lloyd, D. K. (1991). Quantitative aspects of capillary electrophoresis. *Trends in Analytical Chemistry, 10*(9), 272-279.

Gutierrez-Adan, A., Maga, E. A., Meade, H., Shoemaker, C. F., Medrano, J. F., Anderson, G. B., et al. (1996). Alterations of the physical characteristics of milk from transgenic mice producing bovine kappa-casein. *Journal of Dairy Science, 79*(5), 791-799.

Haasnoot, W., Smits, N. G. E., Kemmers-Voncken, A. E. M., & Bremer, M. G. E. G. (2004). Fast biosensor immunoassays for the detection of cows' milk in the milk of ewes and goats. *Journal of Dairy Research, 71*(3), 322-329.

Hanley, B. P., Xing, L., & Cheng, R. H. (2007). Variance in multiplex suspension array assays: Microsphere size variation impact. *Theoretical Biology and Medical Modelling, 4*, 31.

Harauz, G., Ishiyama, N., Hill, C. M. D., Bates, I. R., Libich, D. S., & Fares, C. (2004). Myelin basic protein: Diverse conformational states of an intrinsically unstructured protein and its roles in myelin assembly and multiple sclerosis. *Micron, 35*(7), 503-542.

Hautala, J. T., Wiedmer, S. K., & Riekkola, M.-L. (2005). Influence of pH on formation and stability of phosphatidylcholine/phosphatidylserine coatings in fused-silica capillaries. *Electrophoresis, 26*(1), 176-186.

Hemar, Y., & Pinder, D. N. (2006). DWS microrheology of a linear polysaccharide. *Biomacromolecules, 7*(3), 674-676.

Hemar, Y., Pinder, D. N., Hunter, R. J., Singh, H., Hebraud, P., & Horne, D. S. (2003). Monitoring of flocculation and creaming of sodium caseinate-stabilized emulsions using diffusing wave spectroscopy. *Journal of Colloid and Interface Science, 264*(2), 502-508.

Hildebrand, M. (2005). Analytics in quality control and in vivo. In J. Knaeblein (Ed.), *Modern Biopharmaceuticals* (Vol. 4, pp. 1556-1579): WILEY-VCH Verlag GmbH & Co.

Hitchin, E., Stevenson, E. M., Clark, A. J., McClenaghan, M., & Leaver, J. (1996). Bovine beta-casein expressed in transgenic mouse milk is phosphorylated and incorporated into micelles. *Protein Expression and Purification, 7*(3), 247-252.

Hjerten, S. (1985). High-performance electrophoresis: Elimination of electroendosmosis and solute adsorption. *Journal of Chromatography, 347*(2), 191-198.

Hjerten, S., & Zhu, M. D. (1985). Adaptation of the equipment for high-performance electrophoresis to isoelectric focusing. *Journal of Chromatography, 346*, 265-270.

Holland, J. W., Deeth, H. C., & Alewood, P. F. (2004). Proteomic analysis of kappa-casein micro-heterogeneity. *Proteomics, 4*(3), 743-752.

Holt, C. (1992). Structure and stability of bovine casein micelles. In B. C. Anfinsen, D. S. Eisenberg, J. T. Edsall & F. M. Richards (Eds.), *Advances in Protein Chemistry* (Vol. 43, pp. 63-151): Elsevier Science & Technology Books.

Horka, M., Ruzicka, F., Horky, J., Hola, V., & Slais, K. (2006). Capillary isoelectric focusing of proteins and microorganisms in dynamically modified fused silica with UV detection. *Journal of Chromatography, B, 841*(1-2), 152-159.

Horne, D. S. (2002). Casein structure, self-assembly and gelation. *Current Opinion in Colloid & Interface Science, 7*(5,6), 456-461.

Horne, D. S. (2006). Casein micelle structure: Models and muddles. *Current Opinion in Colloid & Interface Science, 11*(2,3), 148-153.

Horvath, J., & Dolnik, V. (2001). Polymer wall coatings for capillary electrophoresis. *Electrophoresis, 22*(4), 644-655.

Hu, S., Jiang, J., Cook, L. M., Richards, D. P., Horlick, L., Wong, B., et al. (2002). Capillary sodium dodecyl sulfate-DALT electrophoresis with laser-induced fluorescence detection for size-based analysis of proteins in human colon cancer cells. *Electrophoresis, 23*(18), 3136-3142.

Huang, T.-L., & Richards, M. (1997). Development of a high-performance capillary isoelectric focusing technique with application to studies of microheterogeneity in chicken conalbumin. *Journal of Chromatography, A, 757*(1 + 2), 247-253.

Huang, Y.-F., Hsieh, M.-M., Tseng, W.-L., & Chang, H.-T. (2006). On-line concentration of microheterogeneous proteins by capillary electrophoresis using SDS and PEO as additives. *Journal of Proteome Research, 5*(2), 429-436.

Huang, Y.-F., Huang, C.-C., Hu, C.-C., & Chang, H.-T. (2006). Capillary electrophoresis-based separation techniques for the analysis of proteins. *Electrophoresis, 27*(18), 3503-3522.

ICH (Q2R1), Validation of analytical procedures: Test and methodology, International Conference on Harmonization of Technical Requirements for Registration of Pharmaceuticals for Human Use C.F.R. (2005).

Jagschies, G. (2008, October). Where is biopharmaceutical manufacturing heading? *BioPharm International,* 1-6.

Johnsson, B., Loefaas, S., & Lindquist, G. (1991). Immobilization of proteins to a carboxymethyldextran-modified gold surface for biospecific interaction analysis in surface plasmon resonance sensors. *Analytical Biochemistry, 198*(2), 268-277.

Kellar, K. L., & Iannone, M. A. (2002). Multiplexed microsphere-based flow cytometric assays. *Experimental Hematology, 30*(11), 1227-1237.

Kelner, D. N., & Bhalgat, M. K. (2007). Analytical strategy for biopharmaceutical development. In A. A. Shukla, M. R. Etzel & S. Gadam (Eds.), *Process Scale Bioseparations for the Biopharmaceutical Industry* (Vol. 31, pp. 395-418): Taylor and Francis Group.

Kilar, F. (2003). Recent applications of capillary isoelectric focusing. *Electrophoresis, 24*(22-23), 3908-3916.

Krause, S. O. (2006, June). A guide for testing biopharmaceuticals. Part 2: Acceptance criteria and analytical method maintenance. *BioPharm International,* 12-18.

Kumar, S., Clarke, A. R., Hooper, M. L., Horne, D. S., Law, A. J. R., Leaver, J., et al. (1994). Milk composition and lactation of beta-casein deficient mice. *Proceedings of the National Academy of Sciences of the United States of America, 91*(13), 6138-6142.

Kundu, S., & Fenters, C. (1995). Isoelectric focusing of monoclonal antibodies by capillary electrophoresis. *Journal of Capillary Electrophoresis, 2*(6), 273-277.

Kuo, C.-Y., Chiou, S.-S., & Wu, S.-M. (2006). Solid-phase extraction and large-volume sample stacking with an electroosmotic flow pump in capillary electrophoresis for determination of methotrexate and its metabolites in human plasma. *Electrophoresis, 27*(14), 2905-2909.

Laemmli, U. K. (1970). Cleavage of structural proteins during the assembly of the head of bacteriophage T4. *Nature, 227*(5259), 680-685.

Laible, G., & Wells, D. N. (2007). Recent advances and future options for New Zealand agriculture derived from animal cloning and transgenics. *New Zealand Journal of Agricultural Research, 50*(2), 103-124.

Lee, H. G. (1997). Rapid high-performance isoelectric focusing of monoclonal antibodies in uncoated fused-silica capillaries. *Journal of Chromatography, A, 790*(1 + 2), 215-223.

Leong, M. M., & Fox, G. R. (1990). Luminescent detection of immunodot and western blots. *Methods in Enzymology, 184*, 442-451.

Little, M. J., Paquette, D. M., & Roos, P. K. (2006). Electrophoresis of pharmaceutical proteins: Status quo. *Electrophoresis, 27*(12), 2477-2485.

Lucy, C. A., MacDonald, A. M., & Gulcev, M. D. (2008). Non-covalent capillary coatings for protein separations in capillary electrophoresis. *Journal of Chromatography, A, 1184*(1-2), 81-105.

Luke, F., Doina, N., & Simon, A. (2002, December). Patenting in the biopharmaceutical industry: Comparing the US with Europe. *Drug Plus International* 14-20.

Lupi, A., Viglio, S., Luisetti, M., Gorrini, M., Coni, P., Faa, G., et al. (2000). alpha-1 Antitrypsin in serum determined by capillary isoelectric focusing. *Electrophoresis, 21*(15), 3318-3326.

Maatta, J. A., Coffey, E. T., Hermonen, J. A., Salmi, A. A., & Hinkkanen, A. E. (1997). Detection of myelin basic protein isoforms by organic concentration. *Biochemical and Biophysical Research Communications, 238*(2), 498-502.

Manso, M. A., Leonil, J., Jan, G., & Gagnaire, V. (2005). Application of proteomics to the characterisation of milk and dairy products. *International Dairy Journal, 15*(6-9), 845-855.

Marchesseau, S., Mani, J. C., Martineau, P., Roquet, F., Cuq, J. L., & Pugniere, M. (2002). Casein interactions studied by the surface plasmon resonance technique. *Journal of Dairy Science, 85*(11), 2711-2721.

Mazzeo, J. R., & Krull, I. S. (1991). Capillary isoelectric focusing of proteins in uncoated fused silica capillaries using polymeric additives. *Analytical Chemistry, 63*(24), 2852-2857.

McMahon, D. J., & Oommen, B. S. (2008). Supramolecular structure of the casein micelle. *Journal of Dairy Science, 91*(5), 1709-1721.

Melo Eduardo, O., Canavessi Aurea, M. O., Franco Mauricio, M., & Rumpf, R. (2007). Animal transgenesis: State of the art and applications. *Journal of Applied Genetics, 48*(1), 47-61.

Meri, S., & Baumann, M. (2001). Proteomics: Posttranslational modifications, immune responses and current analytical tools. *Biomolecular Engineering, 18*(5), 213-220.

Miksik, I., Sedlakova, P., Mikulikova, K., Eckhardt, A., Cserhati, T., & Horvath, T. (2006). Matrices for capillary gel electrophoresis: A brief overview of uncommon gels. *Biomedical Chromatography, 20*(6-7), 458-465.

Morcol, T., & Bell, S. D. (2001). *Method for processing milk*.

Morcol, T., He, Q., & Bell, S. J. D. (2001). Model process for removal of caseins from milk of transgenic animals. *Biotechnology Progress, 17*(3), 577-582.

Mosher, R. A., & Thormann, W. (2002). High-resolution computer simulation of the dynamics of isoelectric focusing using carrier ampholytes: The post-separation stabilizing phase revisited. *Electrophoresis, 23*(12), 1803-1814.

Mueller, K. M., Gempeler, M. R., Scheiwe, M.-W., & Zeugin, B. T. (1996). Quality assurance for biopharmaceuticals: An overview of regulations, methods and problems. *Pharmaceutica Acta Helvetiae, 71*(6), 421-438.

Muller-Renaud, S., Dupont, D., & Dulieu, P. (2004). Quantification of kappa-casein in milk by an optical immunosensor. *Food and Agricultural Immunology, 15*(3-4), 265-277.

Muller-Renaud, S., Dupont, D., & Dulieu, P. (2005). Development of a biosensor immunoassay for the quantification of alfa-S1-casein in milk. *Journal of Dairy Research, 72*(1), 57-64.

Myszka, D. G., & Rich, R. L. (2000). Implementing surface plasmon resonance biosensors in drug discovery. *Pharmaceutical Science & Technology Today, 3*(9), 310-317.

Niemann, H., Halter, R., Carnwath, J. W., Herrmann, D., Lemme, E., & Paul, D. (1999). Expression of human blood clotting factor VIII in the mammary gland of transgenic sheep. *Transgenic Research, 8*(3), 237-247.

Nikolov, Z. L., & Woodard, S. L. (2004). Downstream processing of recombinant proteins from transgenic feedstock. *Current Opinion in Biotechnology, 15*(5), 479-486.

Nolan, J. P., & Mandy, F. (2006). Multiplexed and microparticle-based analyses: Quantitative tools for the large-scale analysis of biological systems. *Cytometry Part A, 69A*, 318-325.

Nuyens, J. H., & VanVeen, H. H. (1999). *Isolation of lactoferrin from milk*.

Nye, S. H., Pelfrey, C. M., Burkwit, J. J., Voskuhl, R. R., Lenardo, M. J., & Mueller, J. P. (1995). Purification of immunologically active recombinant 21.5 kDa isoform of human myelin basic protein. *Molecular Immunology, 32*(14/15), 1131-1141.

O'Donnell, R., Holland, J. W., Deeth, H. C., & Alewood, P. (2004). Milk proteomics. *International Dairy Journal, 14*(12), 1013-1023.

Oettinger, H. F., Al-Sabbagh, A., Jingwu, Z., LaSalle, J. M., Weiner, H. L., & Hafler, D. A. (1993). Biological activity of recombinant human myelin basic protein. *Journal of Neuroimmunology, 44*(2), 157-162.

Otzen, D. E. (2002). Protein unfolding in detergents: Effect of micelle structure, ionic strength, pH, and temperature. *Biophysical Journal, 83*(4), 2219-2230.

Pallandre, A., de Lambert, B., Attia, R., Jonas, A. M., & Viovy, J.-L. (2006). Surface treatment and characterization: Perspectives to electrophoresis and lab-on-chips. *Electrophoresis, 27*(3), 584-610.

Pampel, L., Boushaba, R., Udell, M., Turner, M., & Titchener-Hooker, N. (2007). The influence of major components on the direct chromatographic recovery of a protein from transgenic milk. *Journal of Chromatography, A, 1142*(2), 137-147.

Parker, W., & Song, P. S. (1992). Protein structures in SDS micelle-protein complexes. *Biophysical Journal, 61*(5), 1435-1439.

Planning, S. (2007). Assays for determination of protein concentration. *Current Protocols in Protein Science, Unit 3.4*, 1-29.

Playne, M. J., Bennett, L. E., & Smithers, G. W. (2003). Functional dairy foods and ingredients. *Australian Journal of Dairy Technology, 58(3)*, 242-264.

Pollock, D. P., Kutzko, J. P., Birck-Wilson, E., Williams, J. L., Echelard, Y., & Meade, H. M. (1999). Transgenic milk as a method for the production of recombinant antibodies. *Journal of Immunological Methods, 231*(1-2), 147-157.

Prabhakar, U., Eirikis, E., & Davis, H. M. (2002). Simultaneous quantification of proinflammatory cytokines in human plasma using the LabMAP assay. *Journal of Immunological Methods, 260*(1-2), 207-218.

Rich, R. L., & Myszka, D. G. (2000). Advances in surface plasmon resonance biosensor analysis. *Current Opinion in Biotechnology, 11*(1), 54-61.

Rich, R. L., & Myszka, D. G. (2001). BIACORE J: A new platform for routine biomolecular interaction analysis. *Journal of Molecular Recognition, 14*, 223-228.

Righetti, P. G. (2004). Determination of the isoelectric point of proteins by capillary isoelectric focusing. *Journal of Chromatography, A, 1037*(1-2), 491-499.

Righetti, P. G., Gelfi, C., & Conti, M. (1997). Current trends in capillary isoelectric focusing of proteins. *Journal of Chromatography, B, 699*(1 + 2), 91-104.

Robinson, W. H. (2006). Antigen arrays for antibody profiling. *Current Opinion in Chemical Biology, 10*(1), 67-72.

Rodriguez-Diaz, R., Zhu, M., & Wehr, T. (1997). Strategies to improve performance of capillary isoelectric focusing. *Journal of Chromatography, A, 772*(1 + 2), 145-160.

Russo, A. T., & Brand, L. (1999). A nanosecond time-resolved fluorescence study of recombinant human myelin basic protein. *Journal of Fluorescence, 9*(4), 333-342.

Sadick, M. (2002). Understanding the puzzle of "well-characterized biotechnology products". *Current Opinion in Biotechnology, 13*(3), 275-278.

Saefsten, P., Klakamp, S. L., Drake, A. W., Karlsson, R., & Myszka, D. G. (2006). Screening antibody-antigen interactions in parallel using Biacore A100. *Analytical Biochemistry, 353*(2), 181-190.

Salamone, D., Baranao, L., Santos, C., Bussmann, L., Artuso, J., Werning, C., et al. (2006). High level expression of bioactive recombinant human growth hormone in the milk of a cloned transgenic cow. *Journal of Biotechnology, 124*(2), 469-472.

Shimura, K., Zhi, W., Matsumoto, H., & Kasai, K.-i. (2000). Accuracy in the Determination of Isoelectric Points of Some Proteins and a Peptide by Capillary Isoelectric Focusing: Utility of Synthetic Peptides as Isoelectric Point Markers. *Analytical Chemistry, 72*(19), 4747-4757.

Sims, R. J., III, & Reinberg, D. (2008). Is there a code embedded in proteins that is based on post-translational modifications? *Nature Reviews Molecular Cell Biology, 9*(10), 815-820.

Stoyanov, A. V., Das, C., Fredrickson, C. K., & Fan, Z. H. (2005). Conductivity properties of carrier ampholyte pH gradients in isoelectric focusing. *Electrophoresis, 26*(2), 473-479.

Strelec, I., Pacakova, V., Bosakova, Z., Coufal, P., Guryca, V., & Stulik, K. (2002). Modification of capillary electrophoresis capillaries by poly(hydroxyethyl methacrylate), poly(diethylene glycol monomethacrylate) and poly(triethylene glycol monomethacrylate). *Electrophoresis, 23*(4), 528-535.

Swaisgood, H. E. (2003). Chemistry of the caseins. In P. F. Fox & P. L. H. McSweeney (Eds.), *Advanced Dairy Chemistry* (3rd ed., Vol. 1, pp. 139-201): Academic/Plenum Publishers.

Tang, Q., & Lee, C. S. (1997). Effects of electroosmotic flow on zone mobilization in capillary isoelectric focusing. *Journal of Chromatography, A, 781*(1 + 2), 113-118.

Tauzin, B. (2006). *418 Biotechnology medicines in testing promise to bolster the arsenal against disease* (Report).Medicines in Development, Biotechnology: Phamaceutical Research and Manufacturers of America (www.phrma.org/files/Biotech%202006.pdf).(www.phrma.org/files/Biotech%202006.pdf).

Taylor, J. D., Briley, D., Nguyen, Q., Long, K., Iannone, M. A., Li, M. S., et al. (2001). Flow cytometric platform for high-throughput single nucleotide polymorphism analysis. *BioTechniques, 30*(3), 661-669.

Thoemmes, J., Halfar, M., Gieren, H., Curvers, S., Takors, R., Brunschier, R., et al. (2001). Human chymotrypsinogen B production from Pichia pastoris by integrated development of fermentation and downstream processing. Part 2. Protein recovery. *Biotechnology Progress, 17*(3), 503-512.

Thorsteinsson, M. V., Richter, J., Lee, A. L., & DePhillips, P. (2005). 5-Dodecanoylaminofluorescein as a probe for the determination of critical micelle concentration of detergents using fluorescence anisotropy. *Analytical Biochemistry, 340*(2), 220-225.

Tremblay, L., Laporte, M. F., Leonil, J., Dupont, D., & Paquin, P. (2003). Quantitation of proteins in milk products. In P. F. Fox & P. L. H. McSweeney (Eds.), *Advanced Dairy Chemistry* (Vol. 1, pp. 49-138): Academic/Plenum Publishers.

Tzakos, A. G., Fuchs, P., van Nuland, N. A. J., Troqanis, A., Tselios, T., Deraos, S., et al. (2004). NMR and molecular dynamics studies of an autoimmune myelin basic protein peptide and its antagonist. Structural implications for the MHC II (I-AU)-peptide complex from docking calculations. *European Journal of Biochemistry, 271*(16), 3399-3413.

van Berkel, P. H. C., Welling, M. M., Geerts, M., van Veen, H. A., Ravensbergen, B., Salaheddine, M., et al. (2002). Large scale production of recombinant human lactoferrin in the milk of transgenic cows. *Nature Biotechnology, 20*(5), 484-487.

van Gageldonk, P. G. M., van Schaijk, F. G., van der Klis, F. R., & Berbers, G. A. M. (2008). Development and validation of a multiplex immunoassay for the simultaneous determination of serum antibodies to Bordetella pertussis, diphtheria and tetanus. *Journal of Immunological Methods, 335*, 79-89.

Vanrobaeys, F., Van Coster, R., Dhondt, G., Devreese, B., & Van Beeumen, J. (2005). Profiling of myelin proteins by 2D-gel electrophoresis and multidimensional liquid chromatography coupled to MALDI TOF-TOF mass spectrometry. *Journal of Proteome Research, 4*(6), 2283-2293.

Velander, W. H., Johnson, J. L., Page, R. L., Russell, C. G., Subramanian, A., Wilkins, T. D., et al. (1992). High-level expression of a heterologous protein in the milk of transgenic swine using the cDNA encoding human protein C. *Proceedings of the National Academy of Sciences of the United States of America, 89*(24), 12003-12007.

Vignali, D. A. A. (2000). Multiplexed particle-based flow cytometric assays. *Journal of Immunological Methods, 243*(1-2), 243-255.

Volkin, D. B., Sanyal, G., Bruke, C. J., & Middaugh, R. (2002). Preformulation studies as an essential guide to formulation development and manufacture of protein pharmaceuticals. In N. Stevin & A. Michael (Eds.), *Development and Manufacture of Protein Pharmaceuticals* (Vol. 14, pp. 1-39). New York: Kluwer Academic/Plenum Publishers.

Walsh, G. (2000). Biopharmaceutical benchmarks. *Nature Biotechnology, 18*(8), 831-833.

Walsh, G. (2003). Biopharmaceutical benchmarks 2003. *Nature Biotechnology, 21*(11), 1396.

Walsh, G. (2003). Pharmaceuticals, biologics and biopharmaceuticals. In *Biopharmaceuticals: Biochemistry and Biotechnology* (2nd ed., pp. 1-35): John Wiley and Sons.

Walsh, G. (2006). Biopharmaceutical benchmarks 2006. *Nature Biotechnology, 24*(7), 769-776.

Walsh, G. (2008, October). Biopharmaceuticals: Approval trends in 2007. *BioPharm International,* 1-6.

Wiedmer, S. K., Jussila, M., Hakala, R. M. S., Pystynen, K.-H., & Riekkola, M.-L. (2005). Piperazine-based buffers for liposome coating of capillaries for electrophoresis. *Electrophoresis, 26*(10), 1920-1927.

Wilkins, T. D., & Velander, W. (1992). Isolation of recombinant proteins from milk. *Journal of Cellular Biochemistry, 49*(4), 333-338.

Wlad, H., Ballagi, A., Bouakaz, L., Gu, Z., & Janson, J.-C. (2001). Rapid two-step purification of a recombinant mouse Fab fragment expressed in Escherichia coli. *Protein Expression and Purification, 22*(2), 325-329.

Wright, G., Carver, A., Cottom, D., Reeves, D., Scott, A., Simons, P., et al. (1991). High level expression of active human alpha-1 antitrypsin in the milk of transgenic sheep. *Bio/Technology, 9*(9), 830-834.

Yang, C.-Y., Brooks, E., Li, Y., Denny, P., Ho, C.-M., Qi, F., et al. (2005). Detection of picomolar levels of interleukin-8 in human saliva by SPR. *Lab on a Chip, 5*(10), 1017-1023.

Yeung, K. K. C., Atwal, K. K., & Zhang, H. (2003). Dynamic capillary coatings with zwitterionic surfactants for capillary isoelectric focusing. *Analyst, 128*(6), 566-570.

Zhang, C.-X., Xiang, F., Pasa-Tolic, L., Anderson, G. A., Veenstra, T. D., & Smith, R. D. (2000). Stepwise mobilization of focused proteins in capillary isoelectric focusing mass spectrometry. *Analytical Chemistry, 72*(7), 1462-1468.

Zhang, C., & Van Cott, K. E. (2007). Product Recovery from Transgenic Sources. In A. A. Shukla, M. R. Etzel & S. Gadam (Eds.), *Process Scale Bioseparations for the Biopharmaceutical Industry* (Vol. 31, pp. 367): Taylor and Francis Group.

Zor, T., & Selinger, Z. (1996). Linearization of the Bradford protein assay increases its sensitivity: Theoretical and experimental studies. *Analytical Biochemistry, 236*(2), 302-308.

Appendix I

This appendix contains supplementary data provided by Agresearch Ltd.

- The amino acid sequence of the rhMBP

		↓		★
1	**HHHHHH**DVDL	Y**DDDDKR**LNA	FKCEYWSRPM	ASQKRPSQRH
41	GSKYLATAST	MDHARHGFLP	RHRDTGILDS	IGRFFGGDRG
91	APKRGSGKDS	HHPARTAHYG	SLPQKSHGRT	Q**DENPVV**HFF
131	KNIVTPRTPP	PSQGKGAEGQ	RPGFGYGG**RA**	**SDYKS**AHKGF
171	KGVDAQGTLS	KIFKLGGRDS	RSGSPMARR	

Figure 52: The amino acid sequence of the recombinant human myelin basic protein (without the promoter signal peptide). The amino acid sequences representing the epitopes for the monoclonal antibodies employed in this study are underlined. The enterokinase cleavage site is indicated by an arrow. The start of the amino acid sequence of the 17.2 kDa hMBP is indicated by a star.

Table 8: The antibodies used for the detection and the determination of the rhMBP in this study and their corresponding epitopes.

Epitope	Antibody	Cat no.
HHHHHH	HRP-labeled anti-His tag mAb	Pierce (15165)
	Biotin-labeled anti-His tag mAb	Qiagen (34440)
DENPVV	Anti-hMBP mAb	Abcam (ab7349)
RASDYKS	Anti-hMBP mAb	Santa-Cruz (sc-71547)

- Expression pattern of rhMBP in transgenic animals

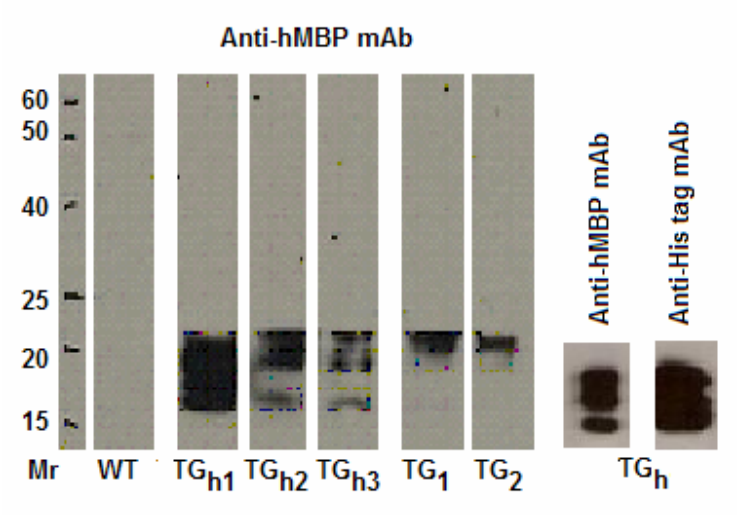

Figure 53: Western blots (left) showing the expression pattern of the rhMBP in the milk of a number of transgenic animals obtained by hormonal induction (TG_{h1-h3}) and natural milking (TG_{1-2}) using anti-hMBP antibody. Western blots (right) showing a comparison of the banding pattern of the rhMBP isoforms in the hormonally induced milk as detected employing anti-hMBP and anti-His tag antibodies.

- Project documentation and ethical approvals

Please refer to the following web page (www.agresearch.co.nz/transgenic/) for the background of this project, the approvals granted and the controls imposed by the New Zealand Environmental Risk Management Authority (ERMA), with respect to dealing with the transgenic animals and their products including milk.

- Poster presented by Agresearch (Queensland, 2004)

Purification of Human Myelin Basic Protein Produced in Transgenic Cows

Brigid Brophy, Mark Dines, Marian Olifent, Jorge Piedrahita, David Wells and Goetz Laible.
AgResearch Ltd, Ruakura Research Centre, Hamilton, New Zealand.

Objective

To purify recombinant human Myelin Basic Protein (rhMBP), expressed as a His tagged fusion protein, from the milk of transgenic cows.

Introduction

- The use of transgenic animals as "bioreactors" has been established as an alternative method for producing recombinant proteins
- MBP was chosen as a proof of principle model to develop bovine bioreactor technology in NZ

Methods

The Construct

- Mouse Whey Acidic Protein (WAP) promoter including 20 amino acid signal peptide
- 6 histidine tag
- Enterokinase cleavage site
- MBP cDNA encoding the 17.2 kDa form
- Bovine growth factor poly adenylation signal
- Expected molecular weight of the rhMBP protein is 21kDA (without the signal peptide)

The Cows

- Transgenic donor cells were generated by cotransfection of the construct and an antibiotic resistance gene (Puromycin A)
- Embryos were generated by Nuclear Transfer with these donor cells
- 9 calves from 2 lines were born
- Lactation in heifers was hormonally induced

Results

Initial Milk Characterisation

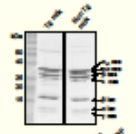

- rhMBP is not visible by Coomassie staining

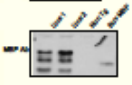

- Antibodies detect multiple protein bands
- MBP and His tag antibodies show similar banding pattern

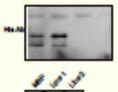

- Antibodies detect similar protein bands for both transgenic lines

- Dot blot analysis showed an expression level of 2-3mg/ml of rhMBP in both lines

Preliminary Purification

- Tested acid precipitation of caseins
  - this co-precipitated rhMBP, suggesting a strong interaction of rhMBP with the casein proteins
- Tested EDTA, arginine and caproic acid for their ability to disrupt the protein interactions
  - established arginine was the most effective in deconstructing the micelles and disrupting the rhMBP/casein interactions
- Evaluated calcium phosphate nanoparticle (CAP) technology (1), ammonium sulphate and PEG as methods to selectively fractionate the proteins prior to chromatography
  - CAP proved the most successful in selectively precipitating the major rhMBP interacting casein (probably α_{s1})
- Tested nickel, ion exchange, size exclusion and hydrophobic interaction chromatography, with and without urea
  - identified a two step chromatography protocol, with the inclusion of urea as the most effective

1. Morcöl,T., Ha, Q.& Bell, S. Model Process for Removal of Caseins from Milk of Transgenic Animals. *Biotechnol. Prog.* 17, 577-582 (2001)

Final Protocol

- Skim milk was treated with an equal volume of 2M arginine
- Proteins (predominantly α_{s1} casein) were precipitated by the addition of CAP particles
- The protein mix was centrifuged and the supernatant recovered
- The rhMBP enriched supernatant was dialysed against binding buffer including 4M urea
- Nickel affinity chromatography was performed

Nickel Affinity Chromatography

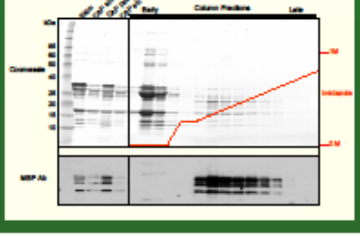

Final Protocol continued

- Pooled rhMBP fractions were subjected to Ion Exchange Sepharose SP FF chromatography

Ion Exchange Chromatography

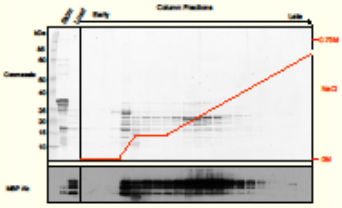

- To remove urea and maintain rhMBP in solution, pooled fractions were dialysed against 0.1N HCl
- The pH was adjusted to distilled water

Final Protein Preparation

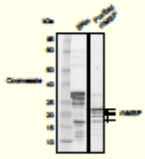

- This process achieved ≥ 90% purity in the final rhMBP preparation

Conclusion

- **Expression from the rhMBP cDNA construct results in multiple protein bands in milk**
- **As rhMBP interacts strongly with other milk proteins, a number of purification procedures were trialled to optimise purification**
- **A multi step procedure involving deconstruction of casein micelles, selective precipitation of proteins and two forms of column chromatography resulted in a rhMBP protein preparation of ≥90% purity**

Acknowledgements

We thank Jacqui Forsyth, Katie Cockrem, Vicki McMillan, Aaron Malthus and Tim Hale for their excellent farm management and Derek Knighton for useful discussion. This work was funded by the New Zealand Foundation of Research, Science and Technology and AgResearch.

Appendix II

In this appendix, milk samples (TGmilk, TGmilk$_h$ and WTmilk) were compared using several techniques. Results of these comparisons are supplementary to those described in Chapters 3 - 6. These results indicate differences noted in the TGmilk$_h$ samples that need to be investigated in-depth in future work.

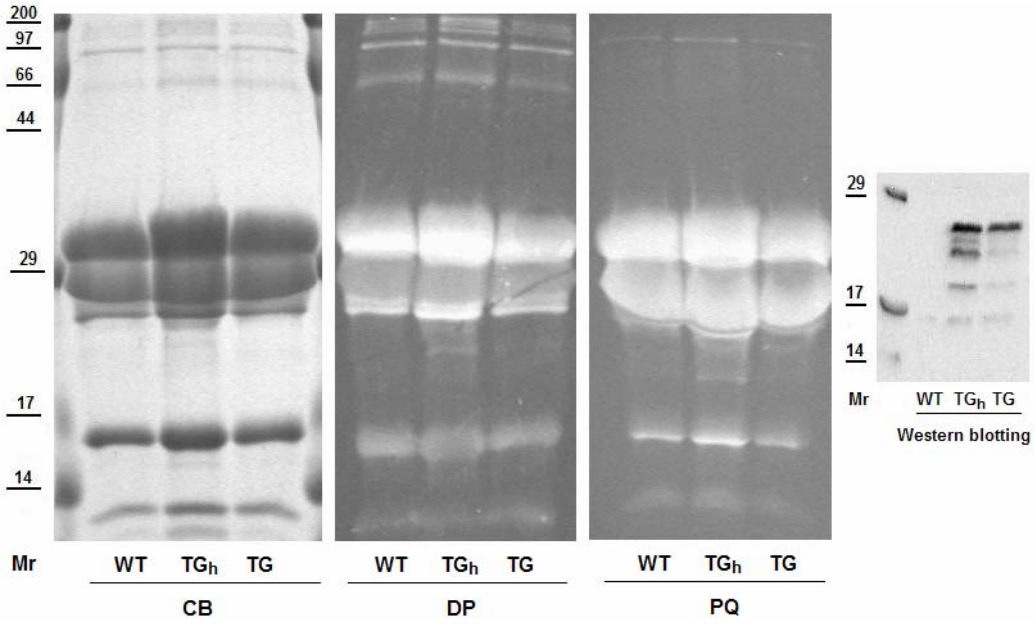

Figure 54: Comparison of milk proteins in the WTmilk, TGmilk$_h$ and TGmilk using three protein stains of different affinities (left). CB: Comassie Blue (a general purpose protein stain), DP: Deep Purple (a highly sensitive fluorescent protein stain more selective to basic proteins) and PQ: ProQ Diamond (a fluorescent protein stain more selective to phosphorylated proteins). Western blots (right) showing a comparison between the three milk types using anti-hMBP antibodies.

- Comparison of TGmilk$_h$ and WTmilk samples employing cation exchange chromatography

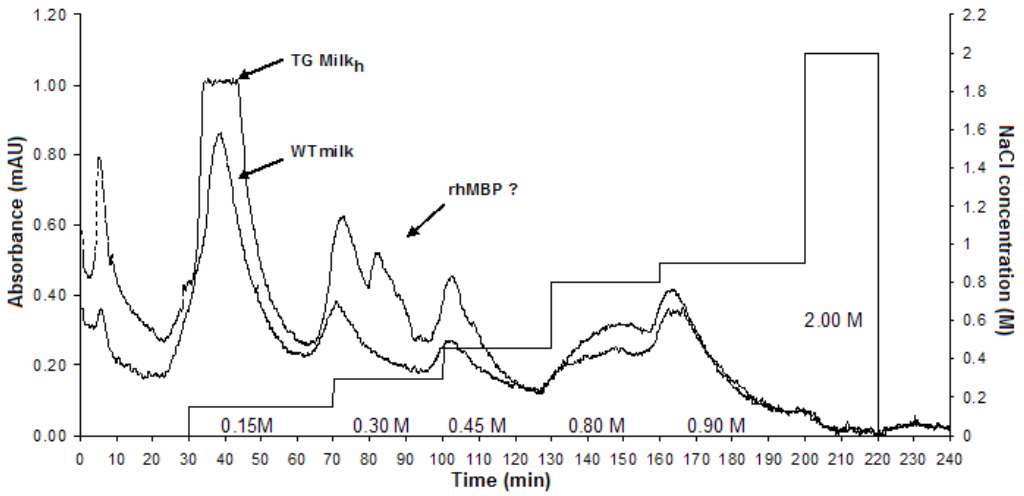

Figure 55: Chromatograms showing a comparison between WTmilk and TGmilk$_h$ with an arrow indicating the extra peak(s) corresponding to the rhMBP. Column: XK 16/20 packed with SP Sepharose BB - cv 20 ml, sample: 30 ml TGmilk loaded at 5.0 ml/min (super loop 50 ml), elution flow rate 5.0 ml/min, loading buffer: 50 mM HEPES (pH 7.0) and elution buffer: 50 mM HEPES (pH 7.0) - 2.0 M NaCl. Equipment: FPLC (Pharmacia, Sweden) with the detector signals interfaced to a computer using a LabPro Data logger.

- Elution pattern of the rhMBP from TGmilk$_h$ samples

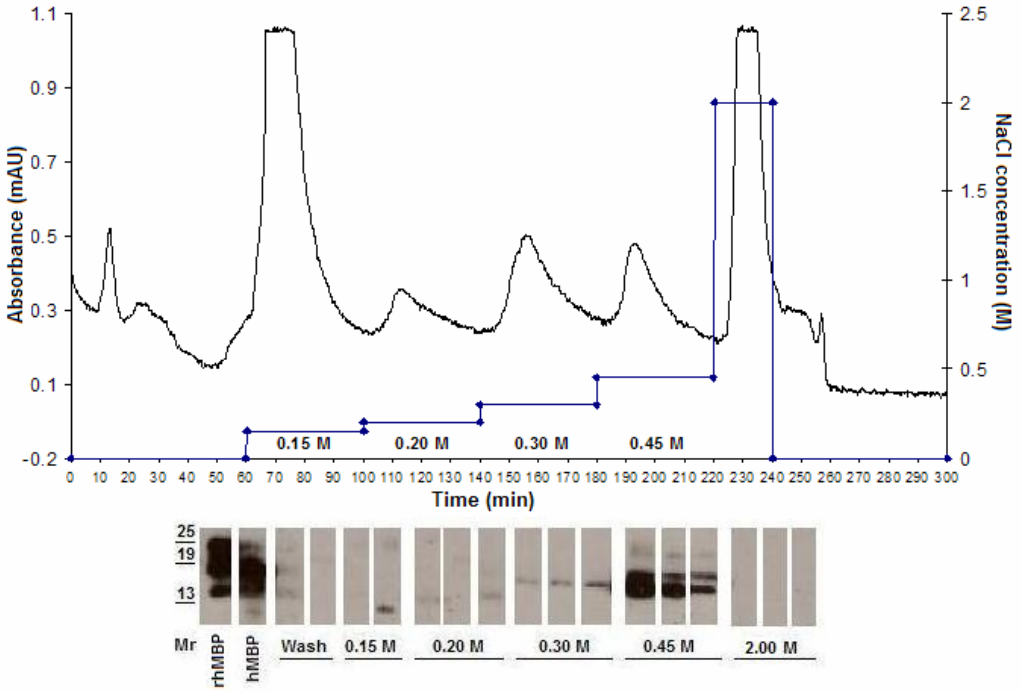

Figure 56: Chromatogram (top) showing a stretched elution pattern over 0.15 - 0.45 M NaCl concentration and the western blotting analysis of the collected fractions (bottom). Column: XK 16/20 packed with SP Sepharose BB - cv 20 ml, sample: 30 ml TGmilk loaded at 5.0 ml/min (super loop 50 ml), elution flow rate 5.0 ml/min, loading buffer: 50 mM HEPES (pH 7.0) and elution buffer: 50 mM HEPES (pH 7.0) - 2.0 M NaCl. Equipment: FPLC (Pharmacia, Sweden) with the detector signals interfaced to a computer using a LabPro Datalogger. The rhMBP standard used in this study was obtained from TGmilk$_h$ samples (Agreserach, Ltd).

- Comparison of WTmilk and the TGmilk samples employing cation exchange chromatography and SDS-PAGE

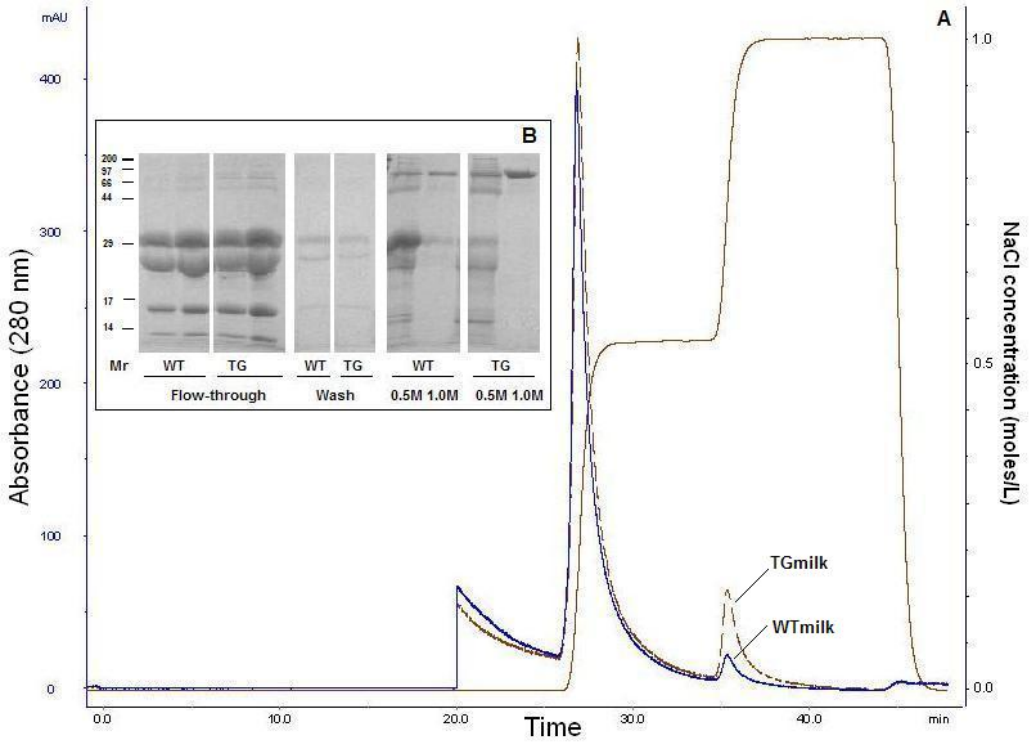

Figure 57: A comparison between the WTmilk and TG milk samples using the optimized purification protocol (sequential loading of the sample) under the same experimental conditions. A: Chromatograms showing a notable difference in the peak obtained at 1.0 M NaCl. B: SDS-PAGE showing more lactoferrin in the TGmilk fraction obtained at 1.0 M NaCl. Column: Tricorn 10/100 packed with SP Sepharose BB - cv 8 ml, sample: 10 ml (2x5 ml) milk loaded at 1.0 ml/min, elution flow rate 5.0 ml/min, loading buffer: 50 mM HEPES (pH 7.0) and elution buffer: 50 mM HEPES (pH 7.0) - 1.0 M NaCl.

- The effects of different chromatographic conditions on column retention

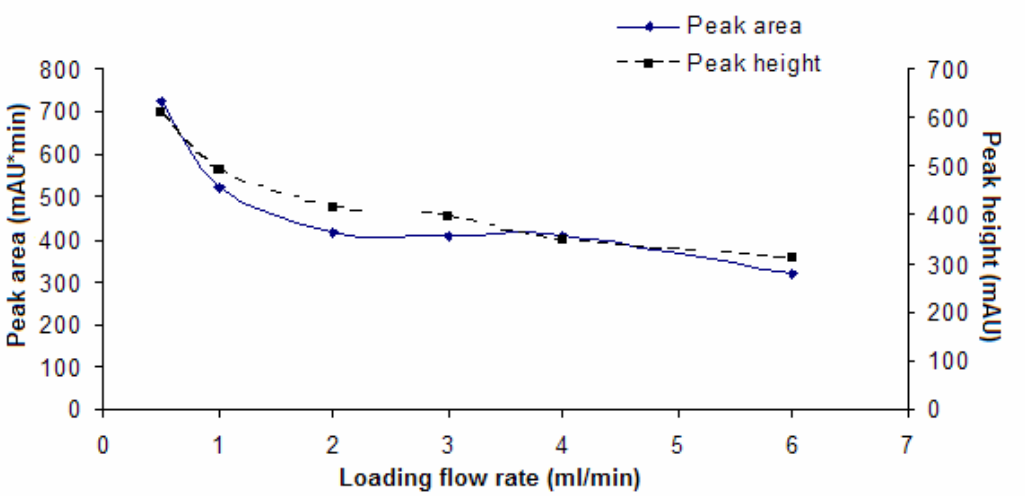

Figure 58: The effect of sample loading flow rate on the total retention of the column. Tricorn 10/100 packed with SP Sepharose BB - cv 8 ml, sample: 10 ml TGmilk loaded at different flow rates, elution flow rate 5.0 ml/min, loading buffer: 50 mM HEPES (pH 7.0) and elution buffer: 50 mM HEPES (pH 7.0) - 1.0 M NaCl (one step).

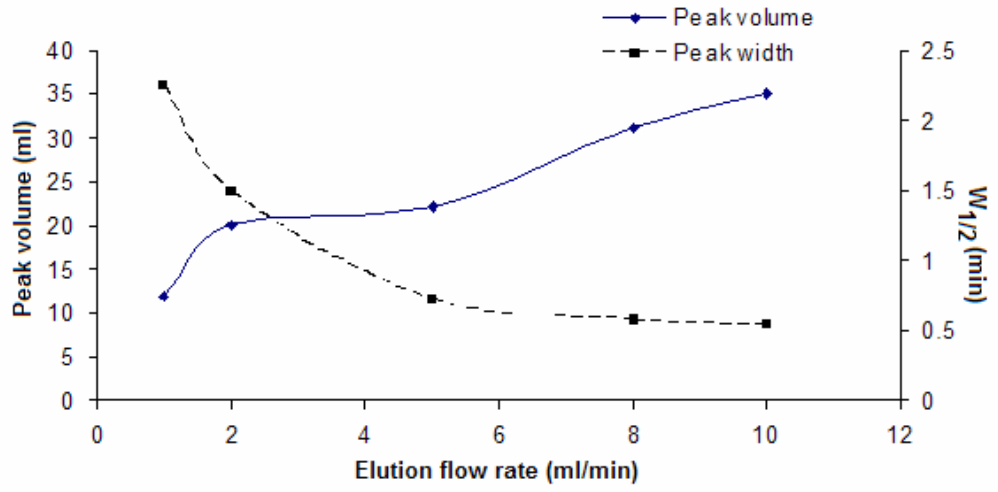

Figure 59: The effect of elution flow rate on the total retention of the column. Tricorn 10/100 packed with SP Sepharose BB - cv 8 ml, sample: 10 ml TGmilk loaded at 1.0 ml/min, loading buffer: 50 mM HEPES (pH 7.0) and elution buffer: 50 mM HEPES (pH 7.0) - 1.0 M NaCl (one step).

- Direct chromatographic recovery of rhMBP employing tangential flow membrane chromatography.

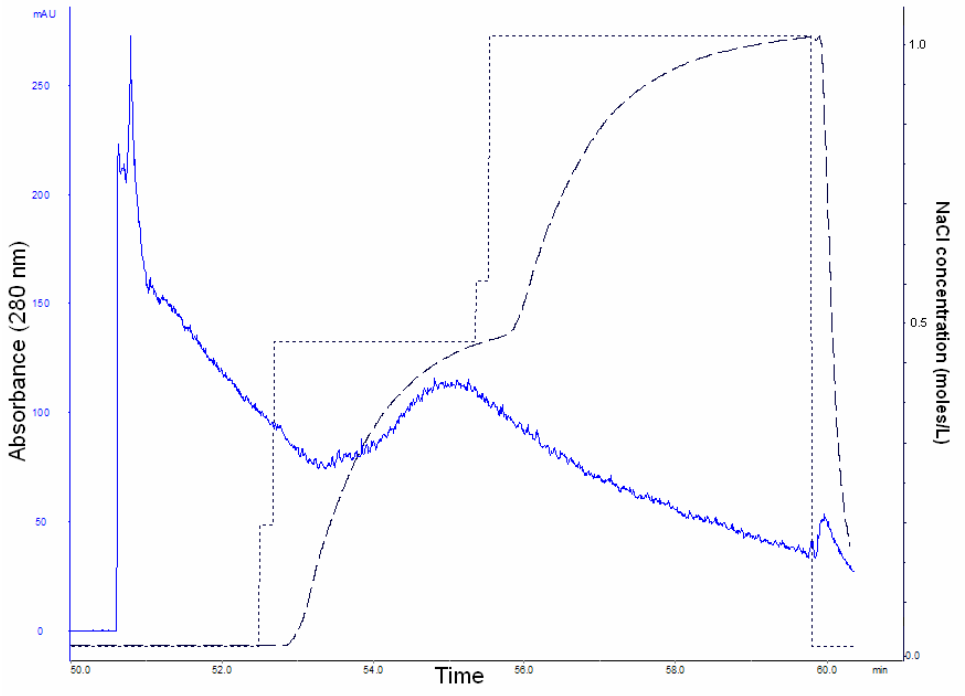

Figure 60: Chromatogram showing a step elution from the cation exchanger membrane unit with the pre-set gradient (dotted line) and the recorded gradient (dashed line) overlaid. Column: Sartobind tangential flow membrane unit - cv 2.5 ml, sample: 50 ml milk loaded at 25.0 ml/min (recycled 5x), elution flow rate 5.0 ml/min, loading buffer: 50 mM HEPES (pH 7.0), elution buffer: 50 mM HEPES (pH 7.0) - 1.0 M NaCl and a two-step elution (5 cv each).

Appendix III

This appendix contains data showing the novel electromigration behaviour of the HEPES buffer in coated and dynamically coated capillaries under the effect of an applied electric field. Further investigations need to be carried out in future work in order to model the phenomenon described herein and to investigate its usefulness in CE applications which involve zwitterionic buffers.

- The electrophoretic migration behavior of HEPES buffer

The electromigration behaviour of the zwitterionic HEPES buffer was studied in PEO dynamically coated and in covalently coated capillaries. HEPES buffer was used as the BGE under negative polarity conditions and was found to generate a reliable and reproducible pseudo-EOF towards the anode. This mobilization force was found to be weaker than conventional EOF and in the opposite direction. The elution pattern of a neutral marker (benzyl alcohol, BA) employing FS capillaries and HEPES buffer as the BGE in the presence and in the absence of PEO polymer was investigated. Results demonstrated the ability of the HEPES system to elute analytes toward the anode upon suppression of the EOF by the dynamic coat achieved using a PEO polymer. In the absence of the polymer, the neutral marker studied was found to migrate towards the cathode under the effect of conventional EOF. This mobilization modality is considerably less vulnerable to capillary wall effects when compared to the traditional EOF which should be of great potential in future applications.

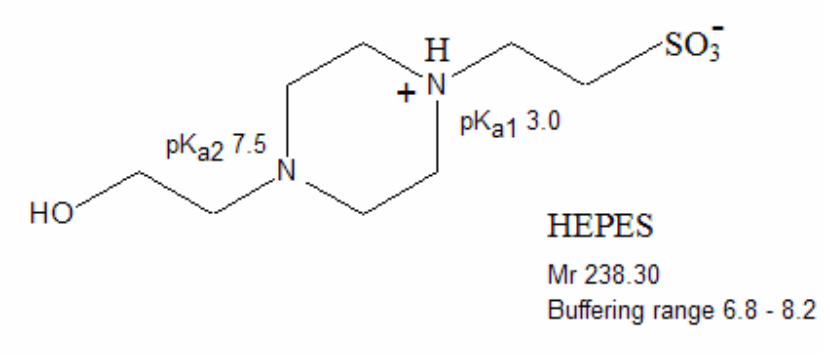

Figure 61: The chemical structure of the zwitterionic HEPES molecule showing the pKa values of the two protonated nitrogens.

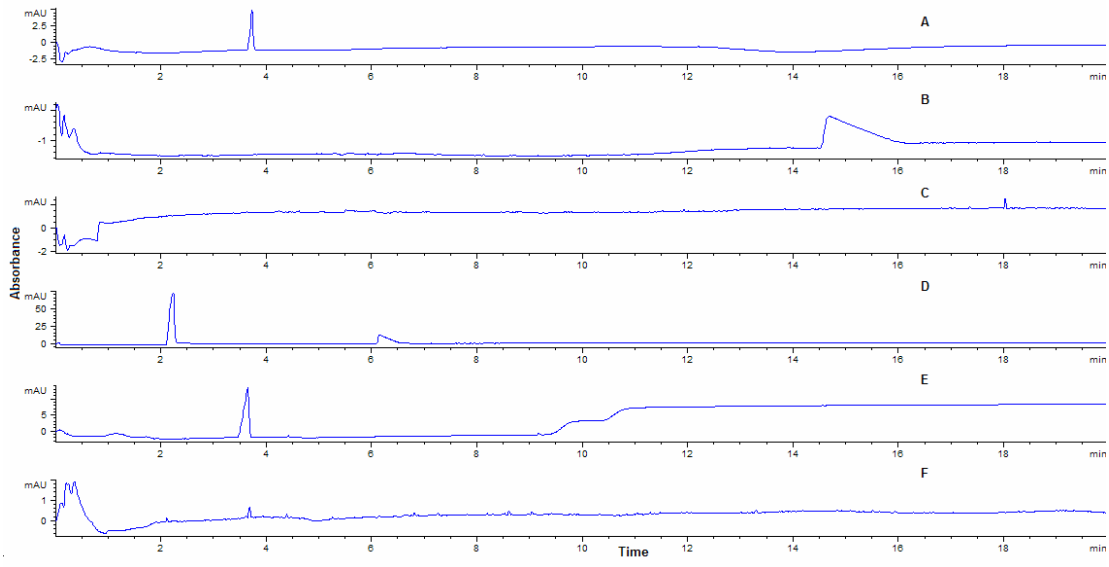

Figure 62: The electromigration behavior of HEPES buffer (pH 7.0), as demonstrated by the direction of the elution of a neutral marker (BA), in FS capillaries of different surface properties and under different polarity conditions. A and B: ZeroFlow coated capillary, negative and positive polarities respectively, C and D: uncoated FS capillary, negative and positive polarities respectively and E and F: PEO dynamically coated capillary, negative and positive polarities respectively. Capillary total / effective length: 33 / 24.5 cm x 50 µm I.D., voltage: 13.75 kV, temperature: 25 °C, detection: UV at 214 nm, hydrodynamic injection: 50 mbar - 10 s and sample: BA.

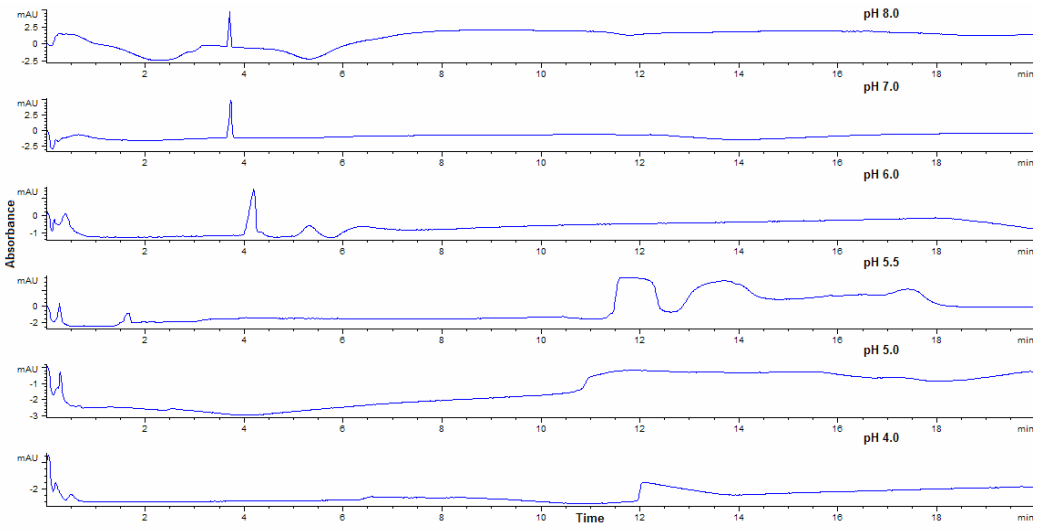

Figure 63: Electrophoregrams showing the impact of the pH of HEPES solutions (pH 4.0 - 8.0) on the elution pattern of a neutral marker (BA). Capillary: ZeroFlow coated capillary, total / effective length: 33 / 24.5 cm x 50 µm I.D., temperature: 25 °C, detection: UV at 214 nm, hydrodynamic injection: 50 mbar - 10 s and sample: BA. The HEPES solution (pH 5.5) represents the pH of 50 mM HEPES in MilliQ water without any pH adjustment.

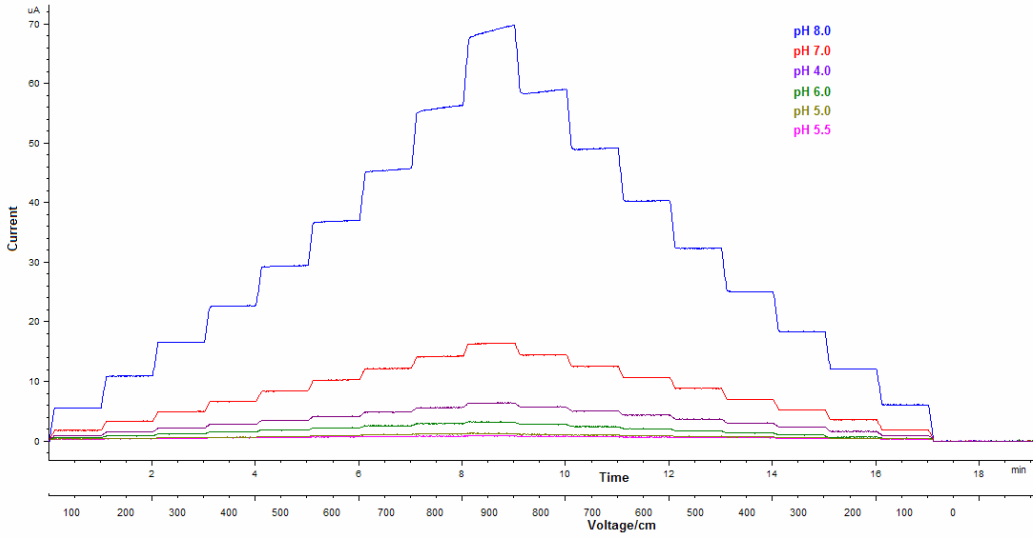

Figure 64: A plot of the electric current recorded upon the application of different voltage values employing a series of 50 mM HEPES buffers / solutions (pH 4.0 - 8.0). Capillary: ZeroFlow coated capillary, total / effective length: 33 / 24.5 cm x 50 µm I.D., temperature: 25 ^{o}C and detection: UV at 214 nm. The HEPES solution (pH 5.5) represents the pH of 50 mM HEPES in MilliQ water without any pH adjustment.

Appendix IV

In this appendix, supplementary data to those described in Chapter 4 are presented.

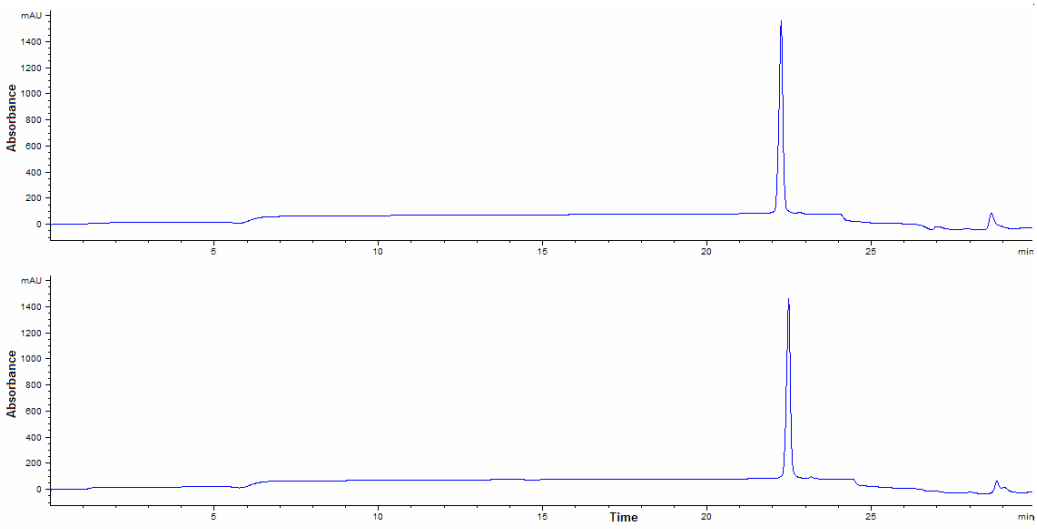

Figure 65: Electrophoregrams showing the effect of the the BGE concentration on the elution pattern of denatured BSA samples prepared in 50 mM (top) and 25 mM (bottom) HEPES buffer (pH 7.0) respectively. Fused silica capillary total / effective length: 72 cm / 63.5 cm x 75 µm I.D., voltage: - 30 kV, temperature: 25 ^{o}C, detection: UV at 214 nm, hydrodynamic injection: 50 mbar - 40 s, BGE: 50 mM (top) and 25 mM (bottom) HEPES buffer (pH 7.0) respectively and sample: 1.0 mg/ml BSA.

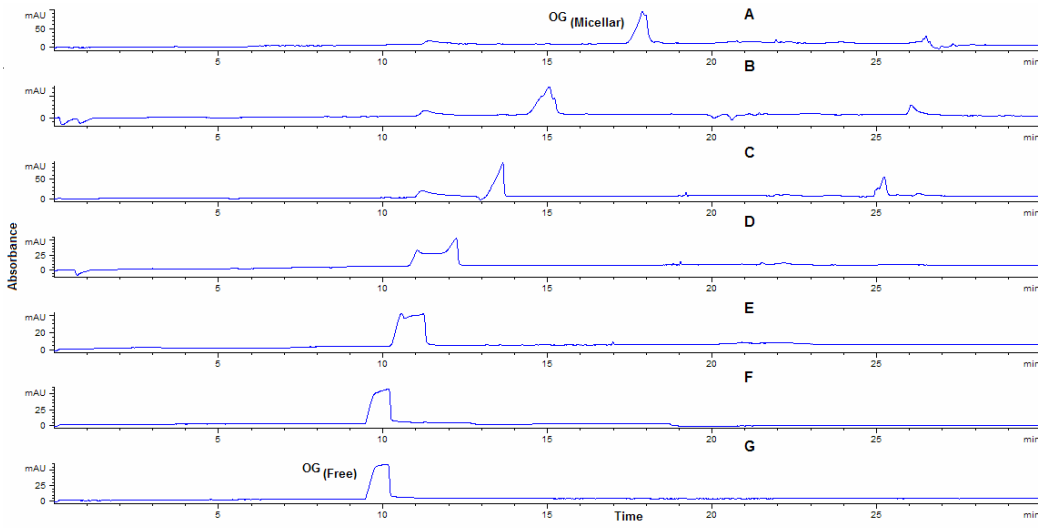

Figure 66: Electrophoregrams showing the migration behavior of the negatively charged orange G marker using different SDS concentration: (A: 35.0, B: 28.0, C: 22.4, D: 17.9, E: 14.3, F: 11.5 and G: 0.0 mM). Fused silica capillary total/effective length: 72 cm / 63.5 cm x 75 µm I.D., voltage: - 30 kV, temperature: 25 ^{o}C, detection: UV at 214 nm, hydrodynamic injection: 50 mbar - 40 s and sample: 4% v/v OG in 50 mM HEPES buffer (pH 7.0). These results confirmed the existence of two different populations of OG (free and micellar) in the capillary lumen. The shift in the migration time of the OG second peak indicated an equilibrium between $OG_{(Free)}$ and $OG_{(Micellar)}$.

Table 9: Comparison between the Bio-Plex and the SPR immunoassays for the determination of the rhMBP concentration.

	Bio-Plex Immunoassay	**SPR Immunoassay**
Format	Anti-rhMBP mAb-coupled to polystyrene fluorescent beads	Anti-rhMBP mAb-coupled to CM dextran on a gold surface
Detection	Fluorescence generated by a labeled anti-His tag mAb (requires labeling).	The change in the SPR response upon binding of the analyte to a sensor surface (label free).
Specificity	Full length rhMBP	hMBP / rhMBP
Regression model	4-PL	4-PL
Calibration curve	Sigmoid	Sigmoid - lower part only
LOD	6.04 ng/ml	30.00 ng/ml
Range	9.77 - 10,000.00 ng/ml	46.0 - 5500.0 ng/ml
Sensitivity to kinetics / PTM	+	+++
Analysis time		
Incubation steps:	≈ 90 min / 96 samples	≈ N/A*
Measuring step:	≈ 45 - 60 min / 96 samples	≈ 3 min / samples
Multiplexing	Up to 100 analytes / sample	N/A*
Interaction analysis	N/A*	Yes
Cost	+++ - beads are not reusable	+ - reusable chip#

*** Not applicable.**

 # Depends on the surface regeneration strategy employed.

Appendix V

In this appendix, supplementary data to those discussed in Chapter 5 are presented.

- The effect of various combinations of voltage and pressure values on the elution pattern of the protein standards.

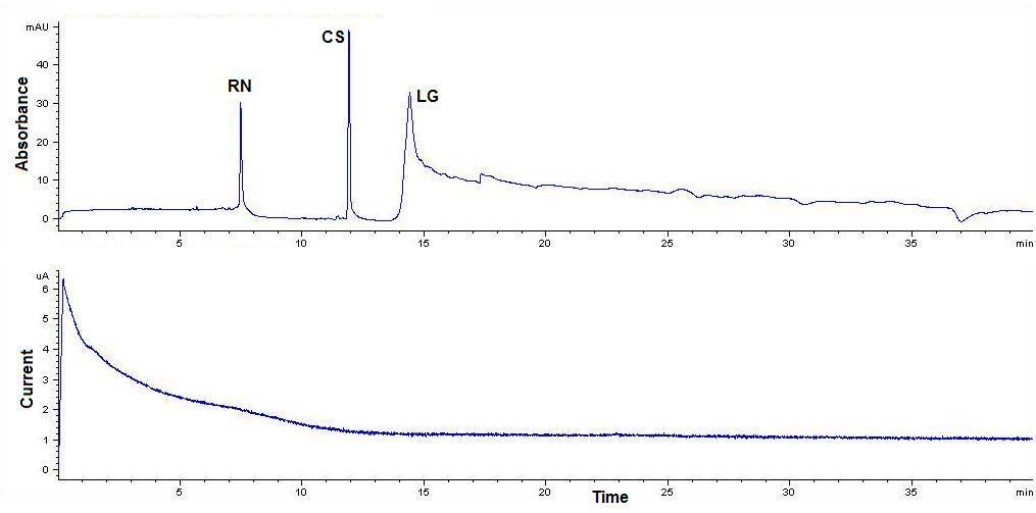

Figure 67: Electrophoregram and current trace obtained using dynamically coated capillaries. Capillary: dynamically coated fused silica, total / effective length: 33 cm / 24.5 cm x 50 µm I.D., anolyte: 91 mM H_3PO_4 in CIEF gel, catholyte: 20 mM NaOH, focusing and mobilization: 10 kV - 0 mbar (after 6 min), temperature: 25 ^oC, hydrodynamic injection: 950 mbar - 2 min and detection: 280 nm. Sample: mixture of four standard proteins: ribonuclease A (RN), carbonic anhydrase II (CS), β-lactoglobulin (LG) and cholecystokinin peptide (CK).

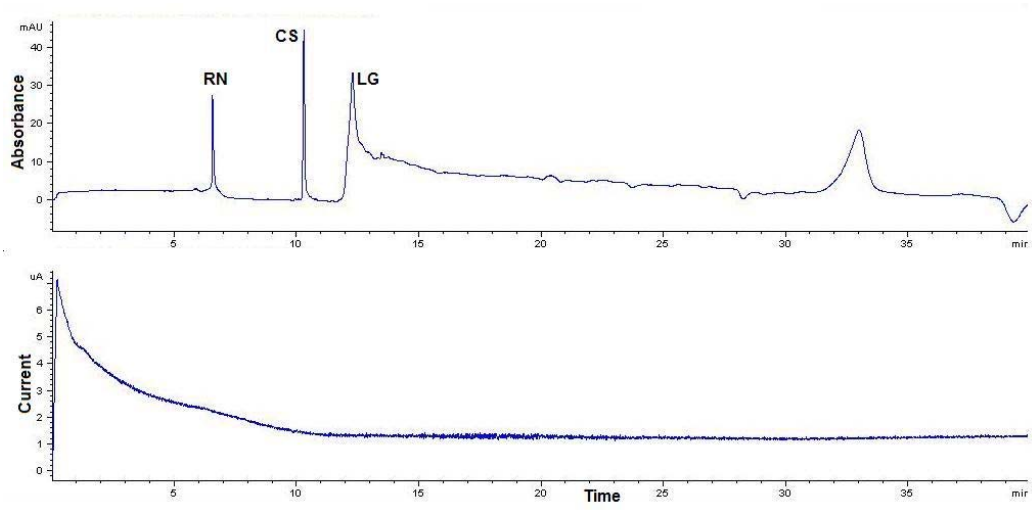

Figure 68: Electrophoregram and current trace obtained using dynamically coated capillaries. Capillary: dynamically coated fused silica, total / effective length: 33 cm / 24.5 cm x 50 µm I.D., anolyte: 91 mM H_3PO_4 in CIEF gel, catholyte: 20 mM NaOH, focusing and mobilization: 15 kV - 0 mbar (after 6 min), temperature: 25 ^oC, hydrodynamic injection: 950 mbar - 2 min and detection: 280 nm. Sample: mixture of four standard proteins: ribonuclease A (RN), carbonic anhydrase II (CS), β-lactoglobulin (LG) and cholecystokinin peptide (CK).

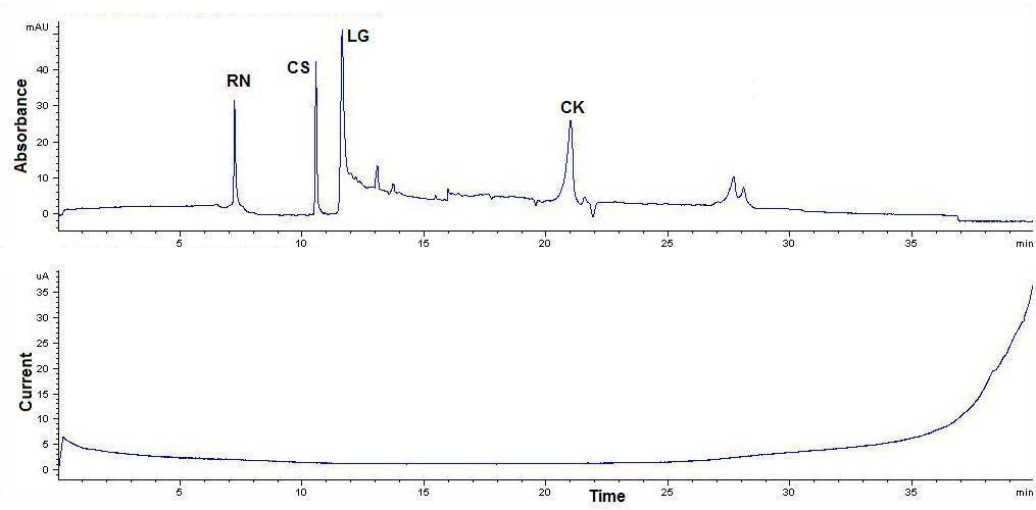

Figure 69: Electrophoregram and current trace obtained using dynamically coated capillaries. Capillary: dynamically coated fused silica, total / effective length: 33 cm / 24.5 cm x 50 µm I.D., anolyte: 91 mM H_3PO_4 in CIEF gel, catholyte: 20 mM NaOH, focusing and mobilization: 15 kV - 10 mbar (after 6 min), temperature: 25 ^oC, hydrodynamic injection: 950 mbar - 2 min and detection: 280 nm. Sample: mixture of four standard proteins: ribonuclease A (RN), carbonic anhydrase II (CS), β-lactoglobulin (LG) and cholecystokinin peptide (CK).

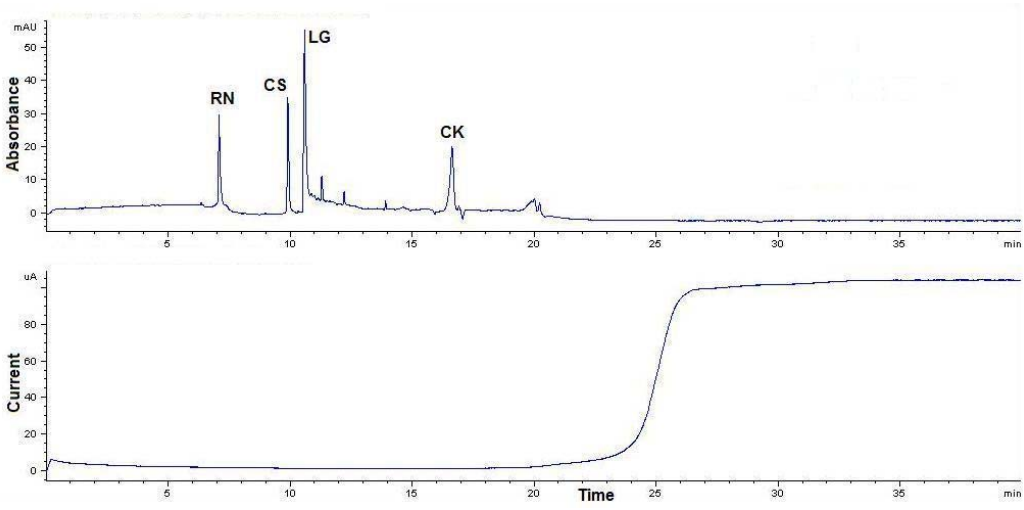

Figure 70: Electrophoregram and current trace obtained using dynamically coated capillaries. Capillary: dynamically coated fused silica, total / effective length: 33 cm / 24.5 cm x 50 µm I.D., anolyte: 91 mM H_3PO_4 in CIEF gel, catholyte: 20 mM NaOH, focusing and mobilization: 15 kV - 20 mbar (after 6 min), temperature: 25 ^oC, hydrodynamic injection: 950 mbar - 2 min and detection: 280 nm. Sample: mixture of four standard proteins: ribonuclease A (RN), carbonic anhydrase II (CS), β-lactoglobulin (LG) and cholecystokinin peptide (CK).

- The effect of the concentration of the anolyte and catholyte solutions

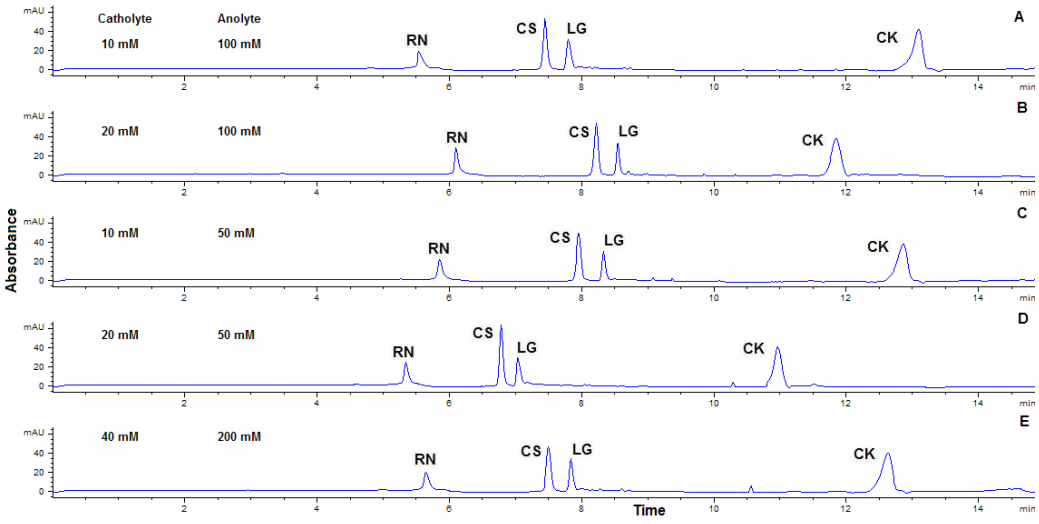

Figure 71: Electrophoregrams obtained using dynamically coated capillaries employing various combinations of anolyte / catholyte concentrations. Capillary: dynamically coated fused silica, total / effective length: 33 cm / 24.5 cm x 50 µm I.D., focusing and mobilization: 15 kV - 35 mbar, temperature: 25 ^{o}C and hydrodynamic injection: 950 mbar - 2 min and detection: 280 nm. Sample: mixture of four standard proteins: ribonuclease A (RN), carbonic anhydrase II (CS), β-lactoglobulin (LG) and cholecystokinin peptide (CK).

- The functionality of PEO polymers

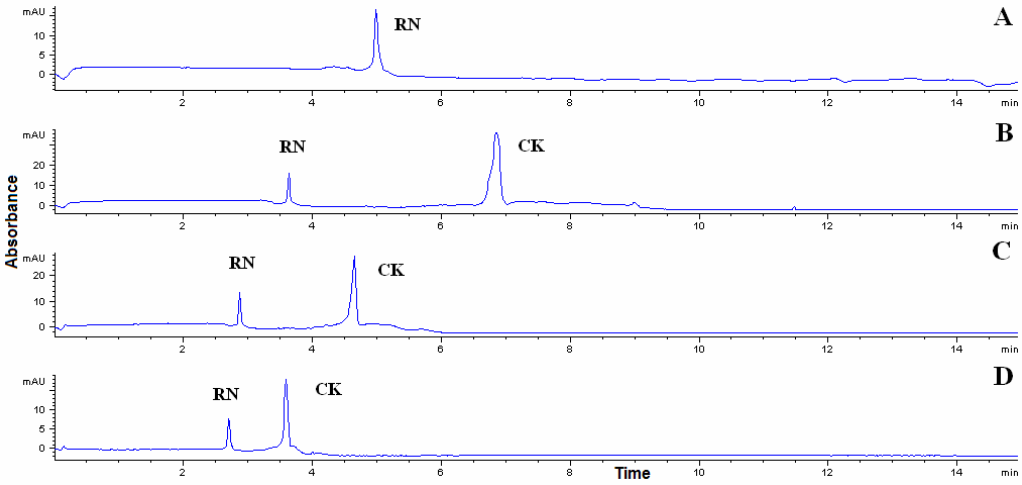

Figure 72: Electrophoregrams obtained using dynamically coated capillaries employing 0.1% PEO 100 in the presence of an increasing hydraulic pressure. Capillary: dynamically coated fused silica, total / effective length: 33 cm / 24.5 cm x 50 µm I.D., anolyte: 100 mM H_3PO_4, catholyte: 20 mM NaOH, focusing and mobilization: 15 kV and 0, 10, 20 and 35 mbar, temperature: 25 ^oC, hydrodynamic injection: 950 mbar - 2 min and Detection: 280 nm. Sample: mixture of four standard proteins: ribonuclease A (RN), carbonic anhydrase II (CS), β-lactoglobulin (LG) and cholecystokinin peptide (CK).

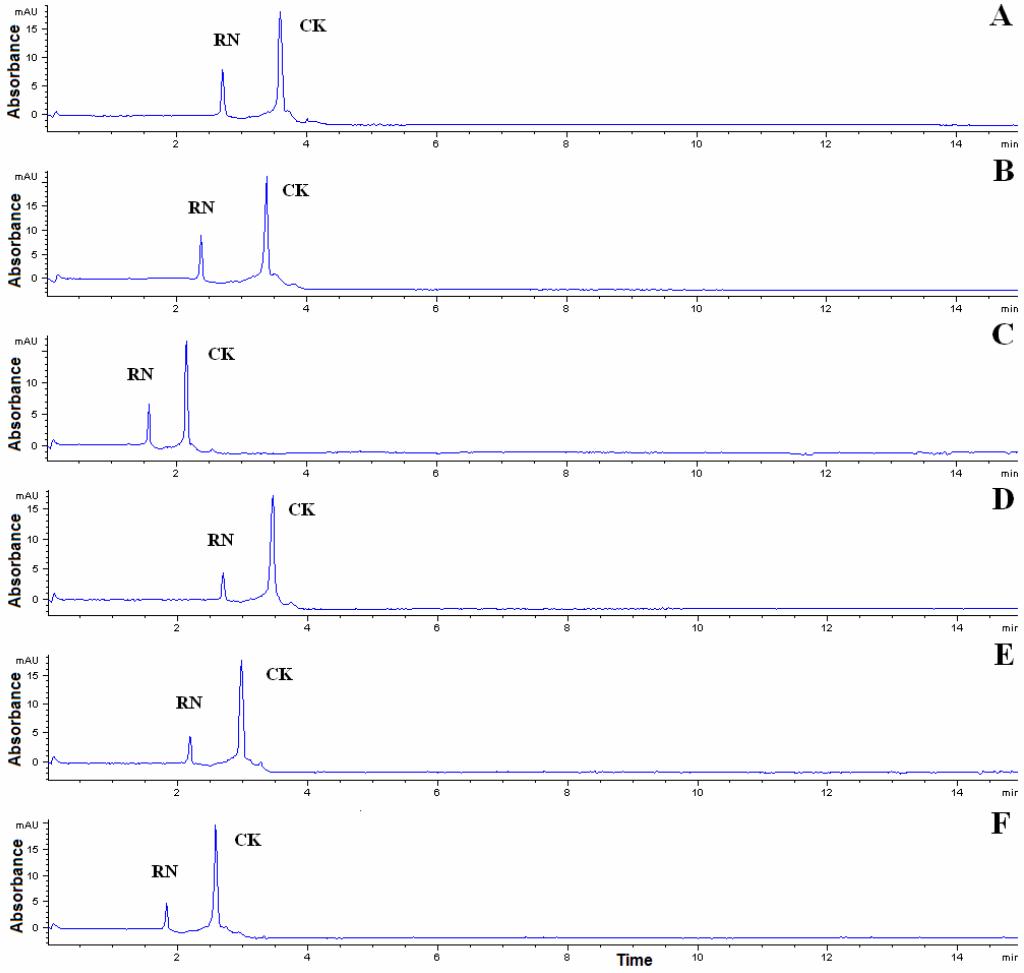

Figure 73: Electrophoregrams obtained using dynamically coated capillaries employing 0.1% PEO 100 (A - C) and 0.1% PEO 600 (D - F) in the presence of an increasing voltage. Capillary: dynamically coated fused silica, total / effective length: 33 cm / 24.5 cm x 50 µm I.D., anolyte: 100 mM H_3PO_4, catholyte: 20 mM NaOH, focusing and mobilization: 10, 15 and 20 kV and 35 mbar, temperature: 25 ^oC, hydrodynamic injection: 950 mbar - 2 min and detection: 280 nm. Sample: mixture of four standard proteins: ribonuclease A (RN), carbonic anhydrase II (CS), β-lactoglobulin (LG) and cholecystokinin peptide (CK).